Transformational Solar Array Option I Final Report

For the interval May 2, 2017 through August 31, 2018

By

Edward Gaddy
Space Exploration Sector
Johns Hopkins University Applied Physics Laboratory
11100 Johns Hopkins Road
Laurel, MD 20723-6099

(240) 228-4289
edward.gaddy@jhuapl.edu

NNC16CA19C
Game Changing Development Program
Extreme Environments Solar Power Project

Prepared for NASA Glenn Research Center, Cleveland, OH 44135

Contents

Authorship

Edward Gaddy is the author on the title page of this report. However, the actual authorship is split between Mark Douglas at DSS; Paul Sharps, Christopher Kerestes and Chris Sulyma at SolAero; and, John Nichols, Chris Drabenstadt, and Edward Gaddy at APL.

Section I: Technical Progress Summary

Introduction

This report summarizes the work performed under NASA contract NNC16CA19C from May 2, 2017 through April 2, 2018. This work is directed toward meeting the goals of the associated NASA NRA and, of course, the requirements of the contract. In brief, the goals are:

- Over 47% beginning of life cell efficiency at 5 AU and -125 °C
- Over 32% end of life efficiency at the blanket level at 50 W m^{-2}, -125 °C and 4E15 1 MeV e cm^{-2}
- Over 8 W kg^{-1} at EOL for the entire array including structure, deployment, and pointing mechanisms using beginning of life performance.
- A stowed packaging density of greater than 66 kW m^{-3}
- An ability to survive launch and numerous deploy retract cycles without degradation
- An output higher than 300 V
- An ability to operate in a plasma generated by xenon thrusters, typically 1E8 cm^{-3} ions with an average energy of 2 eV
- A design compatible with electrostatic and magnetic cleanliness
- Record breaking inverted metamorphic (IMM) 6 junction solar cells
- IMM solar cells that have no anomalous flat spot behavior at low irradiance and low temperature
- A mock-up production line for the low-cost manufacture of spacecraft blanket arrays

The Option I phase of the project continued efforts, started in the base-phase, to eliminate or reduce to very low levels the flat spots that reduce power to an unacceptable value in a significant percentage of cells and to reduce outgassing contamination of the concentrators to acceptable levels. Option I adds tasks to increase the efficiency of IMM cells from those produced in the Base Phase, to eliminate delamination of the coatings that were present in previous versions of the concentrator mirrors, to evaluate pressure sensitive adhesive as a method of fixing solar cell assemblies to blankets, to design a magnetically clean brake for ROSA, to test the robustness of a sample blanket in deploy and retract, to test for the adequate performance of a blanket in vibration and thermal environments, and to define the capital equipment needed to optimize production of the Transformational Array.

Work for this Final Report showed that the greatest likely improvement in the solar cells would be by emphasizing the effort for the IMM4 solar cells and stopping work on other IMM cells. For this phase, the solar cell work was primarily on the IMM4 cells with little work on IMM5 and none on IMM6 cells.

Technical Progress at DSS

The DSS scope of the Transformational Array Phase 1 program consisted of the further development of the FACT concentrator assembly for solar array operation under 5 AU conditions, investigation of various adhesives and solar cell laydown methods to minimize outgassing of the assembly and aid in array manufacture, production of individual solar cell and multi-cell blanket assemblies to support program outgassing and environmental testing, update of the solar array performance analysis from the program base phase targeting a 25 kW solar array system and contribution to the program status reports, meetings and program final report. The detailed DSS tasks for the Transformational Array Phase 1 program are shown below. DSS successfully completed the identified tasks to further advance the flexible solar array technology for the Transformational Array program.

DSS Program Tasks:

- Refine the concentrator coating of the titanium reflectors, coating adhesion layers, and processes to eliminate coating delamination
- Perform thermal cycle testing of the improved coatings and document the lessons learned
- Develop cell laydown processes for both low-outgassing silicone adhesives as well as pressure sensitive adhesives (PSAs)
- Investigate solar array blanket assembly methods to minimize outgassing and reduce array assembly costs
- Provide solar cell blanket assemblies to support outgassing testing at APL as well as other environmental testing
- Develop and design a magnetically clean brake to control the rate of the ROSA solar array deployment.
- Manufacture and deliver two 6” x 6” FACT IMM blanket assemblies with coated reflectors to support APL performance, environmental, and vibration testing
- Update the base phase solar array system level analysis for a 25 kW solar array system (power density, packaging density, 300V capability, xenon plasma operation)

Technical progress

Refinement of Concentrator Coatings

A silver/SiO_2 coating is applied to the concentrators to maximize the light impingement on the solar cell adjacent to the concentrator within the FACT concentrator assembly. A typical concentrator with the coated surface identified is shown in Figure 1.

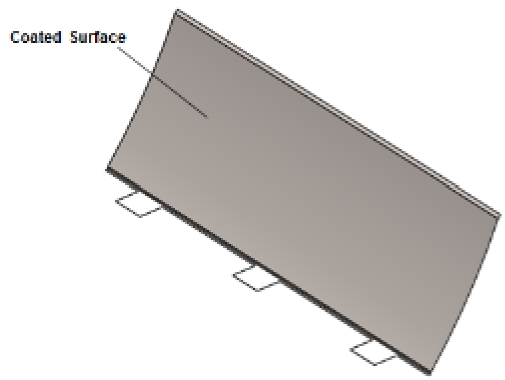

Figure 1. Concentrator Configuration

During an earlier NASA development program, the concentrator was formed using a 0.051-mm-thick stainless steel foil. Coating adhesion to the stainless base metal was identified as a deficiency through both mechanical and thermal cycle testing. To improve the reflective coating adhesion as well as obtain mass benefits, the reflector material was changed to a 0.051 mm-thick titanium foil. Past testing and flight experiments have demonstrated that application of silver/SiO_2 onto titanium foil is a robust reflector system meeting system level requirements. DSS generated a detailed statement of work and a detailed specification for the application of a reflective coating onto a 0.051-mm-thick titanium foil. The reflective part of the coating is 1,500 Å thick silver. Over the silver is 32,000 Å thick SiO_2. The specification detailed materials and coating thicknesses, specular reflectance, orbital thermal environment, coating adhesion tests, coating peel tests, random vibration environment, long term stowage duration, deployment cycling, xenon plum resistance, humidity, UV radiation environment, and charged particle dose. The specification placed emphasis on coating adhesion. The coating/concentrator requirements are summarized in Tables 1 and 2.

Table 1: Coating/Concentrator Requirements

Description	Material Thickness (Angstroms)	Requirement	Comment
Reflector Materials:			
Layer 1: titanium, t=.002 in.	508000		
Layer 2: Thin Adhesion Layer	~ 500		Buellton Advanced Materials to define material and thickness of adhesion layer in order to achieve proper adhesion of the Silver layer and meet the defined reflectance requirement
Layer 3: Silver	1500		
Layer 4: Thin Adhesion Layer	~ 50		Buellton Advanced Materials to define material and thickness of adhesion layer in order to achieve proper adhesion of the SiO2 layer and meet the defined reflectance requirement
Layer 5: SiO2	35000		A thick SiO2 coating is required to meet the RH storage requirement as well as expected orbital degradation
Specular Reflectance of Coated reflector		≥ 0.95	
Storage Environment		< 1% performance degradation of surface after exposure to 90% RH for 60 days	
Orbital Thermal Environment		-175 C to +120 C Thermal Cycles (Qty 2000)	Power reduction of concentrator module less than 1% after 2000 GEO thermal cycles
Coating Adhesion		The silver/SiO2 coating must remain adhered to the titanium base metal following completion of the tape peel test described in Section 5 of the specification.	

Table 2. Coating/Concentrator Requirements (continued)

Test	Environment	Requirement
Electrical	AM0 Large Area Pulsed Solar Simulator (LAPSS)	Excellent optical efficiency and off-point characteristics with assembly meeting power predictions
Random Vibration	15.1 grms random vibration level testing enveloping current launch environments	No measureable shape or performance change
GEO Thermal Cycling	-175 C to +120 C (2000 Cycles)	Power reduction less than 1% after 2000 cycles
LEO Thermal Cycling	-100 C to +120 C (80000 Cycles)	Power reduction less than 1% after 80000 cycles
Long Term Stowage	Stowage duration 3 yrs	No significant reflector shape change or power reduction after long term stowage.
Deployment Cycling	30 stow and deploy cycles	No measurable shape change or power reduction
Xenon Plume Resistance	Xenon Ion Plume at multiple energies and angles	Minimal/pedictable erosion rate of protective coating consistent with analysis
Humidity	90% RH at 22 C for 60 days	No visual degradation with power reduction less than 1%
UV Radiation	>10000 Equivalent Sun Hours	No Coating Degradation
Electrons and Protons	15 Year GEO Dose	No measurable coating degradation

The contractor for this effort, Buellton Advanced Materials, defined a new proprietary coating formulation to improve adherence. They applied the coatings to fifteen 76 mm by 76 mm flat titanium foil coupons. The titanium foil coupons with applied Silver/SiO_2 reflective coating are shown in Figure 2. Per the DSS specification, tape peel tests were performed to verify adhesion of the reflective coating to the base material. The pull test configuration for testing coating adhesion is shown in Figure 3. Coating specular reflectance and thickness were also measured.

Clearly, larger foils will be needed for production arrays; this will be addressed at least theoretically in Option II. In addition, data will be submitted to demonstrate reflectance of greater than 0.95.

Aluminum could be used instead of silver over titanium. The silver was chosen because it has a better reflectance, which is critical to meet the contract's demanding efficiency requirements. In Option II, if awarded, APL will consider $SiO_{1.9}$ rather than SiO_2 due to the former's superior adherence.

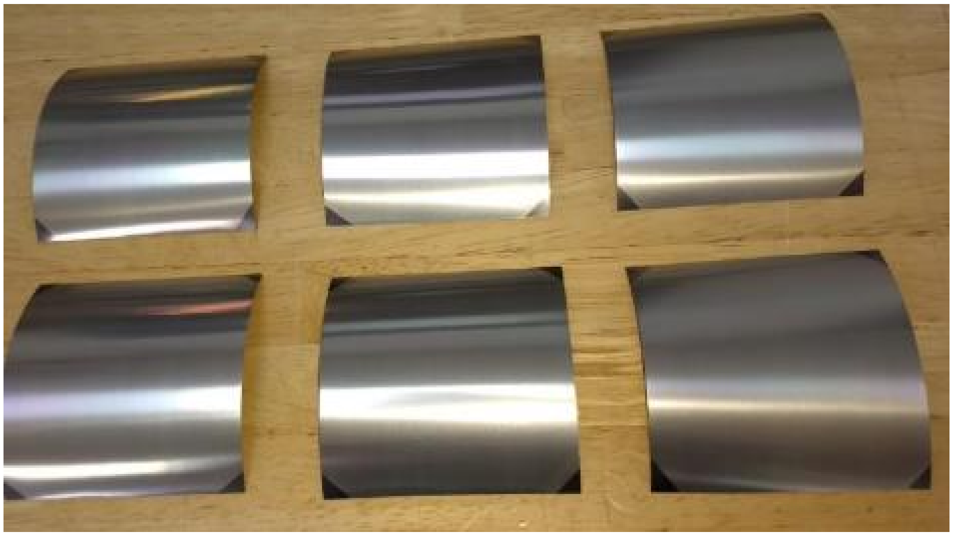

Figure 2: Coated Titanium Reflector Coupons

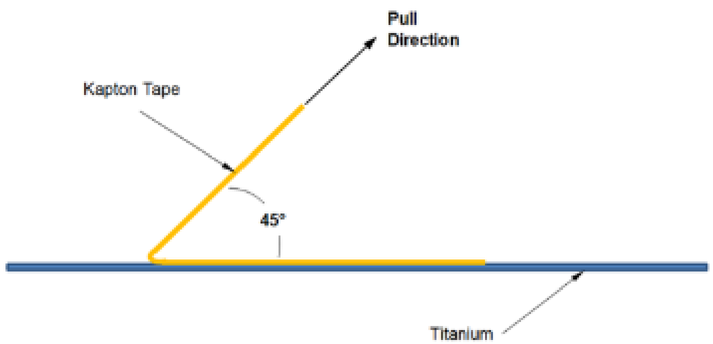

Figure 3: Pull Test Configuration

As shown in Figure 4 and Figure 5, the coated titanium foil coupons successfully passed the specified tape peel testing at Buellton Advanced Materials. After delivery to DSS, the coating peel test was again performed with positive results. Additional thermal cycle testing of the coated titanium foil coupons was performed, again, yielding positive results. Thermal cycle testing is discussed in sections below. Changing the foil material to titanium and adjusting the coating adhesion layers has greatly improved the adhesion of the coating to the base metal.

In Option II a humidity exposure will be performed to demonstrate adhesion of the reflector after exposure to humidity.

Figure 4: Tape Pull Test on Concentrator

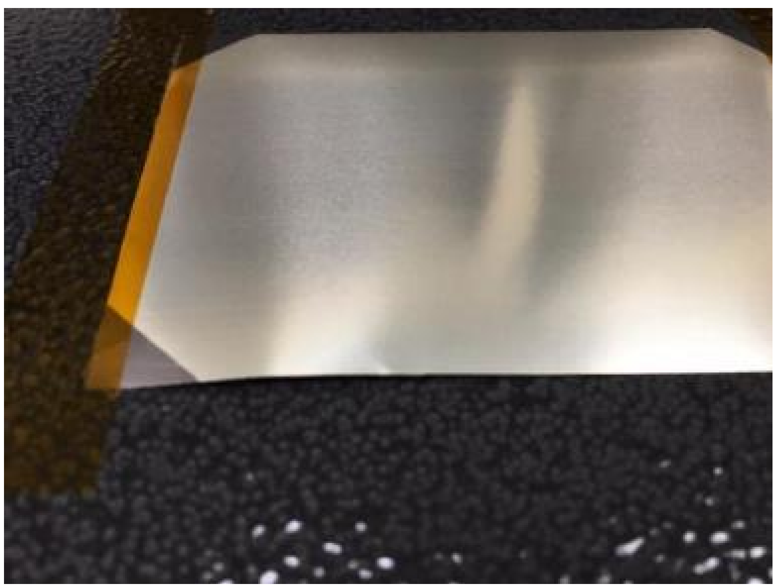

Figure 5: Concentrator Post Tape Peel Adhesion Test (Adhesion test passed)

Cell Bonding Development

DSS was tasked to evaluate both silicone adhesives and pressure sensitive adhesives (PSA)s as materials to secure the interconnected solar cell strings to the underlying Kapton substrate. The selected adhesive must provide a secure bond of the solar cells to the Kapton substrate under all expected terrestrial and orbital environments. Individual SolAero ZTJ solar cells were bonded to a Kapton film substrate using three different silicones/PSAs to evaluate the bonding procedures. The bonded coupons were then subjected to repeat thermal cycling to demonstrate the robustness of the cell-to-Kapton bond. Thermal cycling testing is described in detail below. PSAs are being evaluated as options to conventional silicones because they may aid in the manufacturing process as well as provide a low outgassing adhesive option. A summary of the bonded cell coupon configurations is provided in Table 3. During cell bonding, DSS followed documented laydown processes (material abrading, cleaning, priming, and perforation). One bonded coupon was fabricated using Nusil CV10-2568, the typical adhesive used by DSS during the cell lay down process. Bonding of the solar cell to Kapton using CV10-2568 is shown in Figure 6. The CV10-2568 silicone was applied to the Kapton in a thin, uniform thickness. Tape was used to define the adhesive area that matched the solar cell and was removed from the Kapton after adhesive application. The solar cell was then carefully aligned and placed onto the Kapton/silicone assembly and cured in a weighted configuration. The second coupon, shown in Figure 7, was fabricated using Nusil CV4-1161-5 PSA to secure the solar cell to the Kapton. Nusil CV4-1161-5 has been used successfully to bond solar cells to CubeSats. The remaining two coupons were fabricated using 3M 966 PSA. The first of these coupons was fabricated with one layer of 3M 966 PSA. The second coupon used two layers of the same 3M 966 PSA. Having a thicker PSA bond may provide additional compliance and adhesion during the bond expansion and contraction related to thermal cycling. During cell lay down, the 966 PSA was applied to the back side of the solar cell. Kapton was then carefully rolled onto the assembly producing an assembly without entrapped air. An elevated temperature exposure was used to "set" the 3M 966 PSA and produce a good bond to the cell. The 3M 966 (one layer) thermal cycle coupon is shown in Figure 8. For reference, 3M 966 PSA was used to secure the solar cell mass simulators that solar array blanket within the ISS ROSA flight experiment that launched aboard SpaceX-11 in June 2017. Mass simulators covered the majority of the solar array blanket. The ISS ROSA array performed multiple deploy retract cycles on orbit over a two week period and remained in orbit until February 2018. The ISS ROSA array is shown in Figure 9

Table 3: Bonded Cell Coupon Summary

Cell Type	Substrate	Adhesive	Adhesive Manufacturer	Adhesive Type	Kapton Preparation
SolAero ZTJ	Kapton	CV10-2568	Nusil/Avantor	Silcone - Platinum Cure	IPA Wipe, Abrade, IPA Wipe, Apply Primer
SolAero ZTJ	Kapton	CV4-1161-5	Nusil/Avantor	PSA	IPA Wipe, Abrade, Perforate, IPA Wipe
SolAero ZTJ	Kapton	966 (one layer)	3M	PSA	IPA Wipe, Abrade, Perforate, IPA Wipe
SolAero ZTJ	Kapton	966 (two Layers)	3M	PSA	IPA Wipe, Abrade, Perforate, IPA Wipe

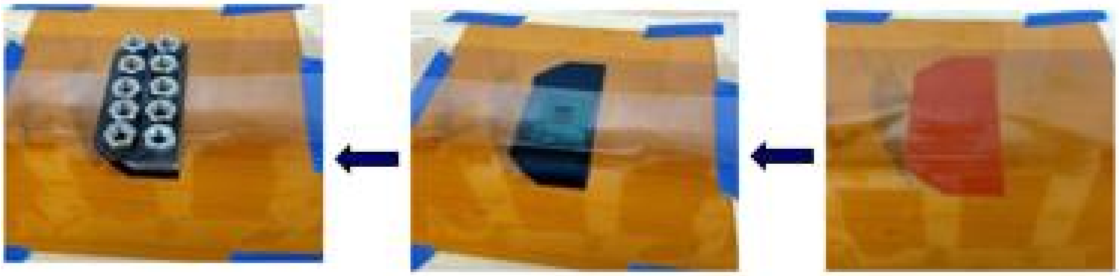

Figure 6: Cell Bonding with CV10-2568

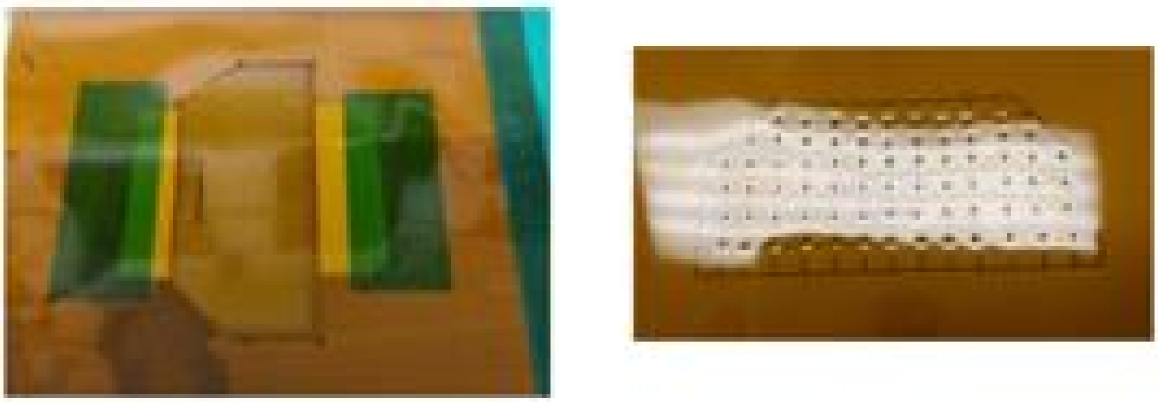

Figure 7: Kapton Perforation and Cell Bonding with CV4-1161-5

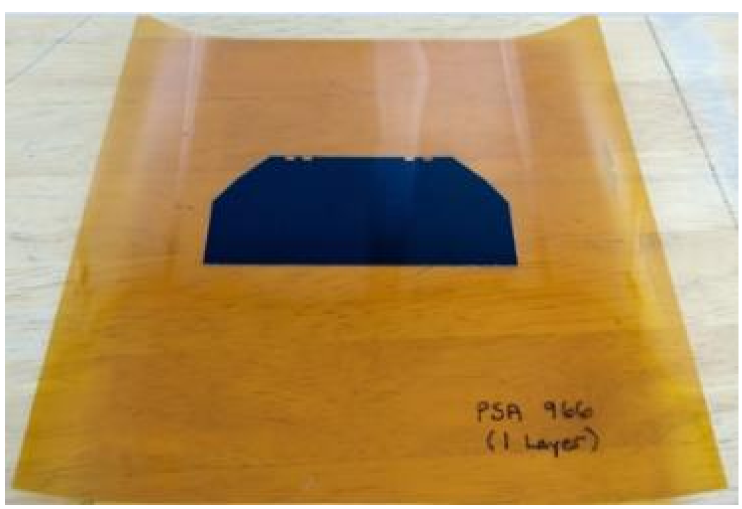

Figure 8: Bonded cell coupon

Figure 9: ISS ROSA Flight Experiment on Orbit

Solar Array Blanket Construction /Improvements

The construction of a typical FACT Reflector Assembly is shown in Figure 10. The reflector assembly consists of coated reflectors, kick up springs, lateral titanium strip elements and a solar cell string bonded to Kapton. Low-outgassing liquid silicones or pressure sensitive adhesives (PSAs) are typically used to assemble the various elements together. PSAs are preferred over liquid silicones because they speed assembly and minimize the tooling required for positioning and clamping of the elements during cure. Once the reflector assemblies are fabricated, they are attached to a tensioned mesh backplane to form the flexible solar array blanket.

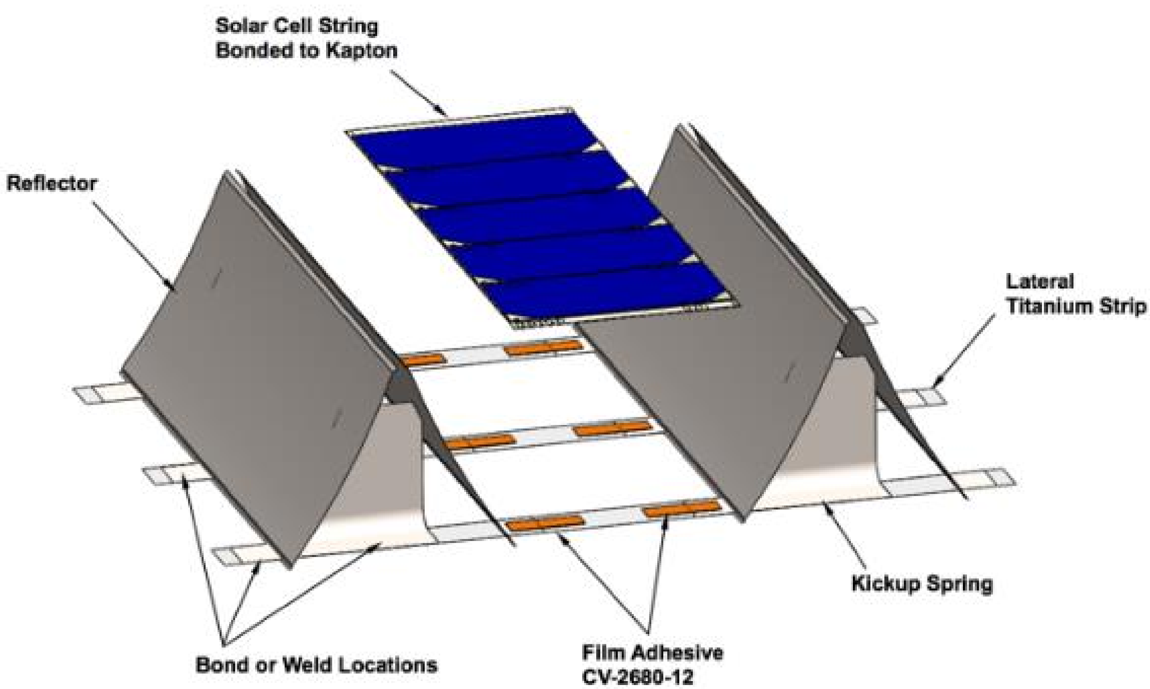

Figure 10: Reflector assembly construction

DSS has baselined Nusil CV-2680-12 film adhesive for the construction of the FACT Reflector Assembly. DSS has significant experience with this adhesive. It is platinum cured, requires a wipe of activator on the surface to which it is to be adhered, and forms strong resilient bonds.

From the manufacturer: the adhesive is a two-part film that cures at room temperature or more rapidly with heat. The adhesive is designed for electronic and space applications that require low outgassing and minimal volatile condensables. It can be used to bond or seal silicone elastomers and some metals and plastics. It is for applications that require shorter work times, easy clean-up, and consistent bond thickness. The adhesive meets or exceeds the ASTM E 595 low outgas requirements. Product details are summarized in Table 4.

One goal of the program is trying to minimize as well as quantify the potential outgas contamination of the reflective concentrators due to the adhesives used within the assembly. DSS has identified titanium spot welding as a method to assemble the FACT Reflector Assembly and minimize outgassing by removing adhesive sources.

Table 4: CV-2680-12 product details

Property	Average Result
Lap Shear	250 psi
Cure System	Platinum
Appearance	Translucent
Application Life	7 hours
CTE	465 ppm/°C
Cure	4 hours at 65° C
Elongation	400%
Tear Strength	115 ppi
Tensile Strength	1450 psi

Titanium weld development

Titanium welds are advantageous for the Transformational Solar Array. Titanium welds reduce the quantity of adhesives used in the construction of the reflector assembly, which has the advantage of reducing outgassing and potential contamination of the reflectors on orbit. Implementation of welding may speed the manufacturing process by eliminating adhesive mixing, and adhesive cure time. In addition, welds provide the potential for automation. The reflector assembly with titanium spot weld locations identified is shown in Figure 11.

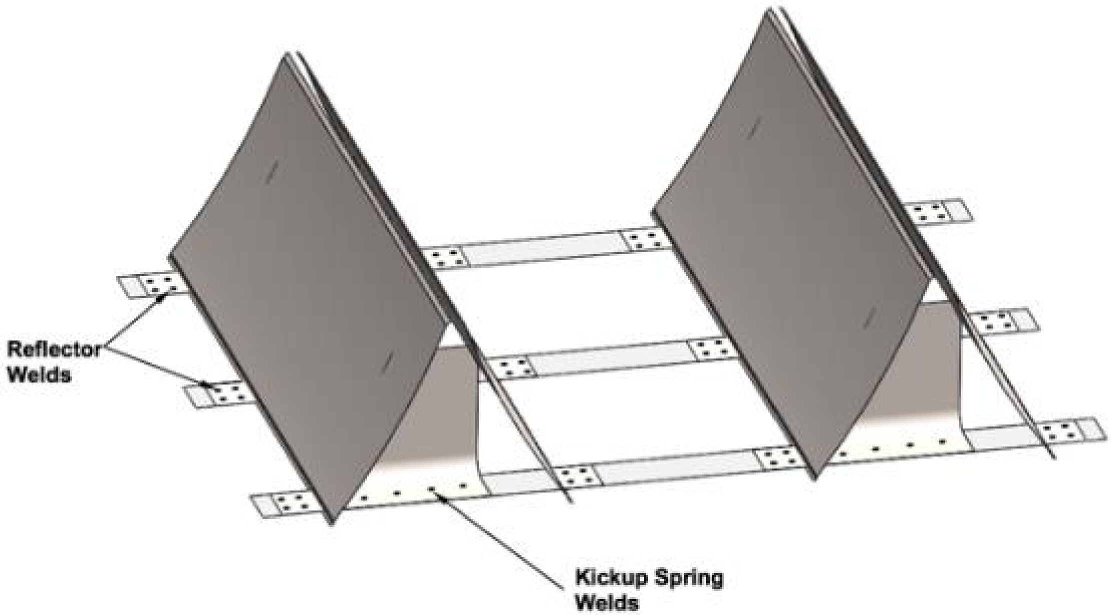

Figure 11: Titanium Welds within the Reflector Assembly

DSS initiated a program to produce a number of welded titanium coupons and perform pull testing on the coupons to determine if welding of the titanium elements within the FACT Reflector Assembly is a viable option for assembly. DSS used a Miyachi welder within the DSS robotic station to develop a weld schedule producing consistent, strong, welds. The welder is shown in Figure 12. A typical weld coupon is shown in Figure 13. Five coupons with a single spot weld were produced. Three coupons with two adjacent spot welds were fabricated. Pull testing of each coupon was performed to determine the ultimate strength of the welded assembly. The pull test configuration is shown in Figure 14.

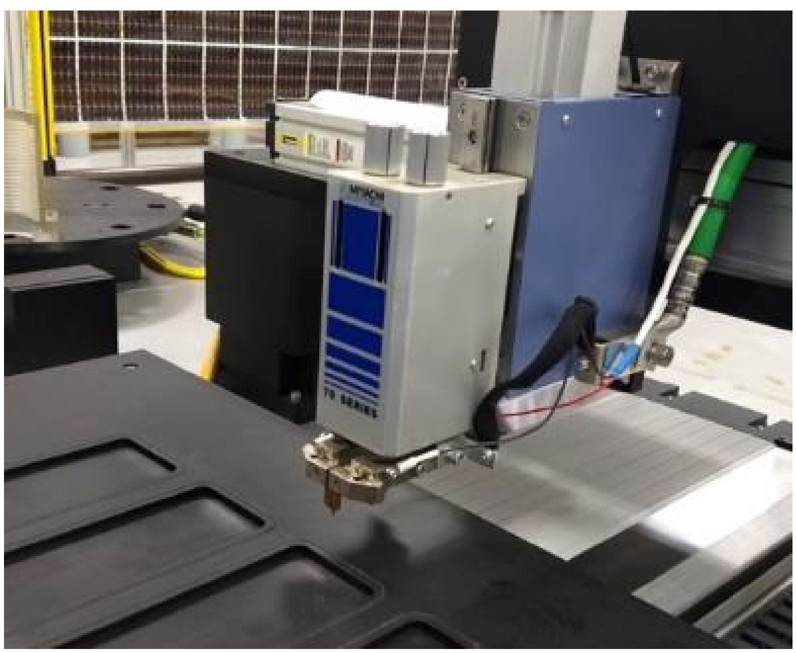
Figure 12: Miyachi 70 series welder

Figure 13: Titanium Spot Weld Coupon

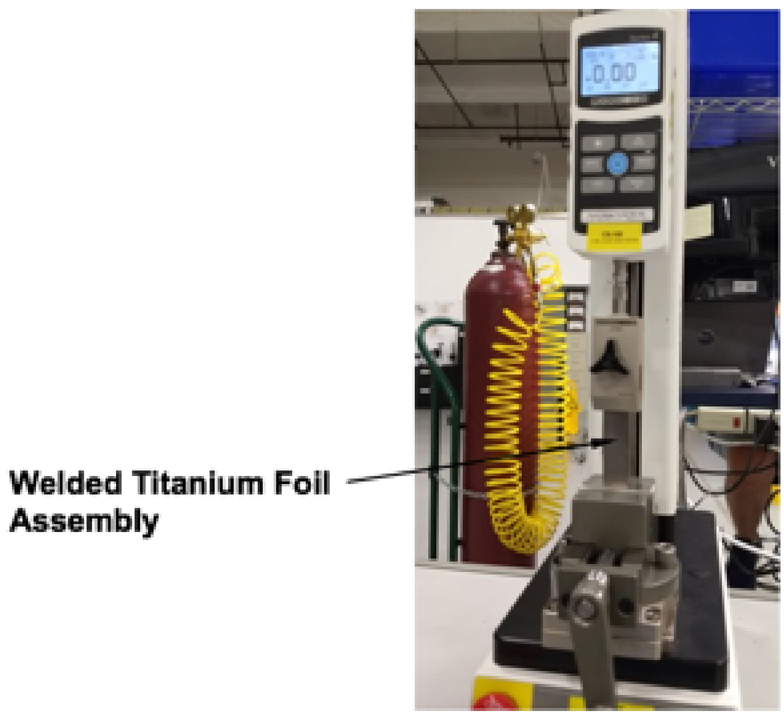

Figure 14: Pull Testing of a Welded Assembly

Welding of the 0.05 mm thick titanium foil strips produced consistent, strong welds as shown in Table 5 below.

Table 5: Measured Shear Load Capability of Welds

Number of Welds in Coupon	Measured Shear Load Capability (lb)
1	16.50
1	16.20
1	16.10
1	16.10
1	16.45
2	23.95
2	26.50
2	24.80

Completion of the weld development program demonstrated titanium welds are a potential fastening method for the titanium elements within the reflector assembly. Subsequent thermal cycle testing of welded titanium foil coupons also yielded positive results.

Thermal Cycle Coupon - Fabrication

DSS fabricated thermal cycle coupons to evaluate: 1) reflector coating adhesion and degradation; 2) adhesives and PSAs used to bond the solar cells to the Kapton substrate with the FACT reflector assembly; 3) the strength of titanium spot welds as a potential attachment method within the FACT reflector assembly. The thermal cycle coupons are discussed below.

Reflector Coating Coupons

Three 76mm by 76 mm titanium foil coupons with reflective coating were selected for repeated thermal cycle exposure. Tape peel adhesion tests were performed on each foil coupon prior to thermal exposure to demonstrate proper adhesion of the coating at ambient temperature. No material removal was observed during the ambient peel testing indicating proper coating adhesion. The foil coupons were then spot bonded to tensioned segment of fiberglass mesh which is identical to the fiberglass mesh backplane within the DSS ROSA array. A reflector coupon secured to the mesh back plane is shown in Figure 15. DSS selected a typical GEO thermal cycle temperature profile (-165°C to +125°C) because it provides the worst case thermal exposure temperature range that a solar array experiences on orbit.

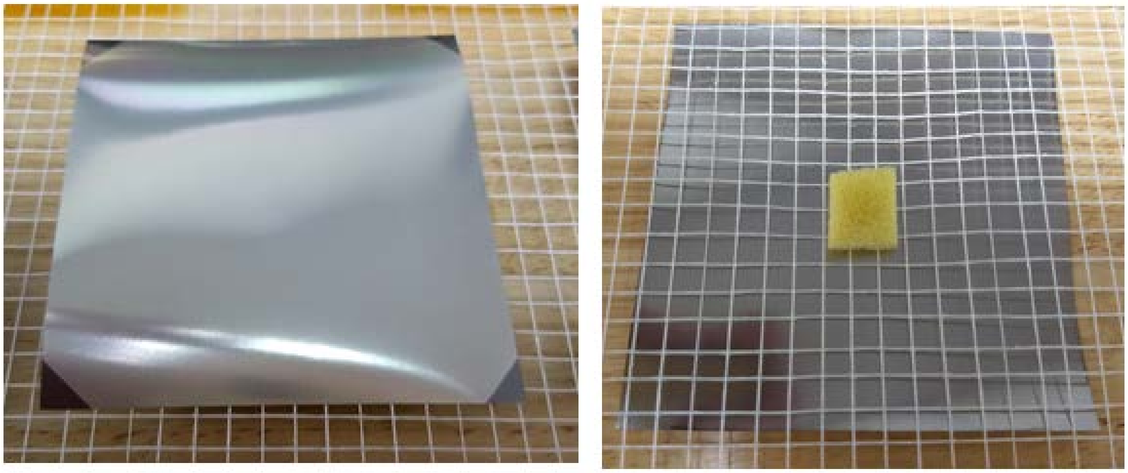

Figure 15: Reflector Thermal Cycle Coupon

Bonded Solar Cell Coupons

Four bonded solar cell coupons were fabricated to undergo thermal cycle testing. The bonded solar cell coupons evaluated the following adhesives: CV 10-2568, CV4-1161-5 PSA, 3M 966 PSA (one layer) and 3M 966 PSA (2 layers). The bonded solar cell coupons were manufactured using the bonded assemblies described in detail within the Cell Bonding Development portion of this report. The Kapton film was cut to a rectangular shape of 82 mm x 108 mm which extended beyond the edges of the bonded solar cell. A summary of the thermal cycle solar cell coupons is shown in Table 6. Each solar cell coupon was spot-bonded to a tensioned segment of fiberglass mesh. The CV10-2568 bonding coupon is shown in Figure 16. Similarly, the CV4-1161-5 PSA bonded cell coupon and the 3M 966 PSA (one layer) coupon are shown in Figures 17 and 18 respectively.

Table 6: Thermal Cycle Bonded Solar Cell Summary

Coupon No.	Cell Type	Substrate	Adhesive	Adhesive Type	Thermal Cycle Temp Range	Attachment to Mesh Backplane
1	SolAero ZTJ	Kapton	CV10-2568	Silcone -Platinum Cure	-165°C to +125°C	Center Spot Bond
2	SolAero ZTJ	Kapton	CV4-1161-5	PSA	-165°C to +125°C	Center Spot Bond
3	SolAero ZTJ	Kapton	966 (one layer)	PSA	-165°C to +125°C	Center Spot Bond
4	SolAero ZTJ	Kapton	966 (two Layers)	PSA	-165°C to +125°C	Center Spot Bond

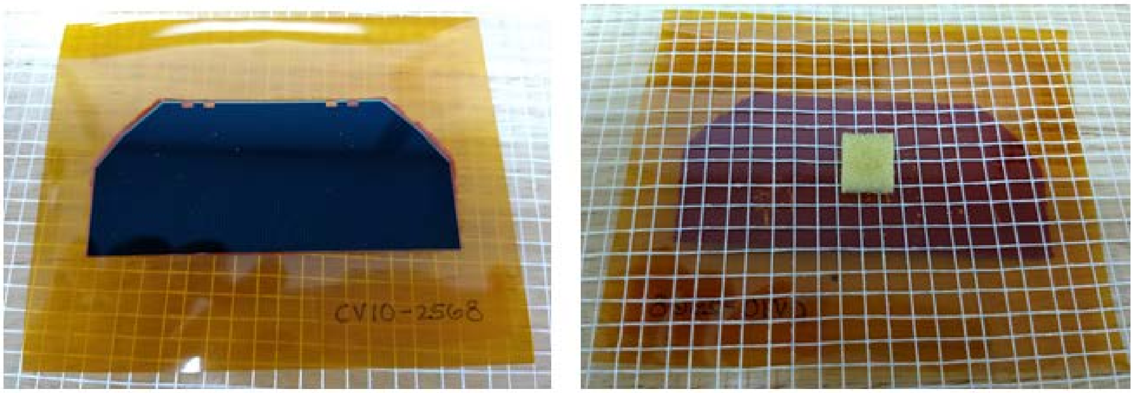

Figure 16: Thermal Cycle Coupon (CV10-2568)

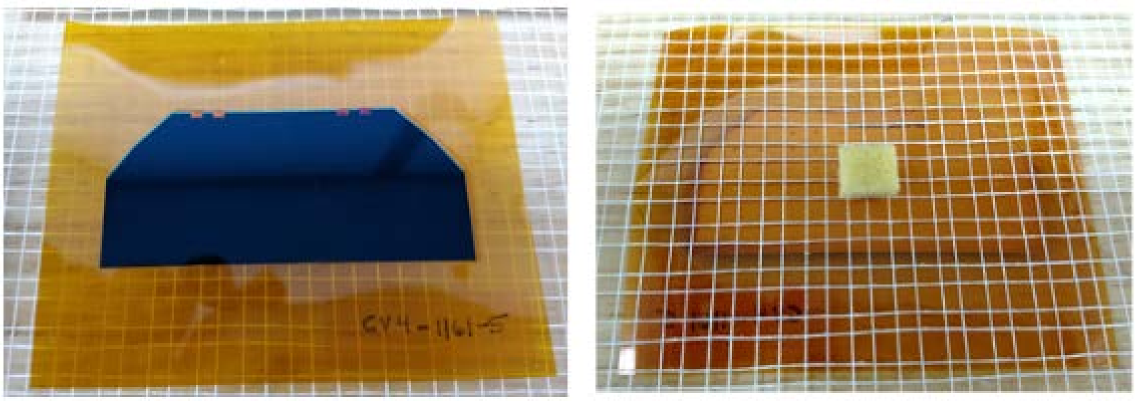

Figure 17: Thermal Cycle Coupon (CV4-1161-5)

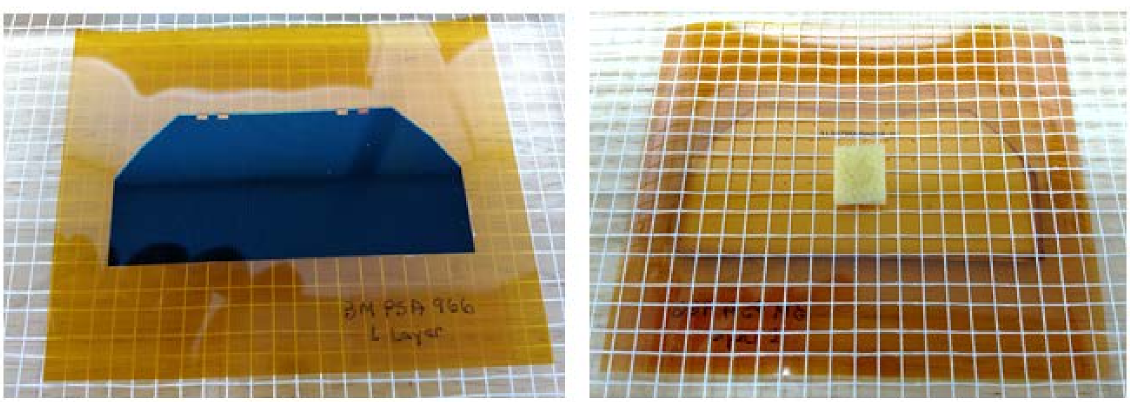

Figure 18: Thermal Cycle Coupon (3M 966 PSA – 1 Layer)

Titanium Weld Coupons

To demonstrate the resilience of the welded attachment when subjected to thermal cycling, DSS fabricated titanium foil weld samples with one, two and four spot welds at the attachment site. The titanium weld coupons are shown in Figure 19. Prior to attachment to the mesh backplane, the welded titanium coupons were wrapped on a typical ROSA array mandrel repeatedly to demonstrate their bending and strain capability. Like the coated reflector and bonded solar cell coupons, the titanium weld coupons were secured to the mesh backplane using a single spot bond.

Figure 19: Titanium Weld Thermal Cycle Coupons

Thermal Cycle Coupon – Testing

The coated reflector, bonded solar cell and welded titanium coupons we secured to a fiberglass mesh backplane and tensioned within an aluminum frame. The front and back side of the thermal cycle coupon assembly is shown in Figures 20 and Figure 21 respectively. The thermal cycle coupon assembly was inserted into the DSS thermal shock chamber that repeatedly moves the coupons between hot and cold regions of the chamber. The thermal shock chamber was set to cycle the samples between -165 °C and +125 °C, typical GEO thermal cycle temperatures. The thermal cycle coupon assembly within the thermal chamber is shown in Figure 22. A number of coupons from different programs were also inserted into the chamber for thermal cycle testing to maximize data collection and reduce the overall program cost. A total of 210 thermal cycles were performed on the thermal cycle coupon. Cell de-bonds, reflector coating degradation and other coupon damage typically occurs very early in the thermal cycle process. The number of thermal cycles performed extended well beyond that period. LN2 costs and competing programs limited the number of thermal cycles within the chamber.

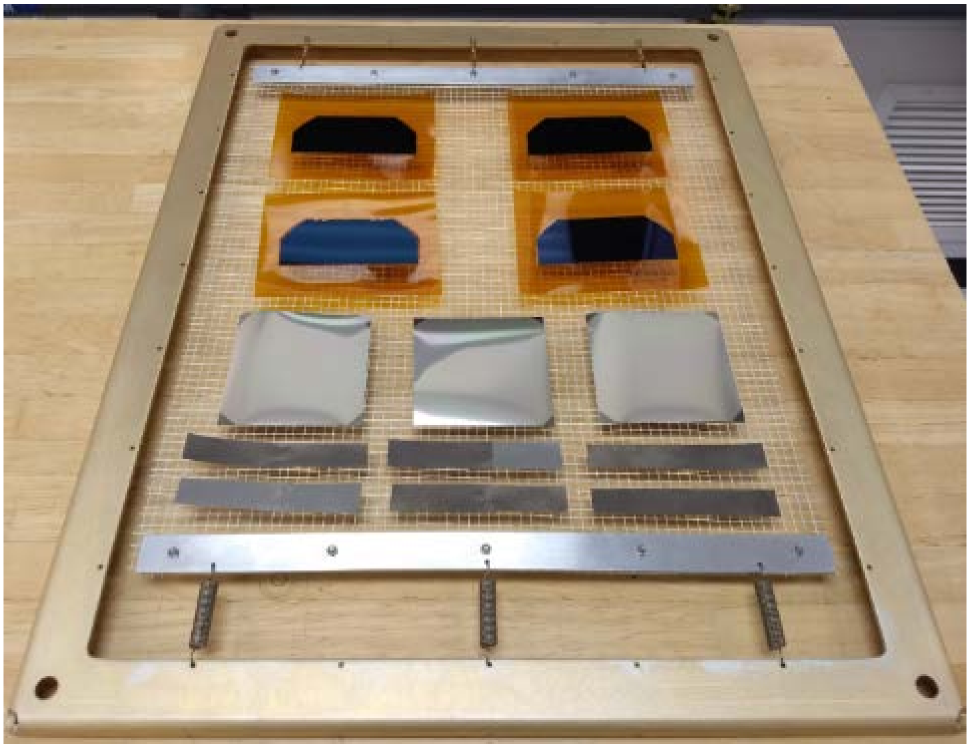

Figure 20: Thermal Cycle Coupon Assembly (Front Side)

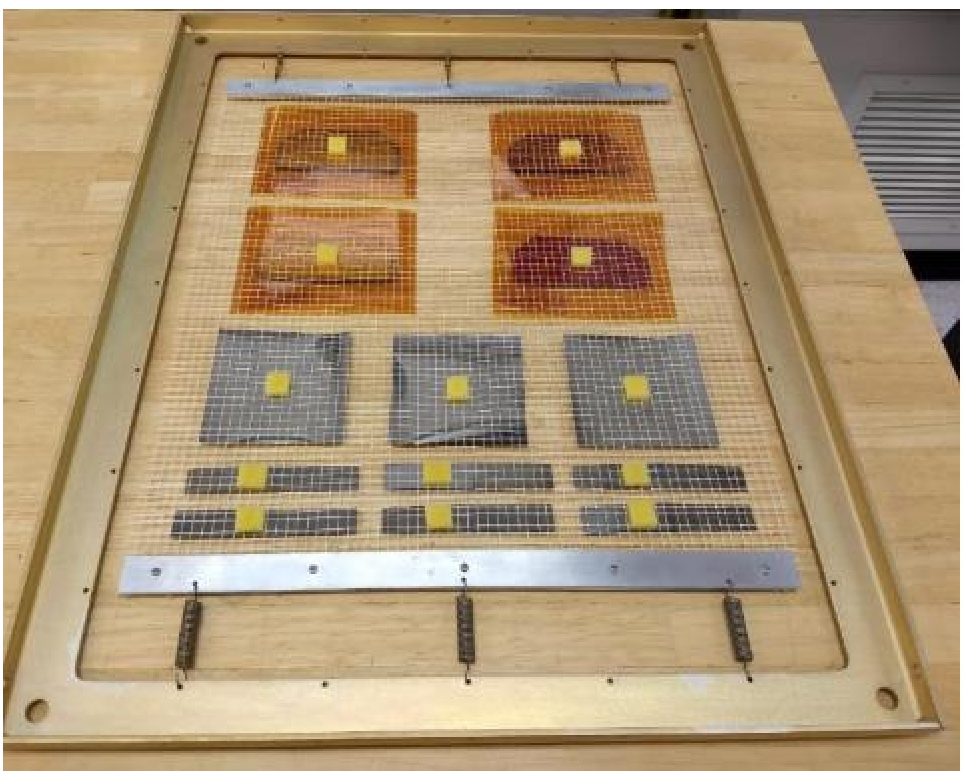

Figure 21: Thermal Cycle Coupon Assembly (Back Side)

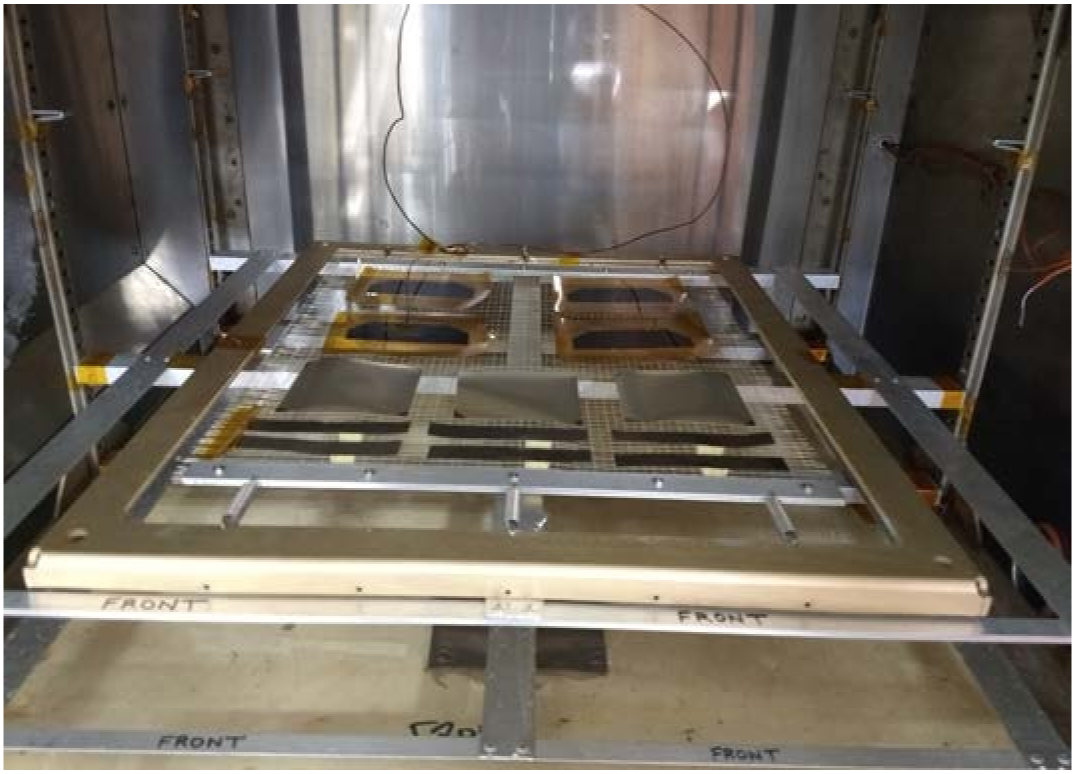

Figure 22: Thermal Cycle Coupon Assembly (Inside Thermal Chamber)

Post Thermal Cycle Test Results

Reflector Coating Adhesion

The individual coated titanium reflector coupons were visually inspected under magnification with no visual degradation of the coating observed. Tape peel test were performed on each coupon to demonstrate adhesion of the reflective coating to the base metal. No removal of material (SiO_2 or silver) was observed during the tape peel tests indicating good adhesion of the reflective coating following thermal cycle testing.

Solar Cell Bonds

The bonded solar cell assemblies were visually inspected under magnification. In addition, attempts were made to peel the Kapton from the cell to evaluate the bond strength of the bond. All solar cells remained securely bonded to the Kapton following thermal cycling. Visual inspection of the CV10-2568, CV4-1161-5 and 3M 966 PSA (one layer) assemblies demonstrated no visual degradation of the solar cell bonds. Under magnification, small lines were visible within the 3M 966 (2 layer) bond indicating possible relative movement between the two layers of adhesive. Completion of the thermal cycle testing demonstrate CV10-2568, CV4-1161-5 PSA and 3M 966 PSA (one layer) as viable cell bonding options when subjected to repeat thermal cycling.

Titanium Spot Weld Samples

The spot welded titanium foil samples were visually inspected under magnification to evaluate damage to the welds or observe any local foil buckling between the weld locations. No damage to any of the welds was observed. The welded samples were then repeatedly wrapped on a mandrel to demonstrate their bending behavior with no degradation observed. Finally, manual pull tests were performed on the samples with no failure observed. Completion of the thermal cycle test demonstrated spot welding of titanium foil as a viable fabrication option for the FACT reflector assembly when subjected to repeat thermal cycling.

Magnetically clean brake

As part of the Transformational Array Program, DSS was tasked to develop and design a magnetically clean brake. This was done even though not required by the contract between Glenn and APL because the contractual requirement is clearly for an array for a scientific spacecraft. It is likely that such a spacecraft will be measuring fields and particles. This will clearly require magnetically clean solar array. The DSS ROSA array typically uses redundant eddy-current dampers within the mandrel assembly to control the rate of array deployment. Eddy current dampers are basically shunted motors and therefore have internal magnets.
DSS has evaluated both friction and continuous rotary viscous dampers as magnetically clean options to limit the rate of deployment of the ROSA array. Due to the relatively slow rate of deployment, DSS determined that the continuous rotary is a good baseline for a magnetically clean brake. Continuous rotary viscous dampers are commercially available and have been used in the past to control the rate of deployment of ROSA solar arrays under ambient conditions. Figure 24 is a photograph of the commercial viscous damper. The disassembled unit is shown in Figure 25. The damper consists of mating concentric thin-walled cylinders that shear the viscous fluid during rotation. The DSS rotational damper development path is shown below

DSS Rotational Damper Development Path:

- Determine the dimensional tolerances of the commercial damper components.
- Determine damper performance equations based on damper geometry, tolerances and fluid viscosity.
- Identify the high-viscosity flight-rated damper fluid.
- Re-engineer commercial damper using flight-approved materials and incorporate a polyimide heater.
- Determine the performance characteristics of the updated damper design and estimate the deployment times for typical ROSA solar arrays

Figure 23: Commercial viscous damper

Figure 24: Internal damper components

DSS derived the equations related to the performance of the rotational damper. The performance of the rotational damper is a function of the size and number of concentric thin-walled cylinders within the assembly, the tolerances between the static and moving components, and the viscosity and temperature characteristics of the viscous fluid. Using SolidWorks, DSS designed a rotary viscous damper based on the commercial version. Plastic components were replaced with flight qualified metal components with appropriate finishes. A silicone viscous fluid with high vacuum capability and a typical operational range of -40°C to +200°C was identified as the fluid for the re-designed damper. A circular polyimide foil heater that is bonded to the damper housing and maintains the damper temperature during operation was also selected. Using the derived damper performance equations, the viscosity of the identified flight-rate fluid and the configuration of the damper, DSS determined the deployment rates of typical ROSA arrays. The designed viscous damper yielded similar performance to the eddy-current dampers producing array deployment times between 2 and 3.5 minutes for DSS large ROSA array systems.

Hardware Deliverables

6" FACT Assemblies - Summary

DSS fabricated a number of single-cell and multi-cell coupons (solar cells bonded to Kapton using various adhesives) during the program to support APL outgassing testing. The program final deliverables are two functional 6" FACT coupons. The first coupon was secured to a tensioned mesh segment within an aluminum frame. The coupon configuration is shown in Figure 25. After delivery, the 6" functional coupon is to be used by APL for electrical performance testing and thermal cycle environmental testing. The second coupon was assembled and integrated into 25-ft-long vibration blanket assembly. The vibration blanket was wrapped on an aluminum mandrel and shipped to APL to complete vibration testing. The fabrication and integration of the 6" x 6" (150mm x 150 mm) FACT assemblies is provided in the sections below.

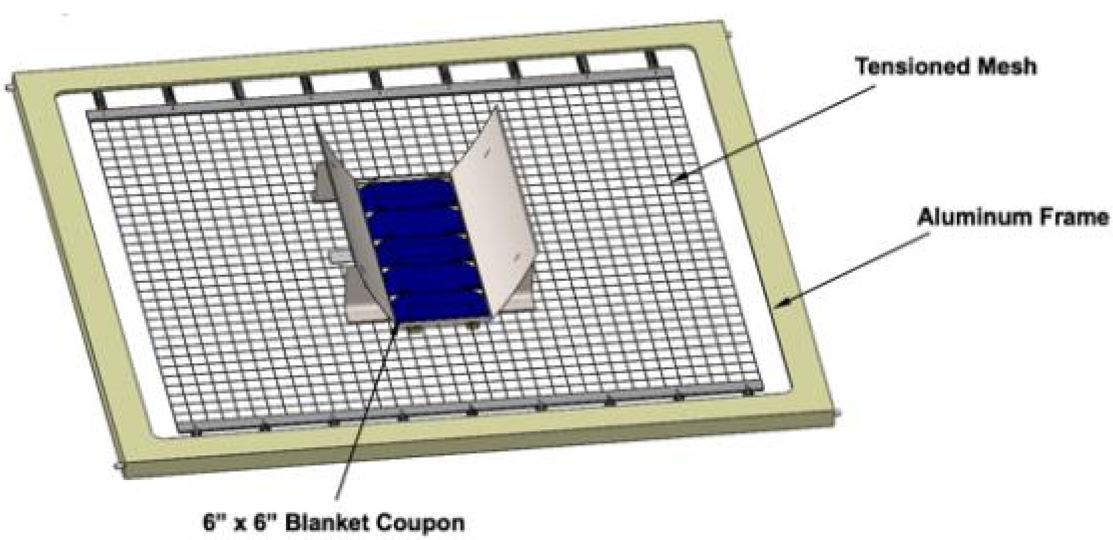

Figure 25: 150 mm by 150 mm FACT Coupon Configuration

FACT Assembly Coupon - Fabrication

DSS received four IMM4 5-cell strings from SolAero for integration into the FACT coupons. I-V performance data was provided by SolAero for the cells in each string. A 5-cell IMM4 string is shown in Figure 26. The IMM4 solar cell strings incorporate Nusil SCV2-2590 Ultra Low Outgassing (ULO) coverglass adhesive. Outgassing testing of this cell/coverglass adhesive combination has been performed by APL. DSS bonded one 5-cell IMM4 string to Kapton film using Nusil CV10-2568. This string was incorporated into the FACT coupon targeted for performance and environmental testing at APL. The second FACT coupon was bonded to Kapton film using 3M 966 PSA. This coupon is to be installed into the vibration blanket assembly. The FACT reflector assembly construction is shown in Figure 27. The reflectors were cut from 0.051 mm titanium stock. A bending operation using a sheet metal brake completed the reflector assemblies. The reflectors were shipped to Buellton Advanced Materials to apply the Silver/SiO_2 reflective coating. Access to the coating chamber drove the delivery schedule of the 6" FACT assemblies to APL. The kick up springs were manufactured using 0.076 mm stainless steel foil. A completed FACT assembly is shown in Figure 28. Integration of the FACT assemblies onto the tensioned mesh segment within the aluminum frame and within the vibration blanket is described in the section below.

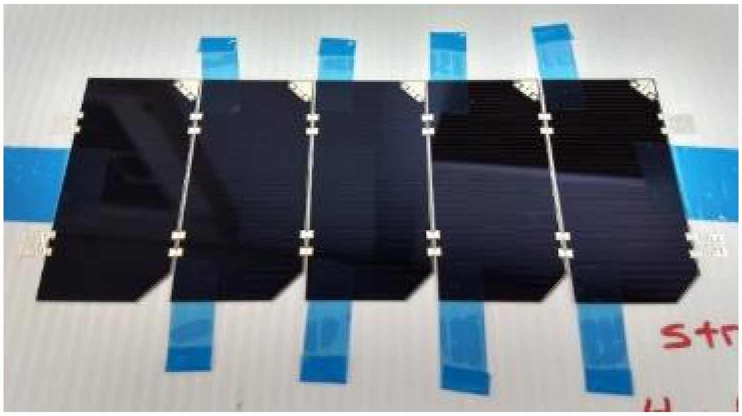

Figure 26: SolAero 5-cell IMM4 String

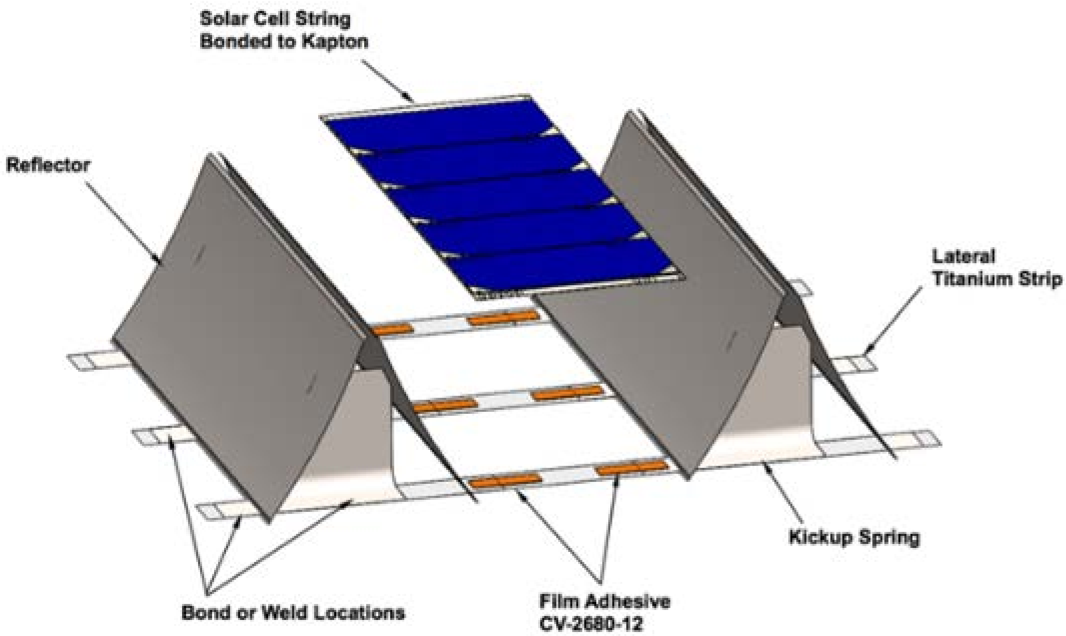

Figure 27: FACT Assembly Construction

FACT Assembly Coupon - Integration

DSS installed one of the 6” FACT coupons onto a mesh backplane tensioned within an aluminum frame. The coupon was spot-bonded to the mesh and strips of polyimide foam were bonded to the back surface to complete the assembly. The completed FACT coupon secured to the mesh is shown in Figure 28. The second 6” FACT coupon was bonded to the mesh backplane of a 25-foot-long vibration blanket. The stowed vibration blanket and mandrel are shown in Figure 29. The majority of the vibration blanket is populated with aluminum mass simulators. The coupon was installed on the end near the mandrel which is the worst loading condition during launch. The mounting location of the FACT coupon within the mandrel assembly is shown in the right side Figure 30 where FACT is set up for electrical test. After coupon installation, the vibration blanket was wrapped neatly on the mandrel. Both the environment test coupon and the vibration coupon within the blanket were packaged for shipment. The two coupons were then shipped to APL to complete further testing: performance, thermal evaluation, vibration testing.

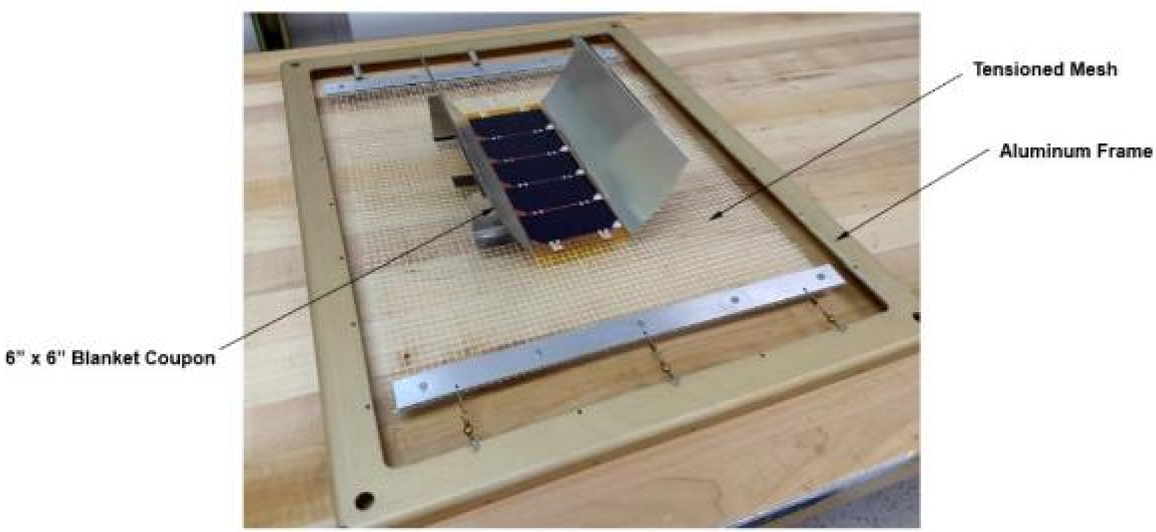

Figure 28: Completed 6” Blanket Coupon Assembly

Figure 29: Stowed Vibration Blanket and Mandrel Assembly

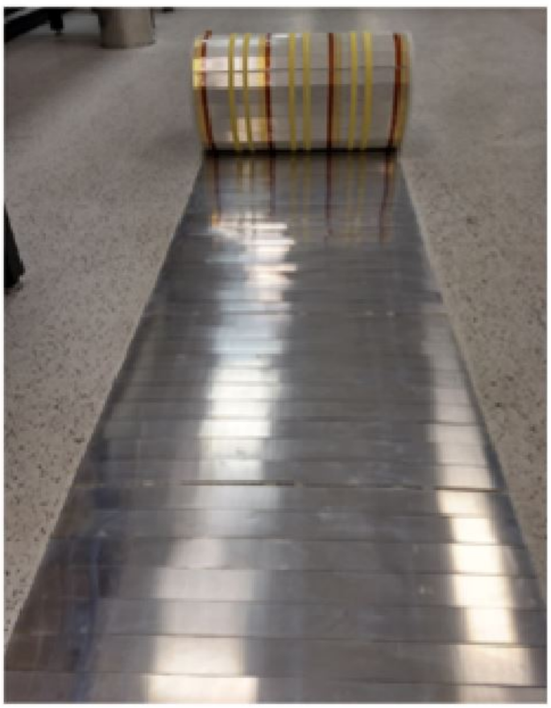

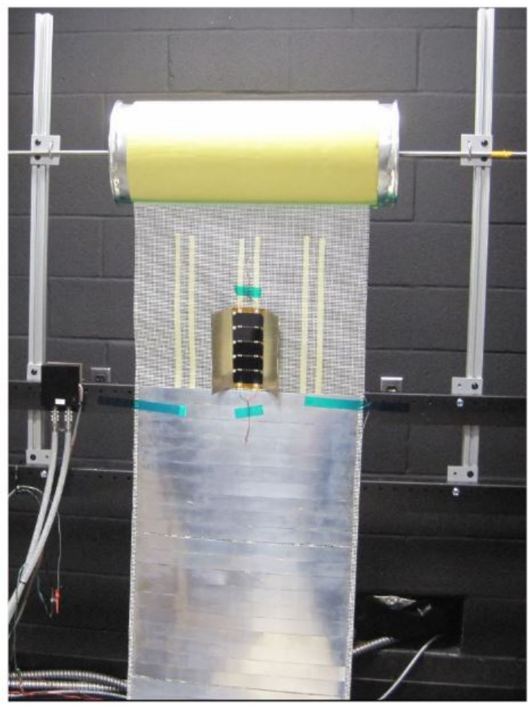

Figure 30: Vibration Blanket on left. FACT on the blanket at set-up for electrical test. The blue tape is GSE.

Analyses

System Level Mass/Power Analyses - Introduction

During the base phase of the program DSS performed system level mass/power analyses for ROSA solar arrays ranging in size from 10 to 35 kW. During the Phase 1 Transformational program, DSS was tasked to update the base phase analyses targeting a 25 kW solar array. In addition, DSS was tasked with updating the base phase analysis that demonstrated 600V and xenon plasma operation. The following analyses were updated and are described below:

Mass properties, power density, packaging density, 300 V operation and xenon plasma operation. The array performance goals for the program are:

- Cell Efficiency: Over 47% BOL cell efficiency at 5 AU and -125°C
- Power density: 50 W m^{-2} EOL at -125°C and 4.15E15 1 MeV e cm^{-2}
- Packaging density: 8 W kg^{-1} at EOL including structure, deployment and pointing mechanism
- Array output higher than 300V
- An ability to operate in a plasma generated by xenon thrusters, typically 1Ecm^{-3} ions with an average energy of 2eV

Due to limited program funds and contractual requirements, bi-prop thrusters were not considered in Option I.

System Mass – 25kW Array

A system level mass analysis was performed for a ROSA 25kW Array populated with IMM FACT concentrator modules. All array subassemblies were included in the analysis (FACT IMM Assemblies, mesh backplane back plane terminator strips, slit booms, mandrel assembly with rate control system, boom deployment/synchronization assembly, blanket tensioning assembly, yoke panel structure/root structure, launch tie-down assemblies, blocking diodes and diode boards and electrical harness assemblies) Measured mass values were used for the IMM FACT concentrator modules as well as relevant subsystems within other DSS large array systems. The estimated wing mass for the 25kW BOL class wing is 113.7 kg.

SolAero IMM Cell Data

For the base program phase, SolAero provided IMM cell performance data and temperature coefficients. The IMM cell data is shown in Figure 31. This cell performance data was used during the Base Phase program to estimate system level BOL array performance for the 25kW array system. For EOL array performance, IMM cell performance data measured by SolAero (5AU, -125C, 4e15 1 MeV electrons) was used. EOL array performance and EOL array specific power are described in the sections below.

BOL Performance

Typical Electrical Output Parameters @AM0 (135.3 mW/cm^2) 28°C	
BOL Efficiency	32.0%
Voc (V)	4.78
Jsc (mA/cm^2)	10.66
Vmp (V)	4.28
Jmp (mA/cm^2)	10.12

EOL Remaining Factors - 1-MeV electrons

No post-radiation annealing

Fluence (e/cm^2)	Voc	Jsc	Vmp	Jmp	Pmp
5E14	0.914	0.987	0.915	0.981	0.898
1E15	0.892	0.966	0.882	0.967	0.853
5E15	0.830	0.870	0.835	0.835	0.697

Annealed to ECSS-E-ST-20-08C Rev.1 post-radiation annealing regiment

fluence (e/cm^2)	Voc	Jsc	Vmp	Jmp	Pmp
5E14	0.923	0.987	0.927	0.982	0.910
1E15	0.900	0.966	0.89	0.977	0.870
5E15	0.841	0.874	0.84	0.848	0.712

Temperature Coefficients

Fluence (e/cm^2)	Voc (mV/°C)	Jsc (μA/cm^2/°C)	Vmp (mV/°C)	Jmp (μA/cm2/°C)
BOL	-9	9.8	-9.3	6.7
5E14	-9.6	9.9	-10.2	5.2
1E15	-9.8	9.7	-10.2	3.3
5E15	-10.7	9	-9.9	7.6

Figure 31: SolAero IMM Cell Performance Data

FACT SPM Performance, 1AU, 28 °C

The FACT reflective concentrator Standard Power Module (SPM) used in the analysis consists of three 10-cell IMM strings with adjacent titanium reflectors that concentrate light onto the solar cell strings. DSS performed a full solar array power analysis to determine the BOL string performance at the SADA/spacecraft connector. The analysis included the following loss factors: LAPSS calibration to AM0, CIC assembly voltage loss, CIC current loss, UV degradation, micro-meteoroid and debris, contamination, cell stringing mismatch, blocking diode voltage drop, wing harness voltage drop. The estimated power output of the FACT SPM at the spacecraft connector is 67.54 W.

FACT SPM Performance, 5AU, -125 °C, Fluence=5E15 e/cm^2

SolAero measured cell performance data for the IMM4 POR cell (cell: 234161-07B, 5AU, -125°C). This was used by DSS to calculate the FACT SPM performance at reduced light intensity and temperature. In addition, the EOL/BOL cell power reduction of 81.6% measured by SolAero was used in the FACT SPM performance estimate. The FACT concentrator power scaling factor of 1.9998866 (Cell Saver test data, 2005 IEEE paper) was also used in the SPM power performance estimate. Combining the measured SolAero cell test data and the measured power scaling factor for a SiO_2 coated 2X concentrator, DSS calculated the FACT SPM performance when the array is operating at 5AU and -125°C and subjected to a fluence of 4E15 e/cm^2. The estimated power output of a single FACT SPM at -125 °C, 5AU, 4E15 e/cm^2 is 2.627 W.

Solar Array Blanket Size (25 kW Array at 1 AU)

The FACT SPM performance at 1 AU was calculated to be 67.54 W, as described above. To meet the desired array power level, 374 FACT SPM modules are required. The SPMs on the solar array blanket for the 25kW array are arranged in 7 columns and 54 rows producing a blanket of length and width of 21.53 meters and 3.32 meters respectively. The array power for this system is estimated to be 25.26 kW.

Wing Specific Power (EOL, 5AU, -125°C, 5E15 e/cm^2)

The wing specific power under LIRT conditions is estimated to be 8.63 W/kg per the table below.

Table 7: Wing Specific Power (EOL, 5AU, -125°C, 4e15 e/cm^2)

Array Power, 28C, 1AU (kW)	Solar Array Wing Power, LILT (W)	Array Mass (kg)	Specific Power , LIRT (W/kg)
25.26	982.49	113.7	8.63

Wing Stowed Power Density

Given the estimated mass of the solar array and the stowed cylindrical volume of the array, the stowed power density of the system was estimated to be 50.87 kW/m^3 per Table 8 below.

Table 8: Stowed Power Density of 25 kW Solar Array System

Array Wing Size (kW)	Array Mass (kg)	Array Wing Power (kW)	Array Width (in)	Stowed Diameter (in)	Stowed Volume (in^3)	Stowed Volume (m^3)	Stowed Power Density (kW/m^3)
25	113.7	25.26	164.8	15.30	30299.1	0.497	50.87

300 V, Xenon Plasma Capability

In a past NASA Phase 2 SBIR (Contract No. NNX12CA22C), DSS produced a FACT concentrator high-voltage coupon to demonstrate operation of the FACT technology at a minimum of 300 V in a plasma environment. The coupon consisted of a 4-cell ZTJ string with two adjacent uncoated stainless steel reflectors, an anodized aluminum radiator and stainless steel springs. The solar cell string was fully grouted using a DSS proprietary process. The assembly was mounted on a fiberglass tensioned backplane. The high voltage coupon is shown in Figure 32. The integrity of the coupon's grouting was verified by DSS using an Insulation Wet Test (IWT) at 500 V. High voltage testing of the module was then performed at JPL per the test plan shown in Figure 33.

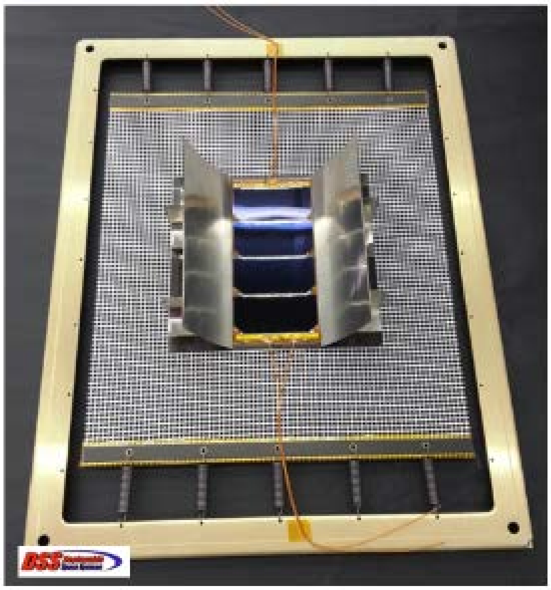

High Voltage FACT Coupon Mounted within Test Frame

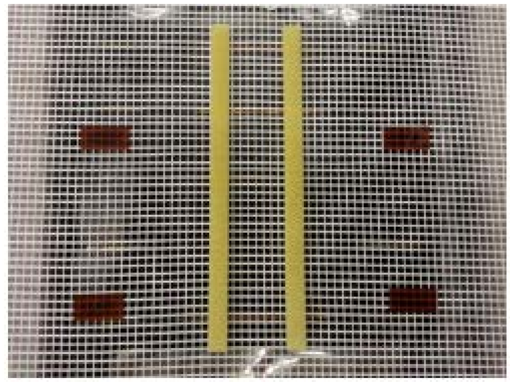

High Voltage FACT Coupon - Rearside

Figure 32: High Voltage FACT Coupon Configuration

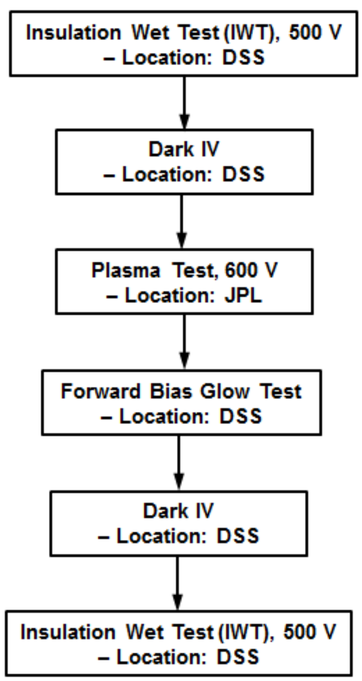

Figure 33: Test plan (high voltage coupon)

The FACT coupon was vacuum baked at 125 °C for 24 hours condition the coupon. The coupon was then inserted into the JPL back of the chamber and subjected to a plasma density of 1.05 x 10^{8} cm^{-3} and electron temperature of 3.3eV. The voltage of the coupon was ramped up in 100 V increments up to 600 V and remained at 600 V for one hour. As shown in Figure 34, the current stayed low at 17µA and dropped to 15µA after 55 min. JPL's assessment of the high voltage FACT coupon is shown below:

"The DSS coupon #11 showed great results in meeting program objectives to demonstrate that solar arrays are capable of performing at desired operational voltage of 300 V in plasma environment. Even at a factor of 2 (600V) of desired operating voltage, the coupon showed minimal current collection during positive bias test. Negative bias test was not performed since the coupon consisted of only one string of cells."

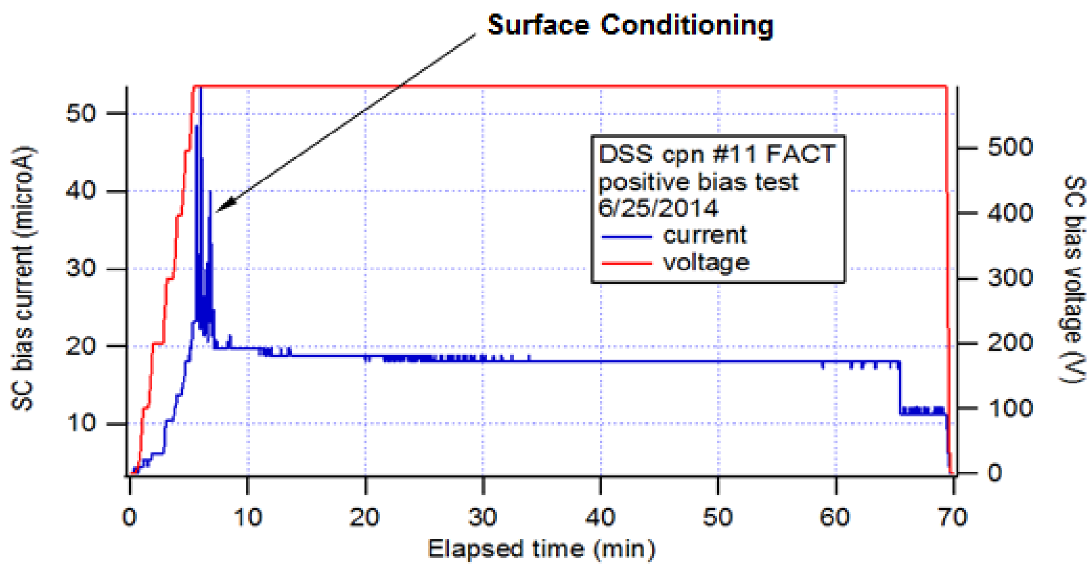

Figure 34: Current Collection of High-Voltage FACT Coupon

Given the positive results from the high-voltage testing, a FACT concentrator array with fully grouted cells is capable of operating at over 300V in a plasma environment. Further testing may be required for a FACT/IMM system to again demonstrate this capability. Cell grouting will likely be required to achieve high-voltage operation.

Program Support / Conclusion

DSS worked directly with APL and SolAero to meet the goals of the Option I Transformational Array program. DSS contributed to program status reports 1 through 3, produced coupons for APL outgas and environmental testing, performed systems level array analysis, developed a magnetically clean brake to control the rate of array deployment and investigated innovative methods to increase the manufacturability of the array and reduce solar array costs.

Technical Progress at SolAero

The IMM solar cell was chosen for the program because of its superior performance under LILT conditions. We present the modeling that was done during Option I for higher performance IMM variants, and also discuss some performance challenges at LILT with the IMM4 device that was chosen.

IMM Cell Down Select

During Option I most of the IMM cells tested were four junctions. As part of Option I, SolAero was to develop a 5 junction cell, with the intent of improving the cell efficiency at LILT conditions. Performance modeling was done for 4, 5, and 6 junction cells at -144 °C to determine the band gap combinations that would provide optimal performance. The best IMM6 cell is better by about 1% absolute efficiency points than the best IMM5 cell, and about 2% absolute efficiency points better than the best IMM4 cell. In terms of ease of manufacture, the IMM4 is likely the easiest device to make due to having fewer junctions. Feedback from NASA-Glenn, midway through Phase 1, resulted in a down selection to the IMM4 cell to use for the remainder of the program.

IMM4 Performance Issues

Seven different variants were fabricated and tested with the aim of improving performance at low temperature. Two of the variants showed positive results in the first evaluation round. Variant 3 as well as a combined Variant 3 and Variant 5 experiment were fabricated and tested to determine if the results were reproducible. An IMM4 baseline was also included, as a control, to ensure that the changes made truly accounted for the performance improvements that were seen. Both 2 x 2 cm^2 and 27.55 cm^2 cells were fabricated and tested under NIRT (Normal Irradiance Room Temperature) and LIRT (Low Intensity Room Temperature). The LIRT testing was done at 4% 1 sun AM0 irradiance. Cells with a fill factor <78% were screened and removed from subsequent testing. Remaining cells were tested at 1 sun AM0. The Isc and FF comparisons for both LIRT and NIRT testing are in Figure 35 and Figure 36. While LILT testing will be the determining factor if the performance issue is resolved on the repeat experiments, the initial test results shown in Figure 35 and in Figure 36 are positive.

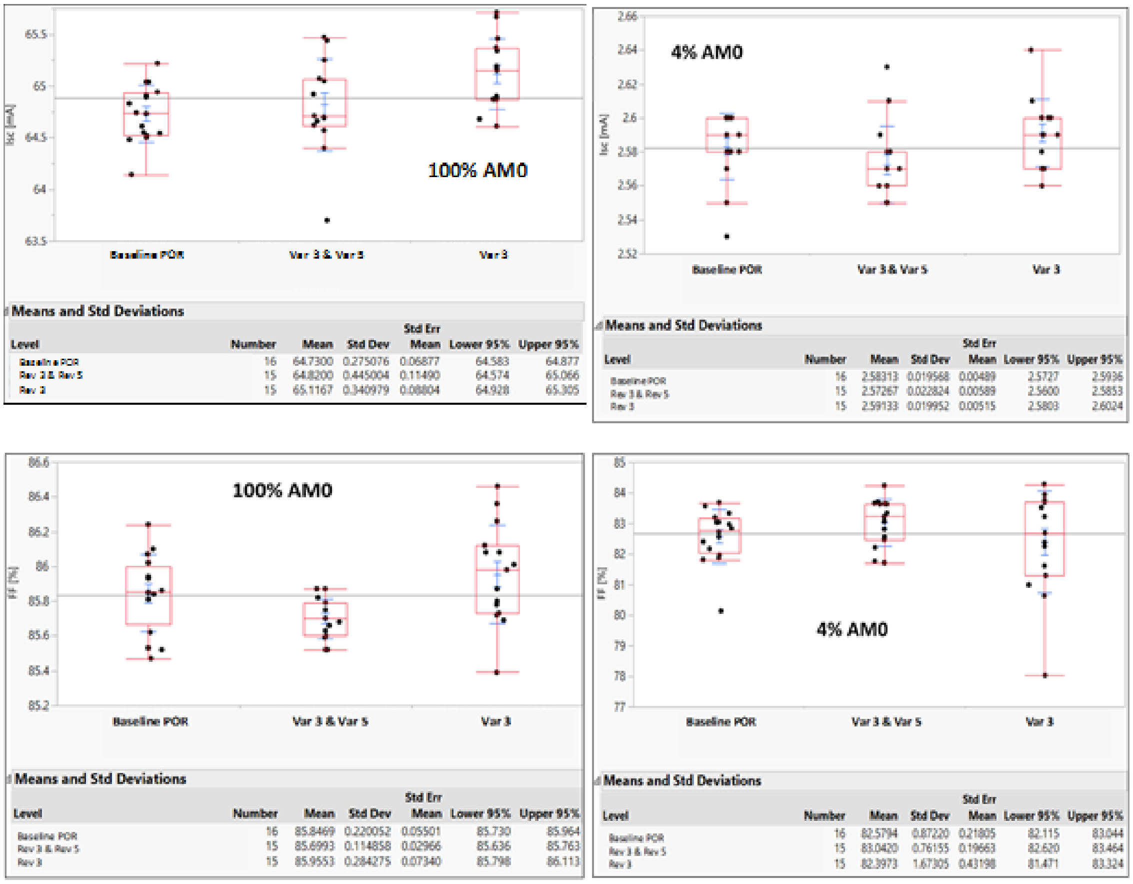

Means and Std Deviations

Level	Number	Mean	Std Dev	Std Err Mean	Lower 95%	Upper 95%
Baseline POR	16	64.7300	0.275076	0.06877	64.583	64.877
Rev 3 & Rev 5	15	64.8200	0.445004	0.11490	64.574	65.066
Rev 3	15	65.1167	0.340979	0.08804	64.928	65.305

Means and Std Deviations

Level	Number	Mean	Std Dev	Std Err Mean	Lower 95%	Upper 95%
Baseline POR	16	2.58313	0.019568	0.00489	2.5727	2.5936
Rev 3 & Rev 5	15	2.57267	0.022824	0.00589	2.5600	2.5853
Rev 3	15	2.59133	0.019952	0.00515	2.5803	2.6024

Means and Std Deviations

Level	Number	Mean	Std Dev	Std Err Mean	Lower 95%	Upper 95%
Baseline POR	16	85.8469	0.220052	0.05501	85.730	85.964
Rev 3 & Rev 5	15	85.6993	0.114858	0.02966	85.636	85.763
Rev 3	15	85.9553	0.284275	0.07340	85.798	86.113

Means and Std Deviations

Level	Number	Mean	Std Dev	Std Err Mean	Lower 95%	Upper 95%
Baseline POR	16	82.5794	0.87220	0.21805	82.115	83.044
Rev 3 & Rev 5	15	83.0420	0.76155	0.19663	82.620	83.464
Rev 3	15	82.3973	1.67305	0.43198	81.471	83.324

Figure 35: Jsc and FF results at NIRT and LIRT for 2 x 2 cm^2 cells for the repeat experiments to resolve the performance issue.

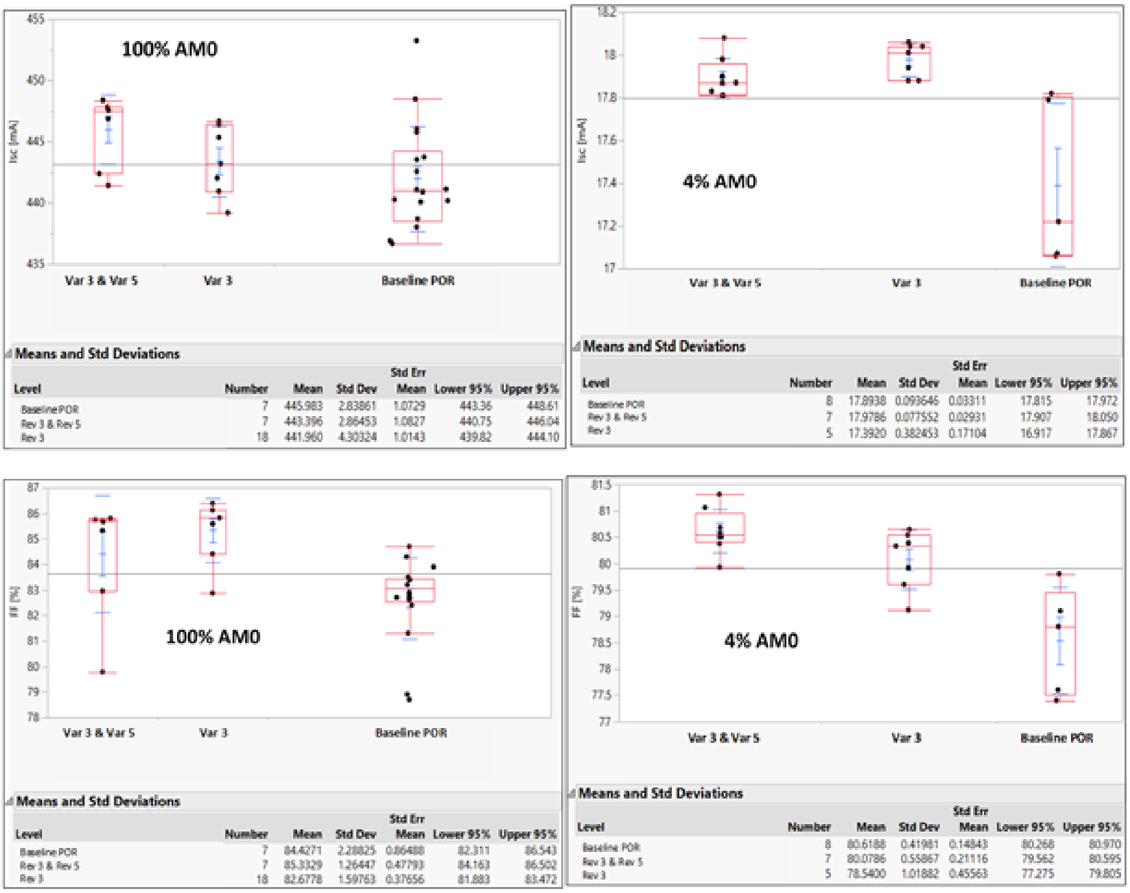

Figure 36: Jsc and FF results at NIRT and LIRT for 27.55 cm^2 cells for repeat experiments. The initial results are positive, with current and FF equal to or greater than the baseline.

Some of the 2 x 2 cm^2 cells from the IMM4 baseline were sent to NIST for irradiation with 1 MeV electrons to a fluence of 4 x 10^{15} e cm^{-2}. Once those cells are returned they will be characterized at room temperature, mounted on LILT test plates along with non-irradiated cells from the same lot, and tested at LILT.

Subsequent to the fabrication of the lots mentioned above, discussions at SolAero raised the possibility of a metal contact (front or back) issue causing the LILT Voc kink. To provide quick feedback on the baseline front metal/standard cap design, and also on the back-metal contact test structures were fabricated. In the front metal/cap layer case the solar cell active junctions were not grown, although the heat load was maintained. The processing of the structure was much quicker, with a back-metal contact included as well as the front metal grid. In the back-metal contact structure case the full cell was grown up to the J4 base, which was undoped, and then the J4 BSF and back contact layer were grown. Selective metal was deposited on the back-contact layer. Both structures were electrically tested while submerged in liquid nitrogen (LN2) to determine if the contacts are ohmic or rectifying at low temperature. The low temperature electrical results revealed linear current-voltage curves, indicative of ohmic contacts. Test probes were submerged in

LN2 to collect a current-voltage curve without contacting a sample to check whether the LN2 was a conductive path. The probes had a very high resistance between the probes when spaced the same distance as the metal pads on the test structures, leading to the conclusion that the front and rear contact are ohmic down to LN2 temperatures (-196^{o}C).

Radiation

Two centimeter by two centimeter IMM4 baseline cells were irradiated with 1 MeV electrons at ambient conditions to a fluence of 4e15 e cm^{-2}. Seven irradiated and non-irradiated cells from the same growth and processing lot were mounted on plates and then tested at LILT (4% sun and -140 °C). The average Pmp for the non-irradiated cells was 5.98 mW for an EOL/BOL of 81.6%, which is quite good for the fluence. It must be kept in mind that while the performance testing was done at LILT, the irradiation was done at ambient temperature and then the samples were tested a number of days later. The best cell performed with an efficiency of 37.2% under LILT conditions of 5AU and -125^{o}C after an irradiation dose of 4e15 1 MeV e-/cm^{2}.

Outgassing Coupons

As part of the outgassing tests to be completed by APL, SolAero made outgassing coupons and strings, six 3x1 coupons using ZTJ CICs, and then four 5x1 (6 inch x 6 inch) strings using IMM4 CICs.

Fabrication of 3x1 ZTJ Coupons

ZTJ CICs with CMG-AR coverglass attached with SCV2-2590 ultra-low outgassing adhesive were interconnected into 3x1 strings, and two of these strings were shipped to DSS for attachment of reflectors, Figure 37. Four of the 3x1 strings were attached to Kapton at SolAero, Figure 38, and then shipped to APL.

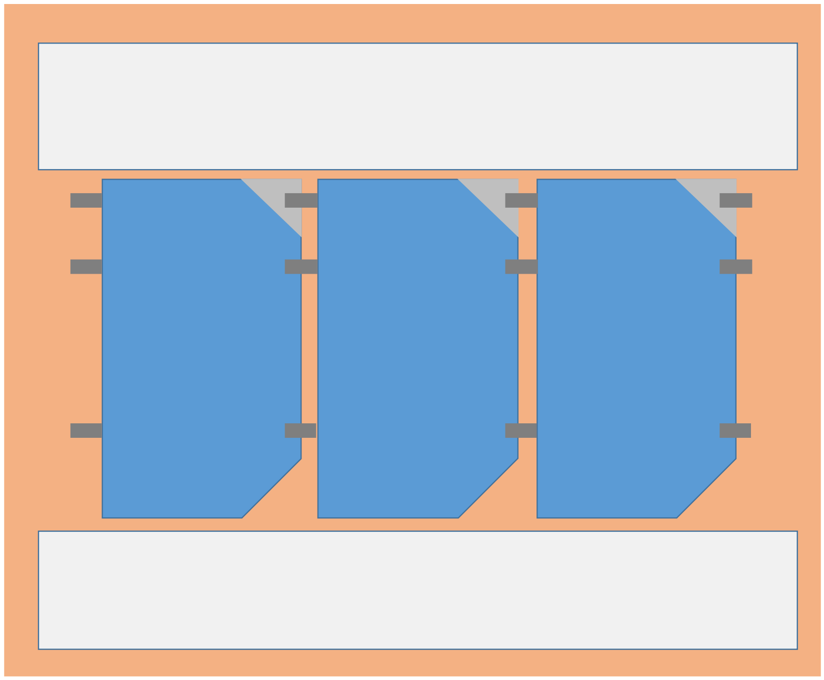

Figure 37: Schematic of the 3x1 ZTJ strings with the location for the DSS attachment of the reflectors.

.

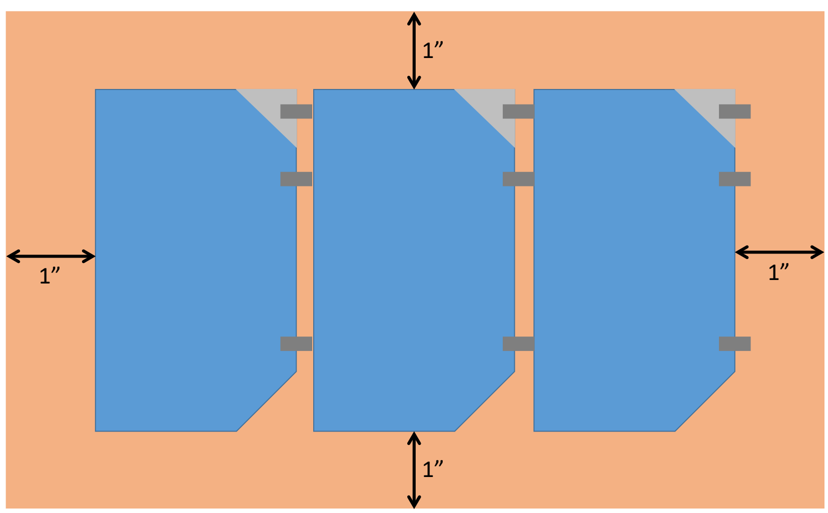

Figure 38: Schematic of the 3x1 ZTJ strings without the reflectors.

Two lots of IMM4 baseline cells were grown and processed for 5x1 (6” x 6”) coupons. The 5x1 strings were assembled, with welded interconnects and bypass diodes, and shipped to DSS for laying down on Kapton and addition of the reflectors.

Fabrication of 5x1 IMM Strings

The four 5x1 (6 inch x 6 inch) IMM4 strings were made using IMM4 CICs with CMG-AR coverglass attached with SCV2-2590 ultra-low outgassing adhesive were interconnected into 5x1 strings. Light IV (LIV) and low intensity, room temperature (LIRT) LIV data for each of the bare cells used in the strings are in Figure 39 and Figure 40. Data for one of the cells is missing for both LIV and LIRT testing, but subsequent string level testing indicated the cell was performing nominally. The layout of the cells (CICs) in the strings are in Figure 41 and Figure 42. The dark IV (DIV) plots for the strings are in Figure 43 and electroluminescense of a completed string is imaged in Figure 44. The DIV measurements ensured functionality of the strings post integration. One sun LIV measurements of the strings were not taken. The strings were sent to DSS for attachment to Kapton and the addition of reflectors.

String 1 LIRT

V_{OC}	J_{SC}	I_{SC}	FF	Efficiency	P_{MAX}	P_{MAX}	J_{MP}	I_{MP}	V_{MP}	Area	P_{IN}	Cal Cell ID
(Volts)	(mA/cm^2)	(mA)	(%)	(%)	(Watts)	(mW/cm^2)	(mA/cm^2)	(mA)	(Volts)	(cm^2)	(W/m^2)	
3.293	16.27	448.45	83.6	32.77	1.234	44.79	15.57	429.04	2.877	27.56	1367	249401-19B
3.272	16.15	445.17	83.7	32.36	1.219	44.24	15.59	429.76	2.837	27.56	1367	249401-21A
3.246	16.29	448.95	82.6	31.95	1.204	43.68	15.62	430.42	2.797	27.56	1367	249401-25B
3.255	16.20	446.52	82.9	32.00	1.206	43.74	15.42	424.92	2.837	27.56	1367	249402-01A
3.291	16.32	449.90	83.3	32.74	1.233	44.76	15.78	434.77	2.837	27.56	1367	249402-01B

String 2 LIRT

V_{OC}	J_{SC}	I_{SC}	FF	Efficiency	P_{MAX}	P_{MAX}	J_{MP}	I_{MP}	V_{MP}	Area	P_{IN}	Cal Cell ID
(Volts)	(mA/cm^2)	(mA)	(%)	(%)	(Watts)	(mW/cm^2)	(mA/cm^2)	(mA)	(Volts)	(cm^2)	(W/m^2)	
3.285	16.29	449.01	83.3	32.63	1.229	44.61	15.72	433.37	2.837	27.56	1367	249401-17B
3.276	16.21	446.87	83.3	32.36	1.219	44.24	15.59	429.73	2.837	27.56	1367	249402-13B
3.239	16.19	446.32	83.0	31.86	1.200	43.55	15.57	429.15	2.797	27.56	1367	249402-07A
3.283	16.25	447.83	83.4	32.53	1.226	44.47	15.56	428.94	2.857	27.56	1367	249402-05B
3.243	16.18	446.03	83.3	31.99	1.205	43.72	15.63	430.86	2.797	27.56	1367	249402-05A

String 3 LIRT

V_{OC}	J_{SC}	I_{SC}	FF	Efficiency	P_{MAX}	P_{MAX}	J_{MP}	I_{MP}	V_{MP}	Area	P_{IN}	Cal Cell ID
(Volts)	(mA/cm^2)	(mA)	(%)	(%)	(Watts)	(mW/cm^2)	(mA/cm^2)	(mA)	(Volts)	(cm^2)	(W/m^2)	
3.260	16.11	444.08	83.5	32.07	1.208	43.84	15.56	428.92	2.817	27.56	1367	249401-09A
3.248	16.10	443.62	83.5	31.94	1.203	43.66	15.39	424.11	2.837	27.56	1367	249401-05A
3.283	16.20	446.36	83.3	32.42	1.221	44.32	15.62	430.55	2.837	27.56	1367	249401-03B
3.254	16.07	442.92	83.5	31.93	1.203	43.65	15.50	427.06	2.817	27.56	1367	249401-03A
NA	NA	NA	NA	NA	NA	NA	NA	NA	NA	27.56	NA	200077-17B

String 4 LIRT

V_{OC}	J_{SC}	I_{SC}	FF	Efficiency	P_{MAX}	P_{MAX}	J_{MP}	I_{MP}	V_{MP}	Area	P_{IN}	Cal Cell ID
(Volts)	(mA/cm^2)	(mA)	(%)	(%)	(Watts)	(mW/cm^2)	(mA/cm^2)	(mA)	(Volts)	(cm^2)	(W/m^2)	
3.279	16.19	446.09	83.5	32.42	1.221	44.32	15.62	430.51	2.837	27.56	1367	249402-17B
3.283	16.17	445.52	83.5	32.40	1.221	44.30	15.61	430.30	2.837	27.56	1367	249401-15B
3.258	16.09	443.40	83.5	32.01	1.206	43.76	15.43	425.13	2.837	27.56	1367	249401-15A
3.251	16.09	443.52	83.6	31.99	1.205	43.73	15.42	424.84	2.837	27.56	1367	249401-13A
3.282	16.19	446.22	83.2	32.35	1.219	44.23	15.70	432.71	2.817	27.56	1367	249401-09B

Figure 39: LIV (one sun) data for the IMM4 bare cells that were integrated into the four 5x1 strings. Data for one of the cells is missing. Otherwise the cells demonstrate excellent 1 sun LIV performance.

String 1 LIRT

V_{OC} (Volts)	J_{SC} (mA/cm^2)	I_{SC} (mA)	FF (%)	Efficiency (%)	P_{MAX} (Watts)	P_{MAX} (mW/cm^2)	J_{MP} (mA/cm^2)	I_{MP} (mA)	V_{MP} (Volts)	Area (cm^2)	P_{IN} (W/m^2)	Cal Cell ID
2.869	0.64	17.62	80.2	26.919	0.041	1.47	0.60	16.52	2.455	27.56	1367	249401-19B
2.844	0.63	17.47	80.7	26.589	0.040	1.45	0.60	16.46	2.435	27.56	1367	249401-21A
2.789	0.64	17.63	78.3	25.559	0.039	1.40	0.60	16.50	2.334	27.56	1367	249401-25B
2.811	0.64	17.59	79.1	25.951	0.039	1.42	0.59	16.33	2.395	27.56	1367	249402-01A
2.866	0.64	17.71	80.2	27.006	0.041	1.48	0.61	16.71	2.435	27.56	1367	249402-01B

String 2 LIRT

V_{OC} (Volts)	J_{SC} (mA/cm^2)	I_{SC} (mA)	FF (%)	Efficiency (%)	P_{MAX} (Watts)	P_{MAX} (mW/cm^2)	J_{MP} (mA/cm^2)	I_{MP} (mA)	V_{MP} (Volts)	Area (cm^2)	P_{IN} (W/m^2)	Cal Cell ID
2.860	0.64	17.61	80.5	26.903	0.041	1.47	0.61	16.79	2.415	27.56	1367	249401-17B
2.834	0.64	17.65	79.0	26.211	0.039	1.43	0.60	16.63	2.375	27.56	1367	249402-13B
2.794	0.64	17.52	78.9	25.648	0.039	1.40	0.60	16.42	2.355	27.56	1367	249402-07A
2.853	0.64	17.70	79.8	26.743	0.040	1.46	0.61	16.69	2.415	27.56	1367	249402-05B
2.802	0.64	17.59	79.6	26.030	0.039	1.42	0.60	16.52	2.375	27.56	1367	249402-05A

String 3 LIRT

V_{OC} (Volts)	J_{SC} (mA/cm^2)	I_{SC} (mA)	FF (%)	Efficiency (%)	P_{MAX} (Watts)	P_{MAX} (mW/cm^2)	J_{MP} (mA/cm^2)	I_{MP} (mA)	V_{MP} (Volts)	Area (cm^2)	P_{IN} (W/m^2)	Cal Cell ID
2.827	0.63	17.48	80.2	26.274	0.040	1.44	0.59	16.40	2.415	27.56	1367	249401-09A
2.811	0.63	17.47	79.9	26.052	0.039	1.42	0.60	16.53	2.375	27.56	1367	249401-05A
2.852	0.64	17.55	80.2	26.626	0.040	1.46	0.60	16.62	2.415	27.56	1367	249401-03B
2.811	0.63	17.45	79.5	25.892	0.039	1.42	0.59	16.29	2.395	27.56	1367	249401-03A
NA	NA	NA	NA	NA	NA	NA	NA	NA	NA	27.56	NA	200077-17B

String 4 LIRT

V_{OC} (Volts)	J_{SC} (mA/cm^2)	I_{SC} (mA)	FF (%)	Efficiency (%)	P_{MAX} (Watts)	P_{MAX} (mW/cm^2)	J_{MP} (mA/cm^2)	I_{MP} (mA)	V_{MP} (Volts)	Area (cm^2)	P_{IN} (W/m^2)	Cal Cell ID
2.847	0.64	17.58	80.3	26.662	0.040	1.46	0.60	16.50	2.435	27.56	1367	249402-17B
2.856	0.63	17.49	80.3	26.629	0.040	1.46	0.61	16.76	2.395	27.56	1367	249401-15B
2.825	0.63	17.40	80.5	26.235	0.040	1.43	0.59	16.37	2.415	27.56	1367	249401-15A
2.818	0.63	17.48	80.1	26.176	0.039	1.43	0.60	16.47	2.395	27.56	1367	249401-13A
2.850	0.64	17.57	80.1	26.638	0.040	1.46	0.60	16.49	2.435	27.56	1367	249401-09B

Figure 40: LIRT data for the IMM4 bare cells that were integrated into the four 5 x 1 strings. Data for one of the cells is missing. Otherwise, all of the cells pass LIRT screening and were suitable for integration into the strings.

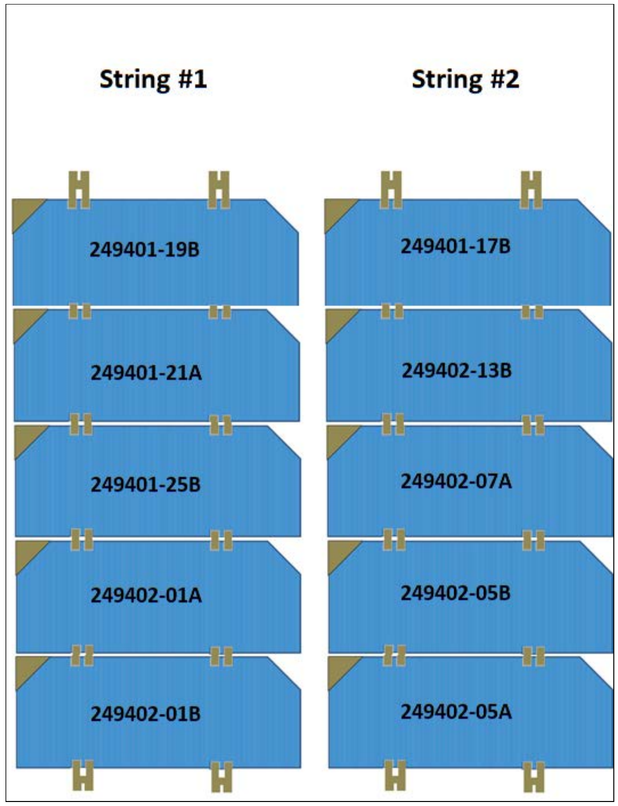

Figure 41: Figure 22. Layout of the CICs in strings 1 and 2.

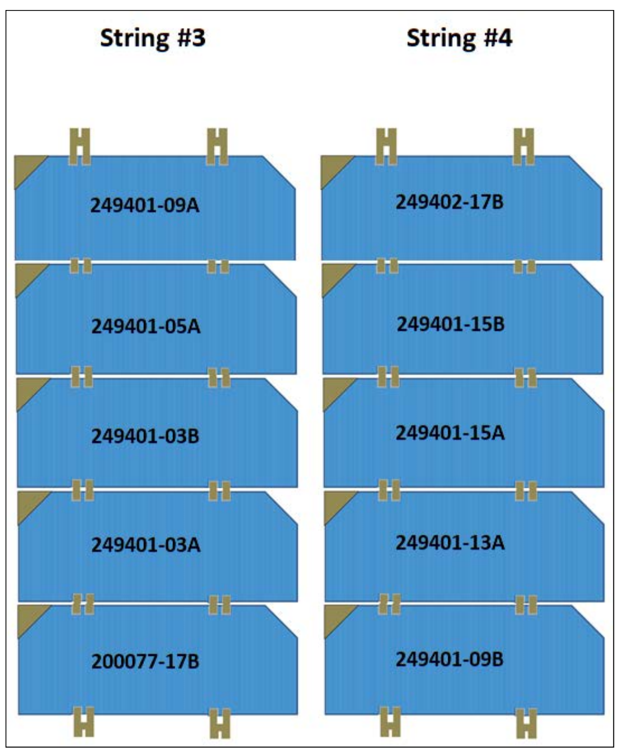

Figure 42: Figure 23. Layout of the CICs in strings 3 and 4.

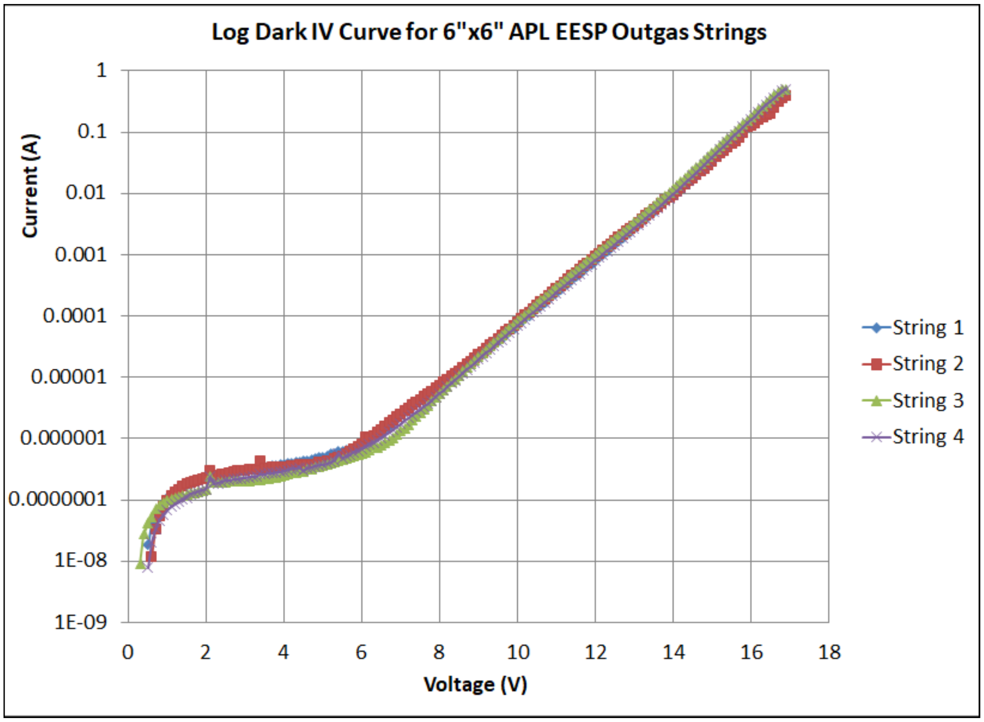

Figure 43: DIV measurements for each of the strings. The curves are excellent, with no indication of shunting in any of the strings.

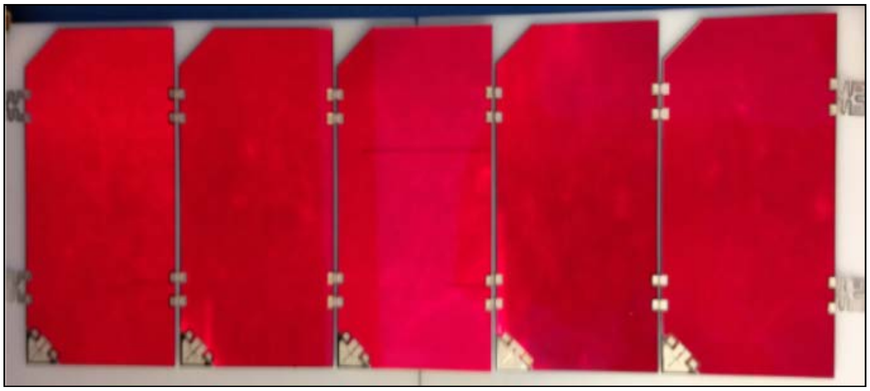

Figure 44 Electroluminescence of a string of IMM4 CICs at room temperature.

Summary of SolAero Work

Efficiency modeling was done for IMM 4, 5, and 6 junction cells, but the IMM4 cell was down selected for the program due to combination of performance and development maturity. Several issues with the IMM4 were observed during LILT testing, preventing the full achievement of optimal performance. While not completely resolved, progress was made in understanding root causes and correcting these issues. Samples for outgassing testing were fabricated.

Technical progress at APL

Thermal modelling

APL thermally modelled the concentrator configuration selected for the Transformational Array. The primary reason for this was to determine the temperature of components assuming a gravity assist from Venus. The hope was that the temperature at Venus would be low enough that rotating the array off axis would not be necessary. The modelling showed this would not be the case.

Figures 45, 46, and 47 show the geometry of the model.

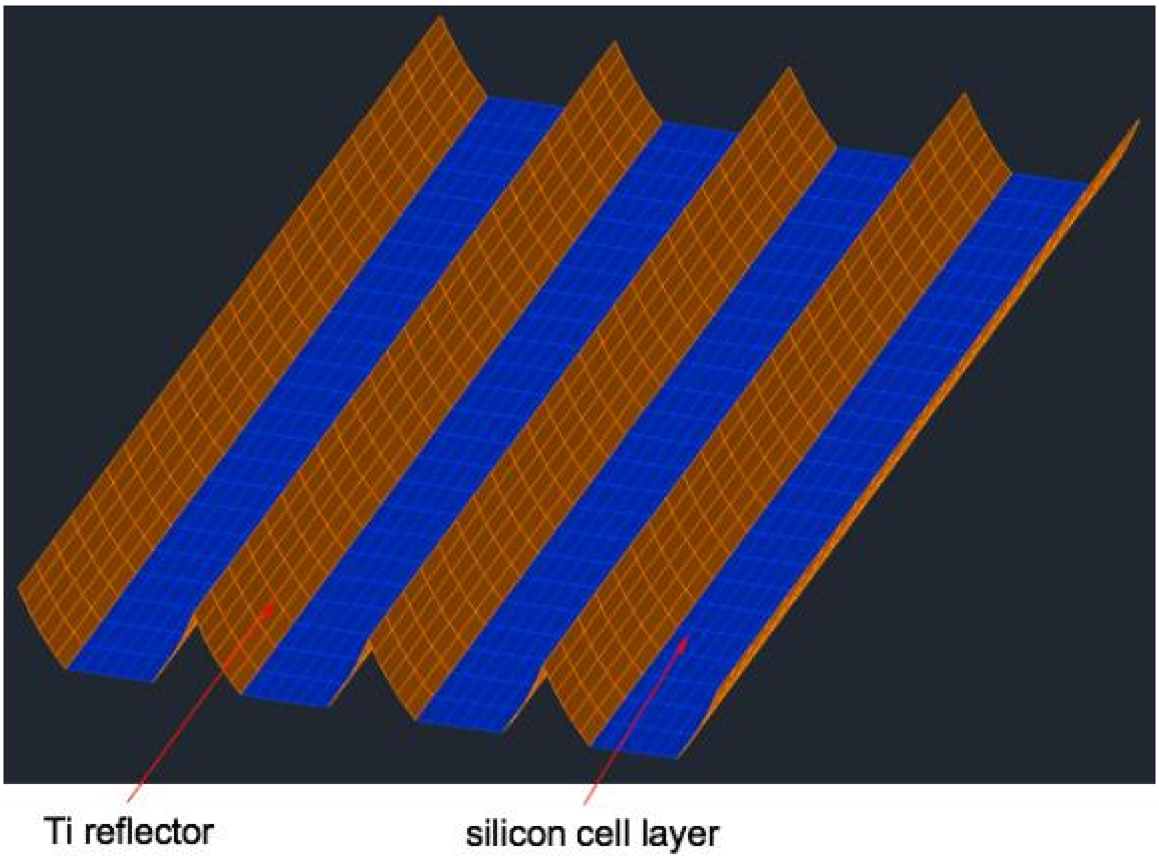

Figure 45: Isometric projection of the thermal model for the Transformational Array

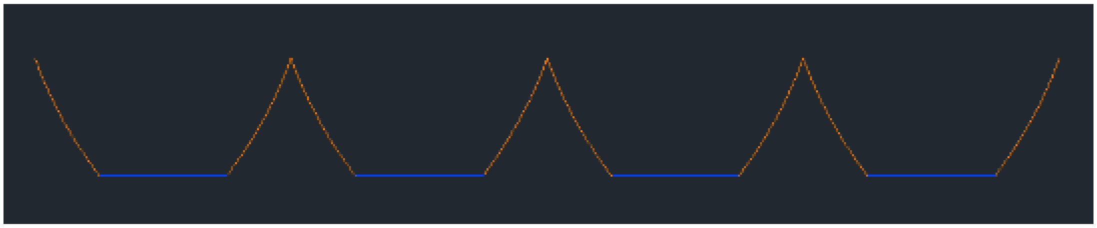

Figure 46: Cross section of the thermal model for the Transformational Array

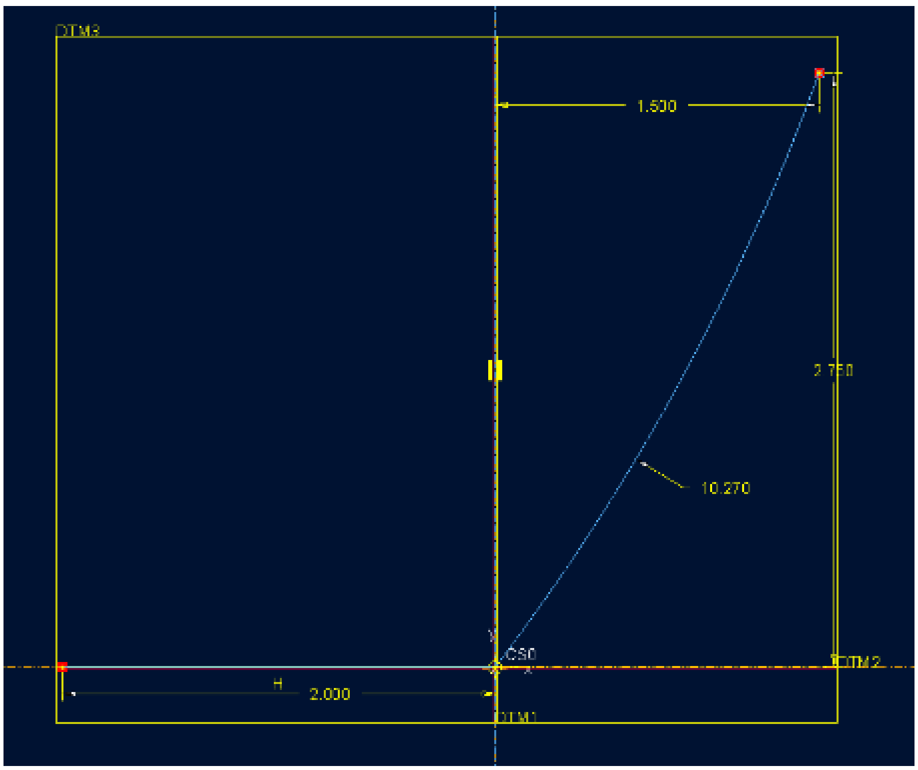

Figure 47: Concentrator geometry dimensions

The model assumes that electrical power is being extracted from the wing and that the cell layer conducts, albeit poorly, in plane. The reflector is assumed to have 100% specularity and 95% reflectivity. The array normal is parallel to the sun vector.

Figures 48 and 49 show the results of the modelling respectively at 1.0 AU and at 0.72 AU. The latter number is roughly the distance of Venus from the sun.

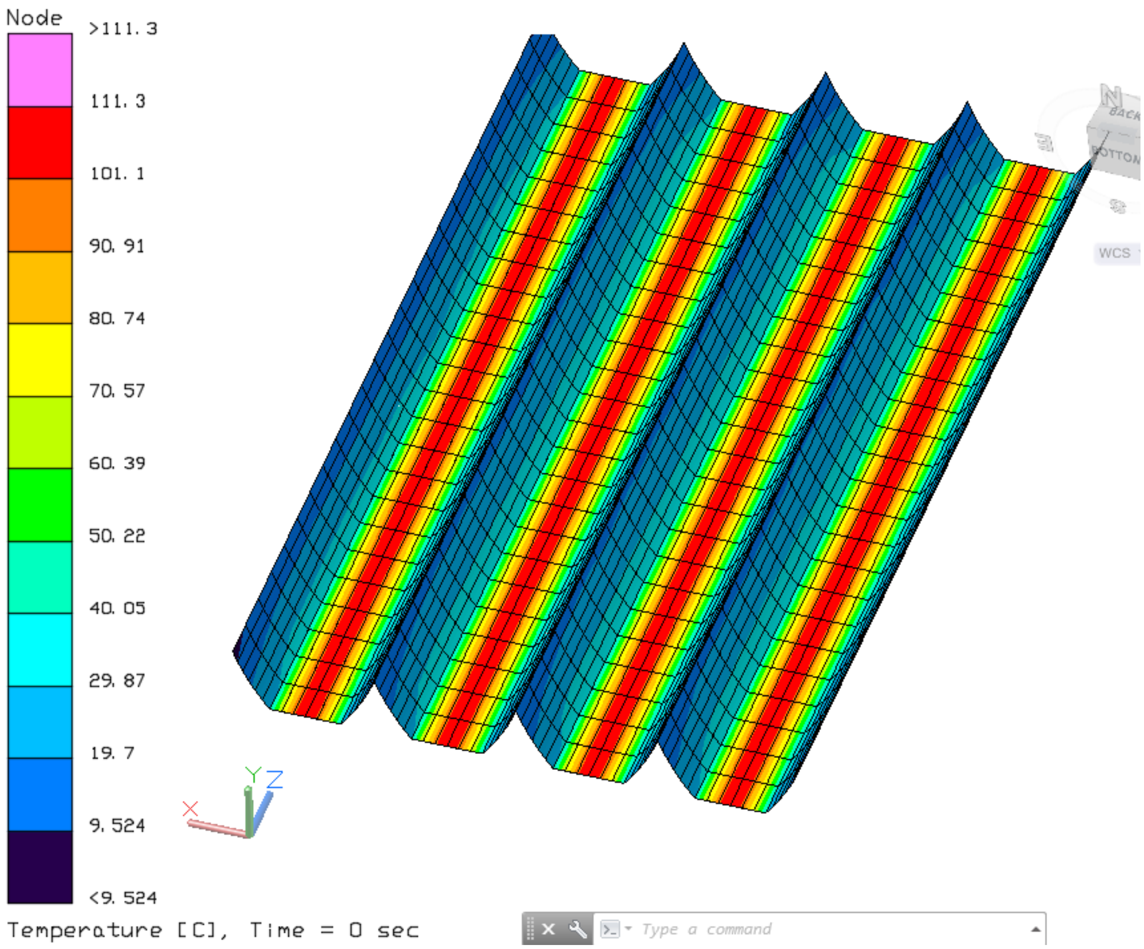

Figure 48: Transformational Array temperatures at 1 AU.

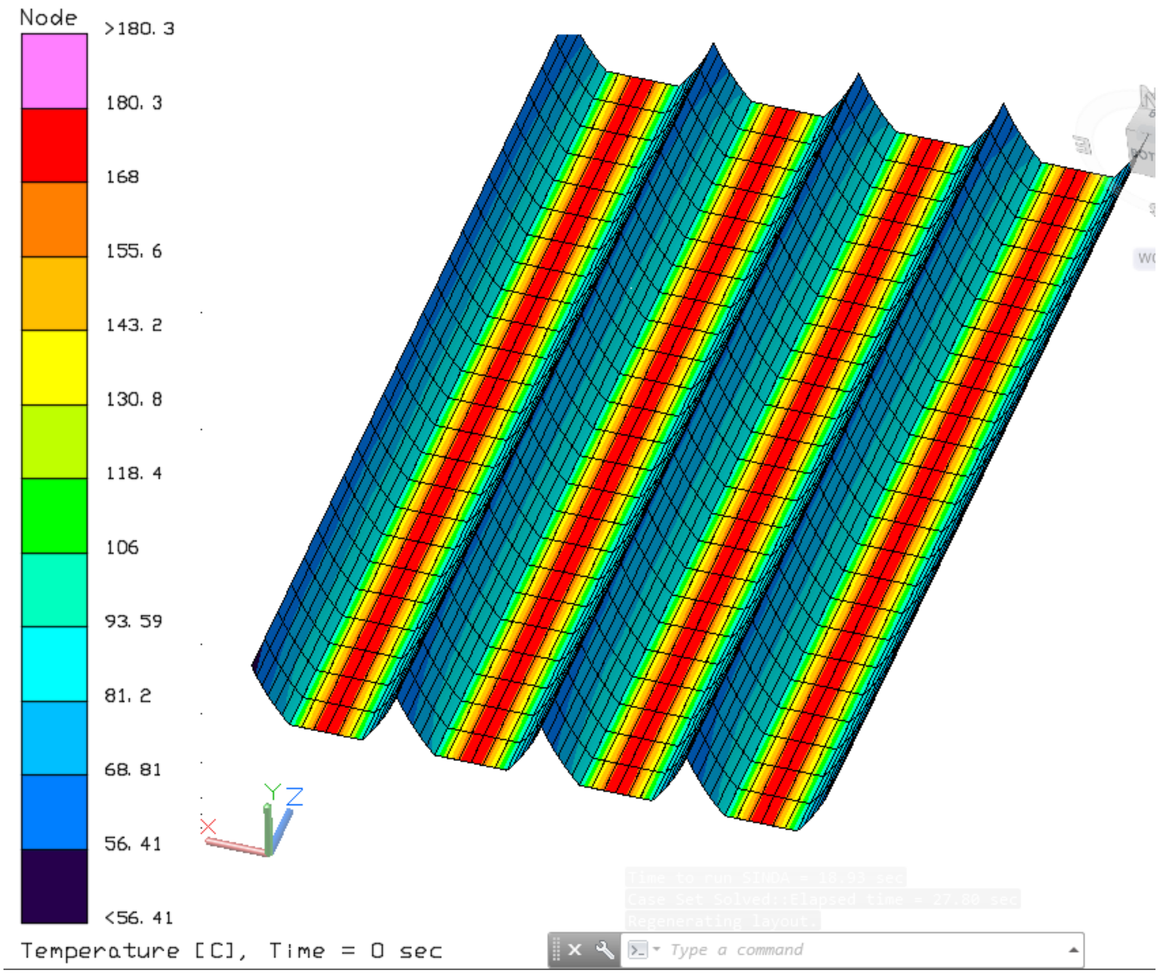

Figure 49: Transformational Array temperatures at 0.72 AU

The thermal modelling demonstrates that the concentrator temperatures are survivable at Venus without rotating the wing. However, they are high enough that it will be necessary to mitigate against outgassing even more than planned or to rotate the wings to attain lower temperatures. Rotating the wing must be performed on an axis perpendicular to string length to attain 1 AU irradiances. This will eliminate the need for outgassing mitigation above what is being done now. A failure could occur that would cause the array to point directly at the sun for an estimated 15 minutes. APL's qualitative estimate is that this will not result in enough outgassing to affect the concentrator performance.

The decrease in string voltage that may occur due to low irradiance on the end cells in a string on array rotation will likely not be a factor because the array receives 50 times more irradiance at Venus and 25 times more irradiance at earth than at Jupiter. This means that adequate current at operating voltage is almost certainly available with the rotated array even thought the operating voltage may be above the peak power voltage.

Outgassing

APL completed outgassing testing aimed at finding the "best" coverglass to cell adhesive. The test measured SCV2-2590 outgassing rates to DC 93-500 outgassing rates measured with identically configured DC 93-500 samples measured in the base phase.

We ran the first test on a single sample. This provided a result but the outgassing rate was difficult to measure because it was low relative to noise. We repeated the experiment with three samples and obtained a better and acceptable signal to noise ratio.

Three samples of SCV2-2590 under a coverglass with an average adhesive mass of 1.17g had a total mass loss of 0.086% after exposure to 150 °C for 72 hours. A single sample of SCV2-2590 under a coverglass with a mass of 1.367 g had a total mass loss of 0.068% under the same outgassing schedule. This compares to a DC 93-500 sample under a coverglass with a mass of 1.424 g that had a total mass loss of 0.128%. So, the DC 93-500 outgassed approximately 57% more than the SCV2-2590. This led us to select SCV2-2590 as the base-line adhesive

An important consideration in the successful development of this solar array is to understand the outgassing potential of the materials and the impact that the outgassing can have on the array's performance. In Option I the goals related to outgassing are as follows:

1. Find the most effective pre-treatment to minimize on orbit outgassing
2. Be able to estimate and quantify anticipated on orbit outgassing
3. Begin to look at effects on concentrator due to outgassing

APL has chosen Nusil Technology's SCV2-2590 as the primary adhesive for the solar array. This adhesive will bond the coverglass onto the cell. To justify the choice of SCV2-2590, APL performed a series of experiments that were completed early in Option 1. A brief synopsis of the results follows.

In the base phase, APL learned how SCV2-2590 outgassed in direct comparison with Dow Corning's DC93-500 adhesive under thermal-only conditions (i.e. no ultraviolet). Table 8 shows the percentage of total mass loss (% TML) after 3 days at 150 °C for a mass of adhesive that is uncovered by glass, thus allowing relatively unrestrained outgassing from a larger surface area (i.e. outgassing primarily through desorption). Table 9 shows the percentage of total mass loss after 3 days at 150 °C for adhesive that is covered by glass, thus having the outgassing occur around the edge of the sample (i.e. outgassing primarily by diffusion). It should be noted that while there is a coverglass on some of these samples, the amount of adhesive used in the samples is much higher (i.e. thicker) than a typical cell-coverglass layer.

Table 8: Uncovered adhesives in effusion cell (% TML by desorption)

Adhesive (Uncovered)	DC93-500	SCV2-2590
Thermal test	150 °C @ 69 hrs.	150 °C @ 71 hrs.
TML% after thermal	TML 0.420%	TML 0.267 %

Table 9: Covered adhesives in effusion cell (% TML by diffusion)

Adhesive (Covered)	DC93-500	SCV2-2590
Thermal test	150 °C @ 70.5 hrs.	150 °C @ 72 hrs.
TML% after thermal	TML 0.128%	TML .089 %

The total mass losses of the competing adhesives are fairly similar, and in fact there is some empirical evidence from work that SolAero has done to suggest that the percent TML's will converge after weeks of exposure at 125 to 150 °C. The advantage of the Nusil adhesive can be seen in the much lower mass of condensable material collected at -20 °C on a Thermal Quartz Crystal Microbalance (TQCM). Not only is the condensable material for the SCV2-2590 an order of magnitude lower than the DC93-500, it also appears to be converging toward zero more quickly, see Figure 50. The overall mass of the condensable material is equal to the area under the curve. With that said, more empirical evidence from SolAero suggests that the amount of condensable from the SCV2-2590 can increase with UV exposure onto the adsorbing surface.

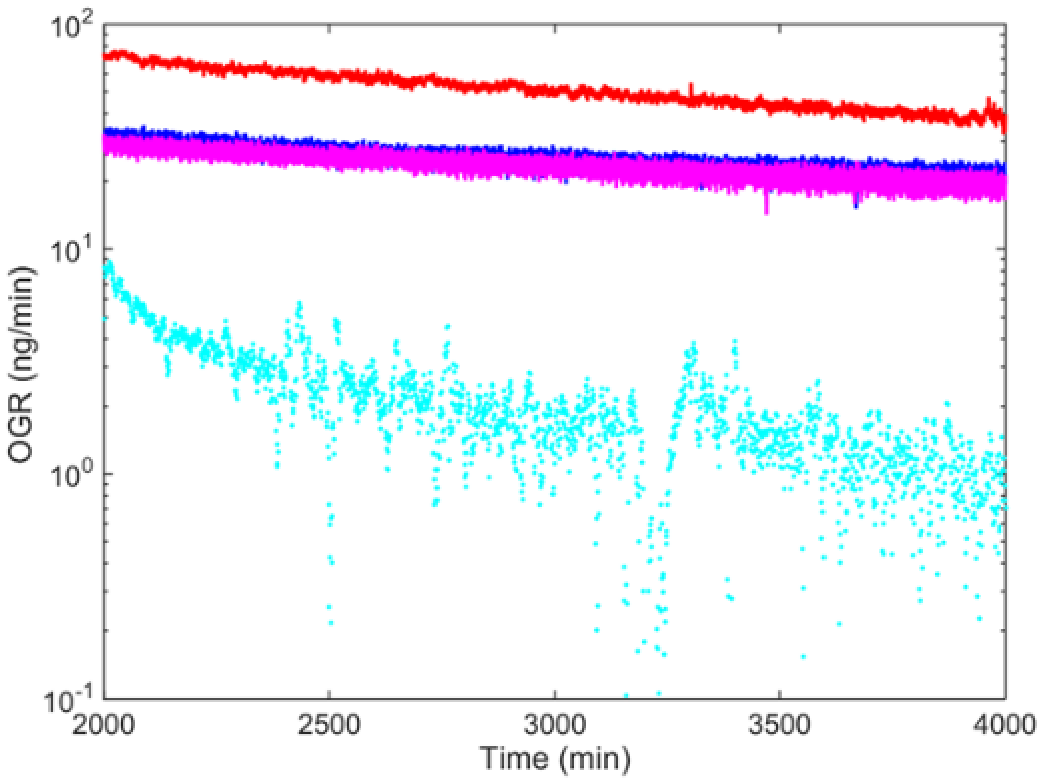

Figure 50: Condensable mass rate (log) of adhesives over time

TQCM Results (Condensable)

- **DC93-500 Uncovered** ----
- **SCV2-2590 Uncovered** ----
- **DC93-500 Covered** ----
- **SCV2-2590 Covered** ----

Once the Nusil SCV2-2590 was selected as the preferred adhesive, the testing focus shifted to developing a pre-treatment (aka conditioning) strategy. Based on results from the base phase and considering time constraints in Option I, APL decided to use a thermal-only vacuum exposure at 150 °C for 14 days. In addition, the samples from this point forward have geometrically accurate thickness. An example of the "thin" samples can be seen in Figure 51.

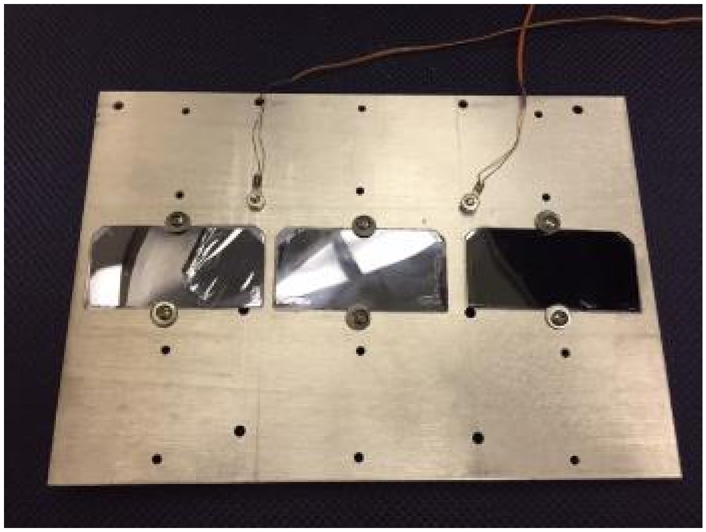

Figure 51: "Thin" samples, which have approximately 0.17 g of adhesive each

Our initial pre-treatment run involved 14 samples (referred to as # 1-14). The samples did have some variation in mass over time from sample to sample, but on average they lost mass very consistently over the 14 days, see Figure 52. Again, the dominant outgassing mechanism is diffusion from the edge of the samples.

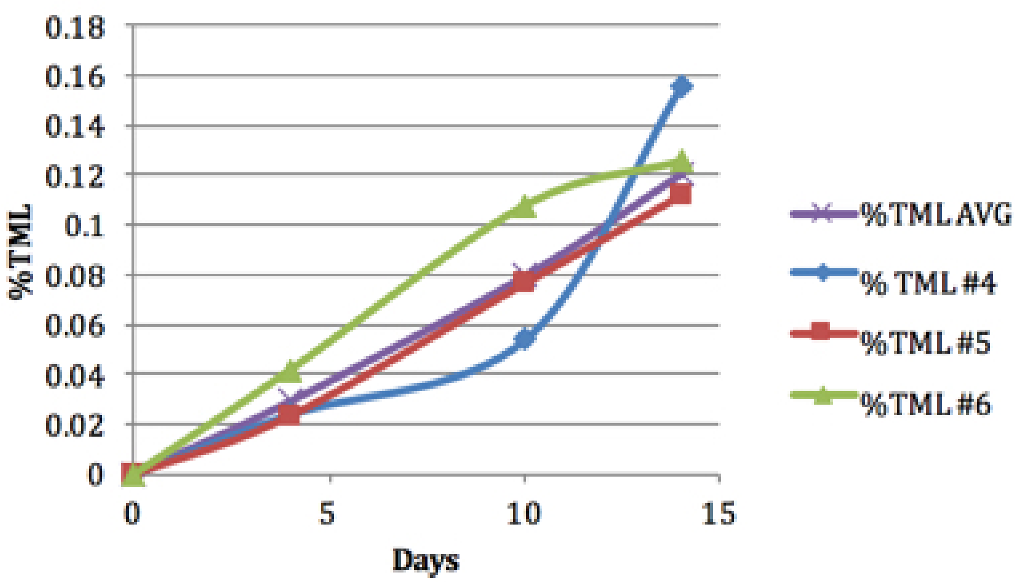

Figure 52: Percent total mass loss vs. days @ 150 °C over 14 days

It is expected that this mass loss trend would continue at the same rate for several more weeks, but it will eventually begin to become asymptotic.

With these 14 conditioned samples and some additional untreated samples, APL began follow-on testing. The first follow-on test was thermal vacuum only; three additional days for samples 4, 5 and 6 at 150 °C. As expected the mass loss continued at the same rate for those three days. Samples 4, 5 and 6 were then exposed to thermal vacuum at 125 °C for three days, but no additional mass loss was observed for those samples. As a control, three untreated samples were run simultaneously, and those samples lost the predicted amount of mass. A summary of the findings can be seen in Table 10.

Table 10: %TML seen in follow on testing

Bake Temp	Bake Time	Condition	TML	Note
125C	3 days	Fresh	0.06%	Nusil claims 0.06%
150C	14 days	Fresh	0.12%	~ linear outgas rate
125C	3 days	Pre-treated at 150C for 14 days	0.00%	-

The % TML from the APL three-day exposure notionally matches the % TML from Nusil Technology, notionally because Nusil data is likely based on ASTM E595 testing of uncovered material for 24 hrs. In addition, APL observed water recovery at 0.01% of the total mass, which is also consistent with published data.

The current follow-on test involved exposing untreated and pre-treated samples to ~2 Suns of ultraviolet light using our calibrated xenon source. The xenon lamp covers the wavelength range of 320 – 1100 nm. The cut-off wavelength of the coverglass is approximately 360 nm, but that can vary slightly depending on the temperature of the glass. The setup configuration and lamp are shown in Figures 53 and 54. The spectrometer used for calibration is shown Figure 55. And the xenon output spectrum is shown as compared to the solar spectrum in the ASTM E490 in Figure 56.

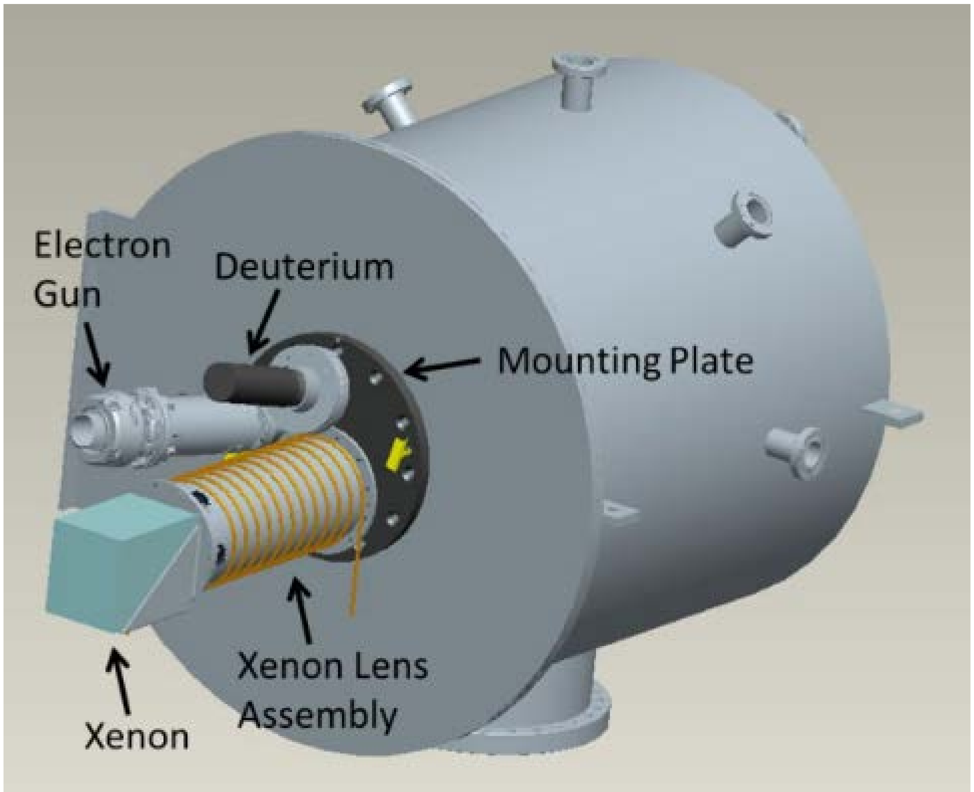

Figure 53: Conceptual drawing of solar simulator sources on CEnT chamber

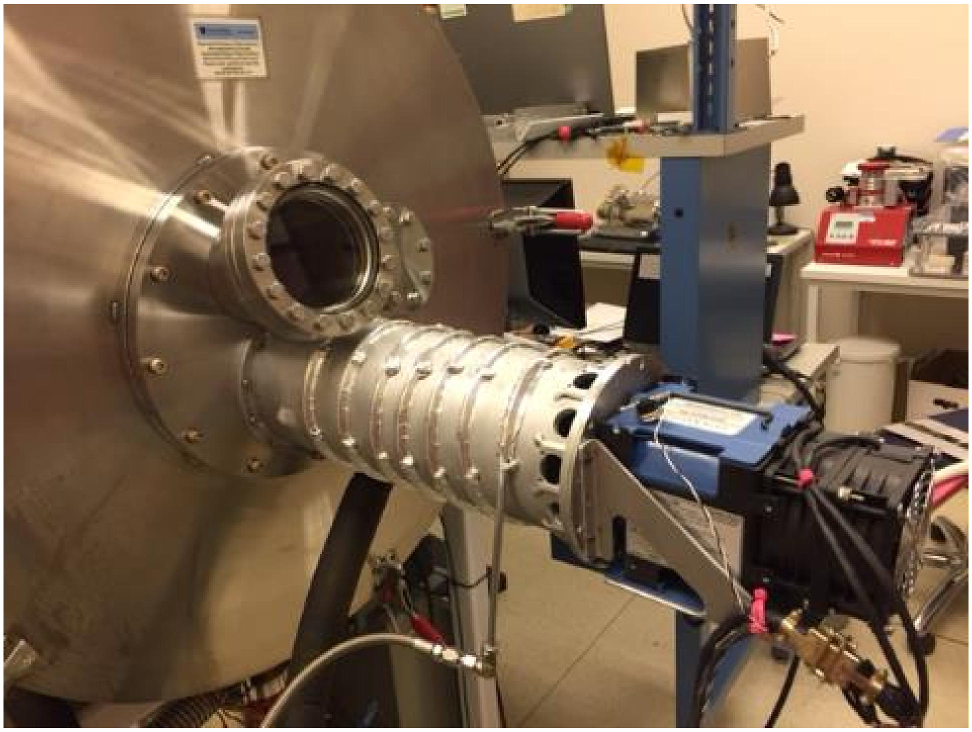

Figure 54: Actual image of xenon lamp configured to CEnT chamber

Figure 55: Spectrometer used for xenon calibration

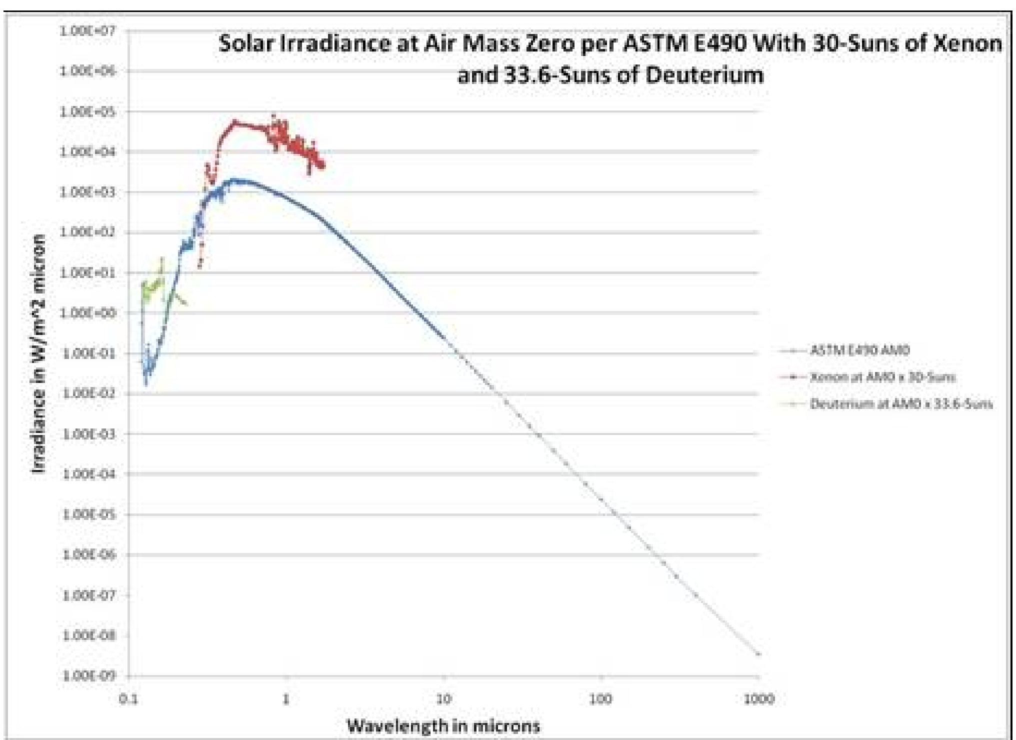

Figure 56: Xenon spectrum (red) overlay against solar spectrum from ASTM E490

The objective of the UV exposure is to determine if the UV changes the outgassing rate for both pre-treated and untreated samples.

The intermediate result of the UV exposure on multiple conditioned samples is shown in Figure 57. The UV exposure was equivalent to approximately 3 Suns. That irradiance level was chosen because it thermally equates to a 150 °C temperature on the samples, which is the temperature at which the samples were conditioned.

Regarding the Figure 56 testing:

- For the initial 17 days, the sample were exposed to 150 °C in vacuum with no UV. There was a consistent mass loss rate.
- For days 17-20, the sample were exposed to 125 °C in thermal vacuum. No additional mass loss was measured
- For the next 83 hours, after day 20, the samples were exposed to ~3 suns of UV, which caused the samples to reach approximately 150 °C (the same as the initial 17 days) – a significant mass loss was observed.

The test results suggest that outgassing at a high temperature does result in a substantial reduction in further outgassing at lower temperature. If temperature were the only environment the Transformational Array would experience, outgassing at a high temperature would eliminate outgassing in flight. Unfortunately, we have also shown that exposure to UV powerfully increases outgassing subsequent to an initial thermal only outgassing. We are now working to determine how to eliminate the UV induced outgassing.

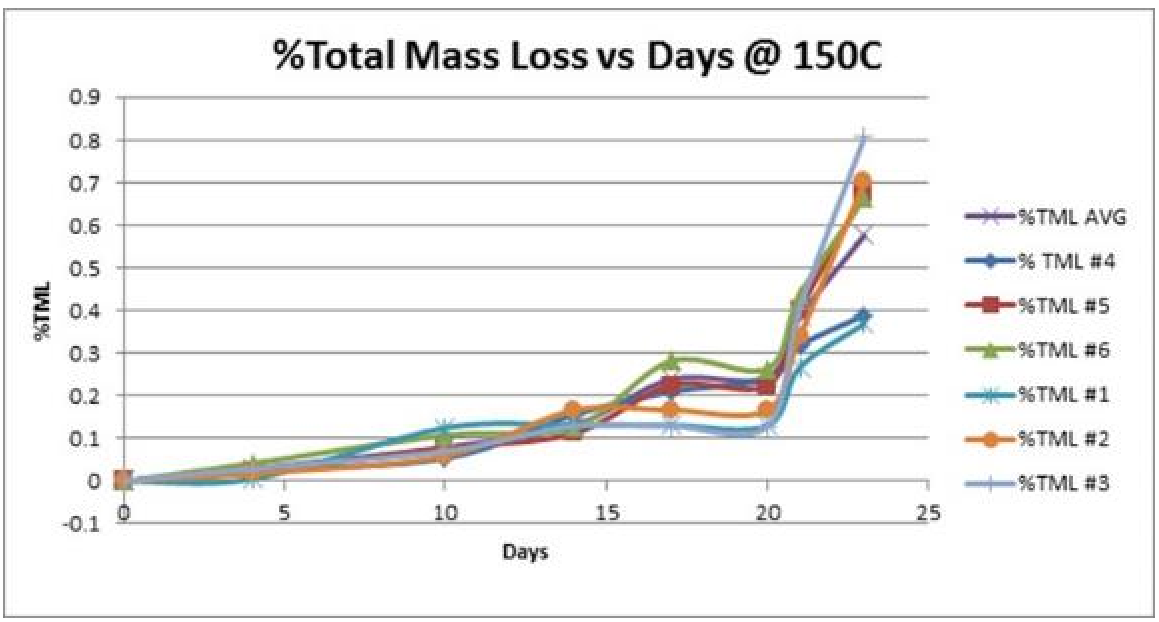

Figure 57: Percent total mass loss versus days at 150 °C. At day 20, APL started illuminating the samples with UV

APL will execute an unplanned test of UV exposure. These same samples will be exposed to ~2 Suns of UV irradiance, which should result in a sample temperature of ~125 °C, to see if the outgassing reduces or disappears completely as it did in the thermal-only test.

The remaining outgassing work for Option 1 consists of testing on mini-arrays. Due to equipment resource conflicts and required repair and calibration of APL's TQCM and RGA, a modified approach to testing of the mini-arrays was utilized.

APL created a crude fixture (to scale) that has unpolished aluminum concentrators with a 3x1 array with similar adhesives. A picture of the setup can be seen in Figure 58.

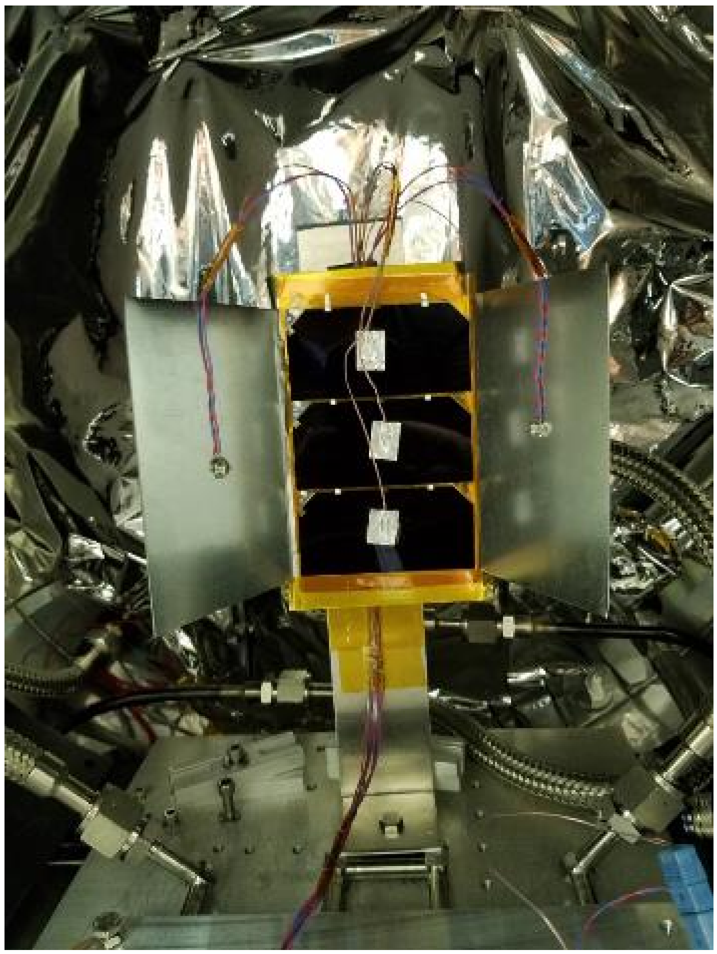

Figure 58: Mini-array crude model

Figure 59 is a view of the setup getting exposed to 3.98 Suns through the chamber viewport. The goal of this test was to quantify the thermal response of the model and to ensure thermal uniformity.

Figure 59: Illuminated “crude” mini-array

The irradiance of 3.98 Suns was a configuration from a previous UV test (unrelated to this task). The thermal performance and uniformity can be seen in Figure 60 below. The temperatures of the concentrators are no shown on the graph because they are not representative of their expected temperature.

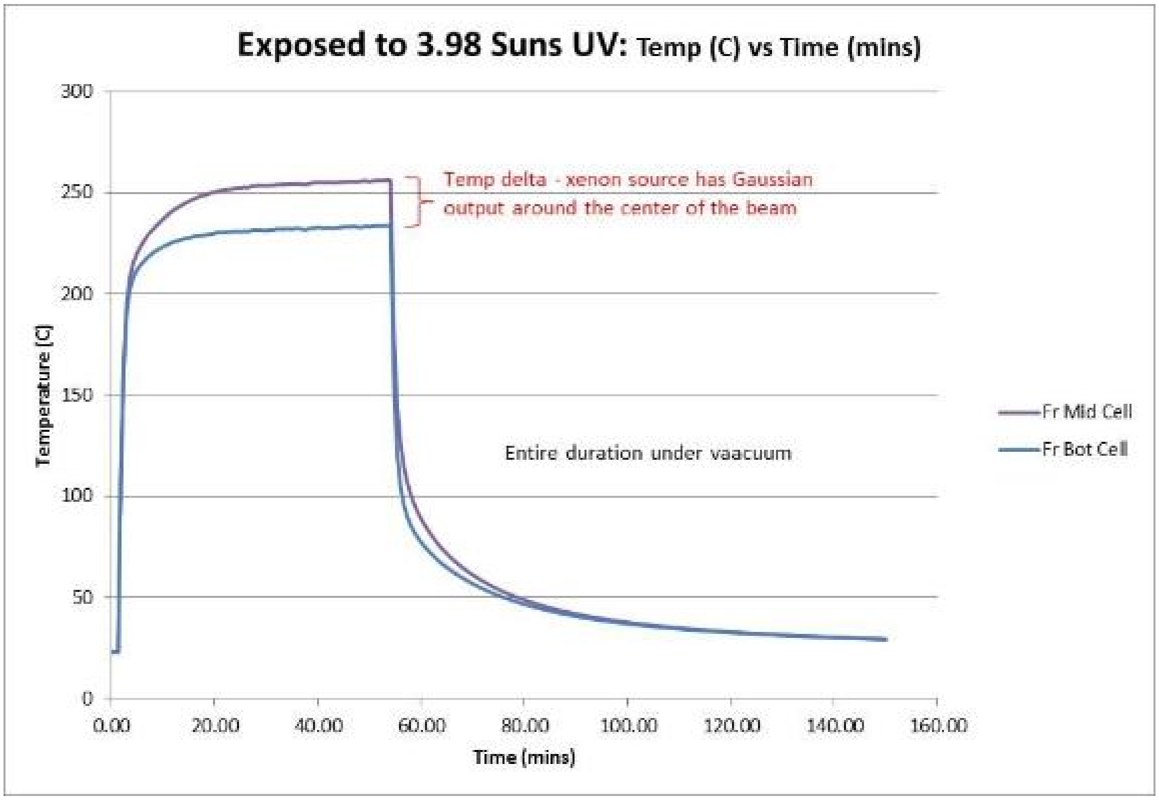

Figure 60: Thermal performance and uniformity of "crude" model

Note the quick heating of the arrays, stable thermal performance over several minutes, and thermal ramp down when the lamp is powered off. Multiple runs were conducted to verify that the thermal behavior is repeatable.

In the Option II Phase, APL will use a mini-array next to a silicon n-oxide coated wafer that is thermally controlled to the predicted values in the 0.72AU case shown in Figure 49.

The 0.72AU case allows higher temperatures (i.e. more outgassing) while remaining applicable to the task. The configuration will be exposed to the appropriate UV setup and ellipsometry will be used to measure any accumulated film thickness on the thermally controlled wafer. The measurements will be taken every 8-16 hrs. A TQCM and RGA will be used in an attempt to quantify the decay in outgassing from the cell adhesives.

In addition, APL will use highly reflective 2-mil aluminum foil for the concentrators in an attempt to better simulate the thermal behavior of the mini-array – somewhat of a thermal model verification.

Performance Testing

Thermal Cycling

APL visually inspected, conducted an electroluminescence test, and ran an I-V characterization on the deliverable 150 mm by 150 mm coupon. Subsequently, APL re-ran these tests. The initial results showed that the string on the panel did not have an ideal curve shape with the short circuit current decreasing more than acceptable between 12 V and about 15.5 V.

Subsequent to 12 thermal cycles between -150 °C to 110 °C the string unacceptably decreased in current at all voltages. This is shown in Figure 61. Both the curve shape and the decrease will be further investigated in Option II. APL has two spare strings, with the same undesirable curve shape that will be returned to SolAero for their confirmation of APL test results and investigation. APL anticipates that this is not a serious issue, in terms of getting it fixed, but this must be done.

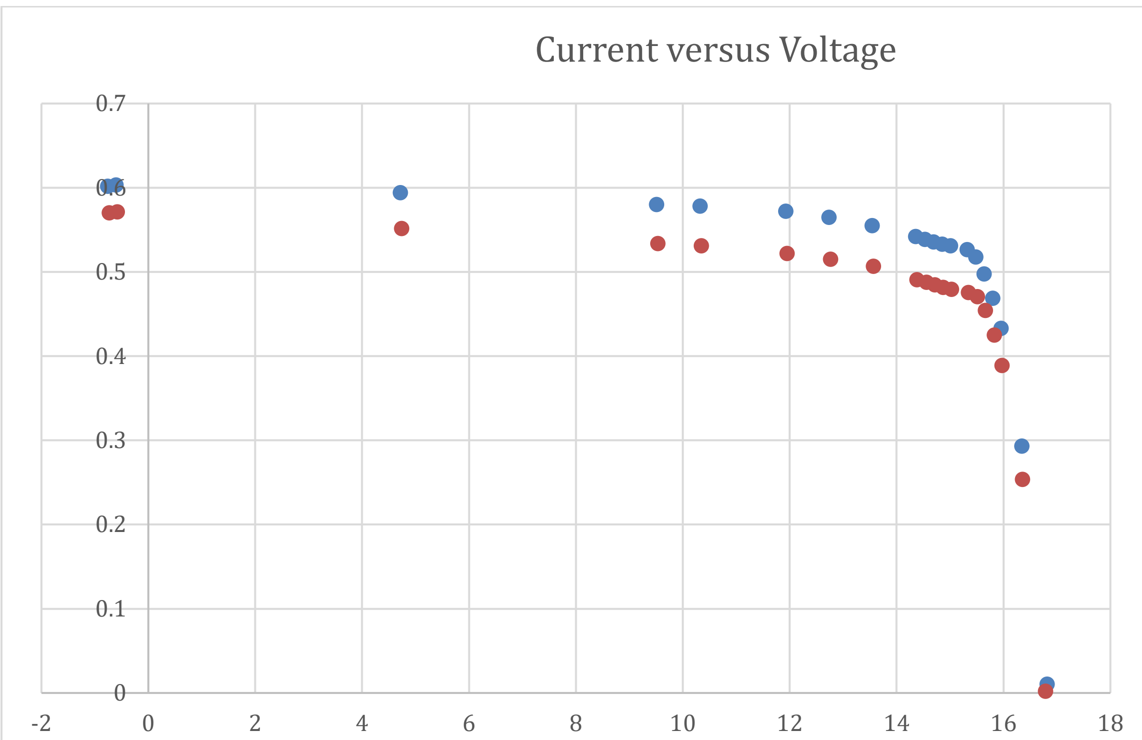

Figure 61: Coupon output before (blue) and after (orange) thermal cycling.

Figure 62 shows the test article, also depicted in Figure 28, in electroluminescence. The darker areas on the two rightmost cells are signs that these cells are shunted, which could explain the less than ideal curve shape. However, these same dark areas appear on SolAero's electroluminescence results, which makes the dark areas less suspicious.

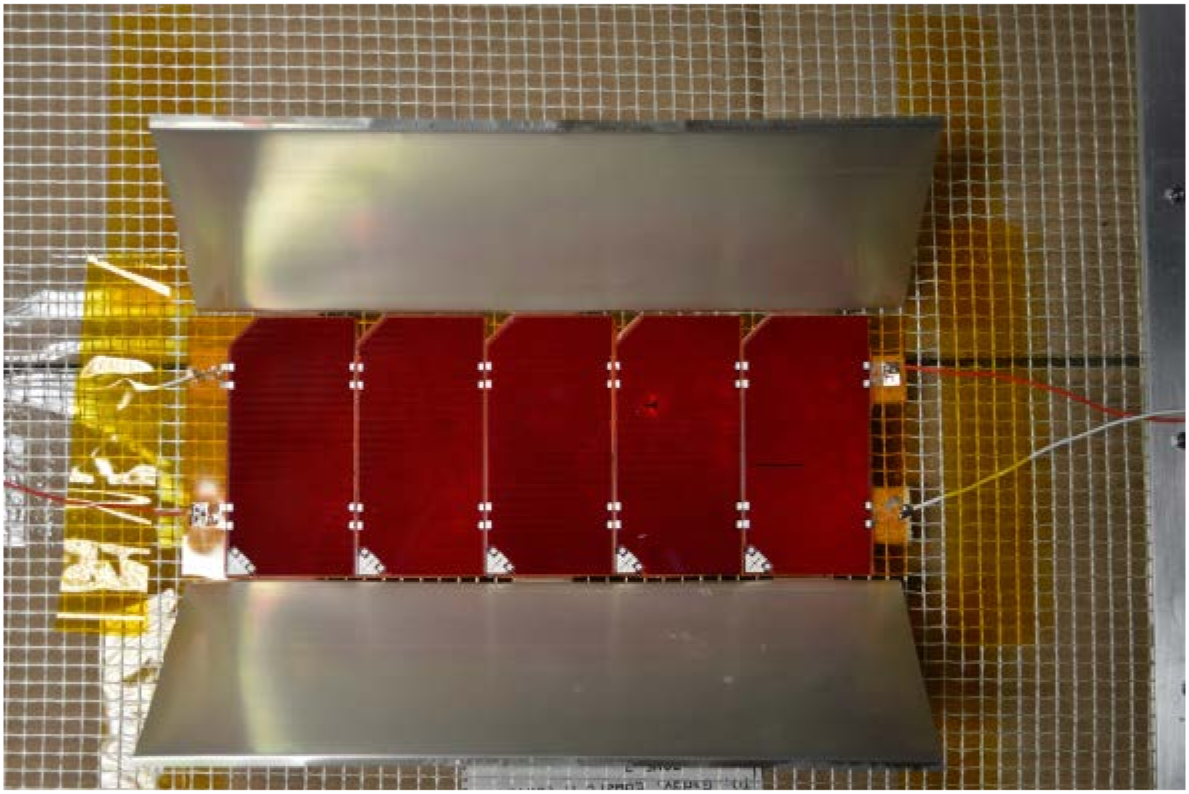

Figure 62: Thermal cycling coupon in electroluminescence.

Vibration

APL subjected the rolled up coupon shown in Figure 29 and Figure 30 to vibration in accordance with the Test Summary Report in Appendix A.

The current versus voltage characterization for this coupon before and after vibration is shown in Figure 63. The coupon's peak power degraded approximately 2.5% after vibration. This is approximately 1.5% outside of the precision of the Large Area Pulsed Solar Simulator used for this test. This degradation is significant to warrant further investigation. This will be undertaken in Option II.

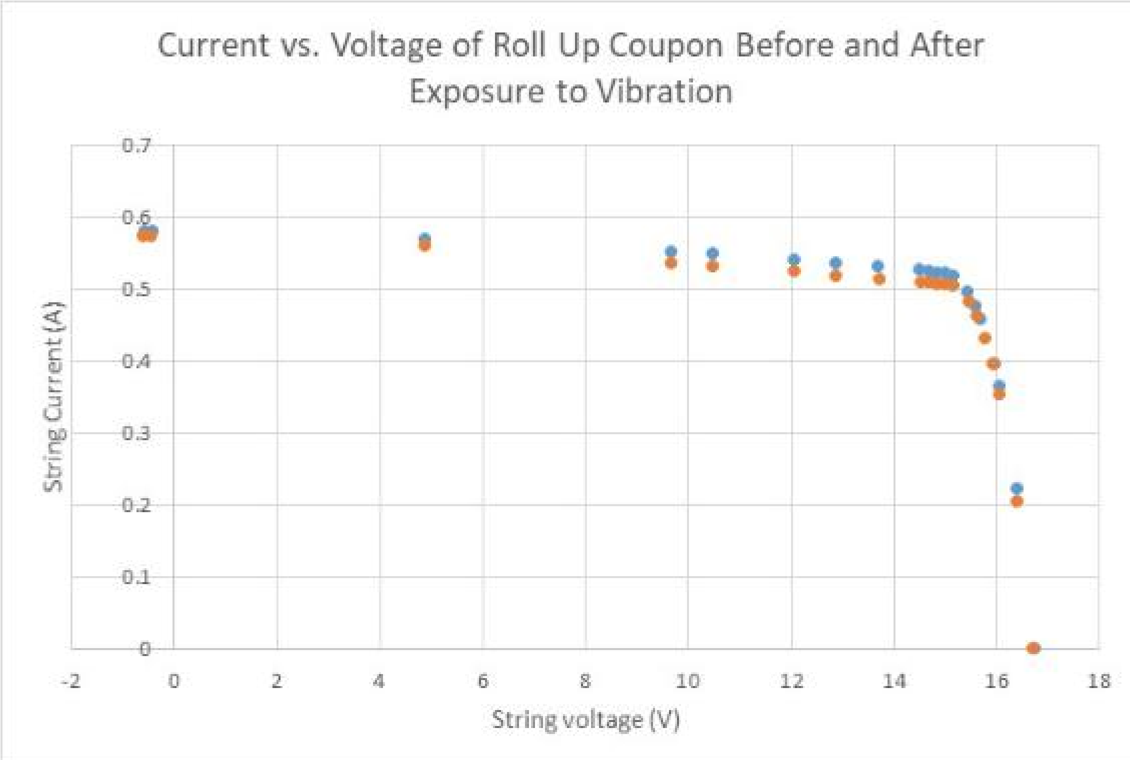

Figure 63: Coupon Output before and after vibration

Conclusions

During the Option I contract, two key performance parameters were exceeded, beginning of life cell efficiency is now computed at 37.2% versus a goal of 35%, and end of life efficiency is at 28.9% versus a goal of 28.9%. The specific power achieved is over a computed 8.6 W kg^{-1} versus a threshold of 8 W kg^{-1}.

SolAero improved the efficiency of the IMM4 solar cells. The company also successfully addressed several of the issues that caused cells that performed well at AM0 to perform relatively poorly at LILT. This improvement has the effect of increasing cell yield. DSS improved the previously unsatisfactory adhesion of the mirror surface on the concentrator substrate. The silver coating is now quite robust having passed tape peel tests and thermal cycling tests. DSS also changed the method of bonding stiffeners to welds rather than adhesive. This reduces cost and mass. Significant knowledge was gained relative to adhesive outgassing most particularly NewForge demonstrated that thermally outgassing adhesive does not stop additional outgassing induced by exposure to UV.

Work to be done includes further improvement of the cell efficiency and cell robustness against poor performance in some fraction of cell production at LILT. Additional effort will be put into improving the reflectance of the concentrator mirrors. DSS's assessment is that this will be readily achieved. Finally, the outgassing from the cover to cell and other adhesives will be improved and means to reduce the deposition of outgassing produce onto the concentrators will be investigated.

TRL Assessment

The following pages contain tables that define APL's assessment of the TRL levels of the Transformational solar array. The pages evaluate TRLs per the NASA definitions that follow.

		Demonstration Unit				Environment							
(green)	Green - TRL 4, 5, 6, 7, 8, 9												
(yellow)	Yellow - TRL 3												
(red)	Red - Below TRL 3												
	White - Unknown												
X	Exists												
Y	Yes												
N	No												
?	Uncertain												
System, Component, Subsystem		**Component**	**Breadboard**	**Prototype**	**Flight Qualified**	**Laboratory Environment**	**Relevant Environment**	**Space Environment**	**Operational Environment (Launch/Space)**	**Analytical Scalability**	**Manufacturing Scalability**	**Overall TRL**	**Rationale for Overall TRL**
System: Solar Array (2 kW)		X	X	X	X	Y	Y	Y	Y	Y	Y	7	A 2 kW ROSA has been fabricated and tested in an operational environment. The array is partially populated with PV including Spectrolab and SolAero product. The deployment roll out booms are purposely large to demonstrate deployment of a 10 kW array. The wing has deployment control, tie downs, everything. This wing will retract. An example of a ROSA has flown on the International Space Station in June 2017.
System: Solar Array (14.1 kW)		X	X	X	in process	Y	Y	N	in process	Y	Y	NA	DSS has built a ROSA array that is in testing for flight qualification (TRL-8) for SSL.

(Green)	Green - TRL 4, 5, 6, 7, 8, 9
(Yellow)	Yellow - TRL 3
(Red)	Red - Below TRL 3
(White)	White - Unknown
X	Exists
Y	Yes
N	No
?	Uncertain

System, Component, Subsystem	Demonstration Unit				Environment							
	Component	Breadboard	Prototype	Flight Qualified	Laboratory Environment	Relevant Environment	Space Environment	Operational Environment (Launch/Space)	Analytical Scalability	Manufacturing Scalability	Overall TRL	Rationale for Overall TRL
Subsystem: Blanket												
Full Blanket	X	X	X	X	Y	Y	Y	Y	Y	Y	7	A 2 kW ROSA blanket has been fabricated and tested in an operational environment.
Blanket Section (Standard Power Module)	X	X	X	X	Y	Y	Y	Y	Y	Y	7	Full size SPMs populated with cells and harness have been fabricated and tested in an operational environment.
Replacement for heat spreader (stiffener)	X	X			N	N	N	Y	Y	Y	5	A coupon with a replacement for the heat spreader, basically a stiffener, is fabricated and thermal cycled. Its mechanical function is satisfactory.
Concentrator Module	X	X	X		Y	Y	N	N	Y	Y	6	The concentrator module for ROSA is at TRL 6. This includes mirrors that are folded for launch and the springs required to place them at the proper angle after the wing is rolled out.
Structure (for 10 kW array)	X	X	X	X	Y	Y	Y	Y	Y	Y	7	The ROSA structure has been fabricated and passed testing in an operational environment

		Demonstration Unit				Environment							
(Green)	Green - TRL 4, 5, 6, 7, 8, 9												
(Yellow)	Yellow - TRL 3												
(Red)	Red - Below TRL 3												
(White)	White - Unknown												
X	Exists												
Y	Yes												
N	No												
?	Uncertain												
System, Component, Subsystem		**Component**	**Breadboard**	**Prototype**	**Flight Qualified**	**Laboratory Environment**	**Relevant Environment**	**Space Environment**	**Operational Environment (Launch/Space)**	**Analytical Scalability**	**Manufacturing Scalability**	**Overall TRL**	**Rationale for Overall TRL**
Component: Solar Cell													
IMM 4 cells		X	X	X	X	Y	Y	Y	Y	Y	Y	7	IMM 4 and IMM 4+ cells are flying on CubeSat’s. We evaluate this as TRL 7. The IMM 4 cells used for the Transformational Array have layers that have slightly different growth parameters and so have a lower TRL.
Strings of IMM cells		X	X	X	X	Y	Y	Y	Y	Y	Y	7	SolAero has successfully demonstrated automated string manufacturing and laydown, robust interconnection methods, and reliable rework. And, strings are already in orbit.
Adhesive		X	X	X	X	Y	Y	Y	Y	Y	Y	9	The proposed adhesives have flown on numerous spacecraft.
Coverglass		X	X	X	X	Y	Y	Y	Y	Y	Y	9	The proposed coverglass has flown on numerous spacecraft, including Juno, a spacecraft that has travelled to 5 AU.

		Demonstration Unit				Environment							
	Green - TRL 4, 5, 6, 7, 8, 9												
	Yellow - TRL 3												
	Red - Below TRL 3												
	White - Unknown												
X	Exists												
Y	Yes												
N	No												
?	Uncertain												
System, Component, Subsystem		**Component**	**Breadboard**	**Prototype**	**Flight Qualified**	**Laboratory Environment**	**Relevant Environment**	**Space Environment**	**Operational Environment (Launch/Space)**	**Analytical Scalability**	**Manufacturing Scalability**	**Overall TRL**	**Rationale for Overall TRL**
Component:	Mirrors	X	X	X		Y	Y	N	N	Y	Y	6	The Transformational Array effort has increased the mirrors, which previously had a delamination issue, from TRL 4 to TRL 6.
Component:	Reduction of outgassing to acceptable levels	X	X			Y	Y	N	N	Y	Y	4	Initial testing in a laboratory environment suggests that the pre-conditioning the adhesive will reduce outgassing to levels that will not contaminate the mirrors.

Green	Green - TRL 4, 5, 6, 7, 8, 9
Yellow	Yellow - TRL 3
Red	Red - Below TRL 3
White	White - Unknown
X	Exists
Y	Yes
N	No
?	Uncertain

System, Component, Subsystem	Demonstration Unit				Environment							Rationale for Overall TRL
	Component	Breadboard	Prototype	Flight Qualified	Laboratory Environment	Relevant Environment	Space Environment	Operational Environment (Launch/Space)	Analytical Scalability	Manufacturing Scalability	Overall TRL	
Component: Structure Assembly												
Motor												Motors are not used.
Deployment Mechanism	X	X	X	X	Y	Y	Y	N	Y	Y	7	A full-size ROSA has been fabricated and tested in an operational environment. This includes the booms that serve as a part of the array's structure as well as to deploy the blanket.
Deployment Brake	X	X	X	X	Y	Y	Y	N	Y	Y	7	A full-size ROSA has been fabricated and tested in an operational environment. This includes the deployment brake.
Hinges	X	X	X	X	Y	Y	Y	N	Y	Y	7	A full-size ROSA has been fabricated and tested in an operational environment. This includes hinges.
Wing tie down	X	X	X	X	Y	Y	Y	N	Y	Y	7	A full-size ROSA has been fabricated and tested in the relevant environment. This includes the wing tie down.
Mandrel tip	X	X	X	X	Y	Y	Y	N	Y	Y	7	A full-size ROSA has been fabricated and tested in an operational environment. This includes the wing mandrel tip.

Meetings and Telecoms

APL presented progress reports verbally and in bulleted form every two weeks.

Section II: Risk Mitigation

At the end of the base phase, one of ten risks identified at the start of the base phase was retired. During the work performed for Option I, risk ID 6 was retired. This risk was for the delamination of the reflective coating on the concentrator. The risk was retired because DSS fabricated coatings that did not delaminate during test. In the following pages, APL re-evaluated the remaining eight risks. The risks are listed in Tables 1 through 4. The risks are against safety, cost, schedule, and technical performance.

Other than risk 6, there have been no substantive change since the Base Phase report.

Table 11: Risk Matrix for Safety

Likelihood	Very High (5)					
	High (4)					
	Moderate (3)					
	Low (2)					
	Very Low (1)		5, 9, 10	2, 3, 4		1, 7
		Minimal (1)	Minor (2)	Medium (3)	Major (4)	Very High (5)
		Consequence				

Table 12: Risk Matrix for Cost Performance

Likelihood	Very High (5)					
	High (4)					
	Moderate (3)					
	Low (2)					
	Very Low (1)				10	1, 2, 3, 4, 5, 7, 9
		Minimal (1)	Minor (2)	Medium (3)	Major (4)	Very High (5)
		Consequence				

Table 13: Risk Matrix for Schedule Performance

Likelihood						
Likelihood	Very High (5)					
	High (4)					
	Moderate (3)					
	Low (2)					
	Very Low (1)				10	1, 2, 3, 4, 5, 7, 9
		Minimal (1)	Minor (2)	Medium (3)	Major (4)	Very High (5)
		Consequence				

Table 14: Risk Matrix for Technical Performance

Likelihood	Very High (5)					
	High (4)					
	Moderate (3)			1		
	Low (2)			2	3, 5, 7	
	Very Low (1)				4, 9, 10	
		Minimal (1)	Minor (2)	Medium (3)	Major (4)	Very High (5)
		Consequence				

Table 15: Threat Risk Consequence Criteria

Consequence	Personnel Safety	Asset Safety	Technical	Schedule	Cost
5 Very High	Death or permanent disability	Loss of flight system or critical asset; prevents mission success	Major impact to mission success; minimum mission success criteria not achievable	Irrecoverable impact to critical path; mission milestones cannot be met	≥ 15% of allocated budget -or- Unrecoverable, requiring outside funding to resolve
4 High	Severe (incapacitating) injury or illness	Major flight system or critical asset damage; impacts mission success	Significant threat to meeting primary mission objectives; minimum mission success criteria remain achievable	Major (≥ 2 weeks) impact to critical path or critical milestones, recoverable within total reserves and with workarounds -or- Major (≥ 4 weeks) impact to non-critical milestones; recoverable using workarounds without impact to critical path	≥ 10% but < 15% of allocated budget -or- Requires de-scope of significant capability or product
3 Medium	Emergency medical treatment for non-permanent injury	Minor flight system damage; repair, or replacement feasible. Moderate asset damage, no threat to mission success	No impact to primary mission objectives, and moderate impact to secondary mission objectives, requirements and technical margins. Minimum mission success criteria remain achievable with margin	Minor (≥2 weeks) impact to critical path or critical milestones, recoverable within minimum reserve profile -or- Moderate (≥ 4 weeks) impact to non-critical milestones; recoverable using workarounds and with only moderate impacts to successor milestones	≥ 5% but < 10% of allocated budget -or- Requires de-scope of secondary capability or product
2 Low	Minor first aid treatment	Negligible flight system damage. Minor asset damage.	No impact to primary mission objectives, and minor impact to secondary mission objective, requirements, and technical margins	No impact to critical path or critical milestones -or- Minor (< 4 weeks) impact to non-critical milestones; recoverable using workarounds and with minor impact to successor milestones	≥ 2% but < 5% of allocated budget -or- Requires significant change in effort with only minor impacts to products and deliverables
1 Very Low	No injury requiring treatment	No flight system or critical asset damage. Minor non-critical asset damage	No impact to full mission success criteria and negligible impact to requirements and technical margins	Negligible impact	≤ 2% of allocated budget -or- requires change in effort but no impact to products or deliverables

Table 16: Risk Likelihood Criteria

Likelihood	Safety (Likelihood of safety event occurrences)	Technical (Likelihood of not meeting mission technical requirements)	Cost/Schedule (Likelihood of not meeting allocated requirement or margin)
5 Very High *Nearly certain*	$P_S > 0.1$	> 60%	>75%
4 High *Highly likely*	$0.01 < P_S \leq 0.1$	$35\% < P_T \leq 60\%$	$50\% < P_{CS} \leq 75\%$
3 Moderate *May occur*	$0.001 < P_S \leq 0.01$	$15\% < P_T \leq 35\%$	$25\% < P_{CS} \leq 50\%$
2 Low *Not likely*	$10^{-5} < P_S \leq 0.001$	$2\% < P_T \leq 15\%$	$5\% < P_{CS} \leq 25\%$
1 Very Low *Very unlikely*	$P_S \leq 10^{-5}$	$0.1\% < P_T \leq 2\%$	$P_{CS} \leq 5\%$

In the following risk evaluations, the safety risk consequence is evaluated with tasks and activities that are directly and uniquely associated with the risk. For example, the risk consequence never includes certain ancillary activities such as transportation of test articles in automobiles or trucks travelling at highway speeds, which would always have a safety risk consequence of 5.

All risks are evaluated with respect to the contract being executed as opposed to the flight of a Transformational Array.

The cost risk requires special elaboration. It is evaluated with respect to the cost of this contract. However, some of the risks listed below do not affect the technical performance of a production Transformational Array but would affect its cost. These risks are put into the Technical Risk category for this contract but not the cost risk as these risks do not affect this contract cost but do affect a goal of the contract - - namely to keep the cost of a production Transformational Array low.

ID 1: IMM solar cells do not meet the power requirements at BOL

Risk Statement: If the IMM cells do not meet or come close to meeting power requirements at beginning of life, it will be difficult or impossible to meet several goals of the contract including cell efficiency at 47%, blanket efficiency of 32%, areal power density of 8 W kg^{-1}, and packing density of 66 kW m^{-3}. This will deplete cost and schedule reserves and if persistent will prevent us from meeting contract goal requirements. The technical consequence of this occurring is lowered from a 4 to a 3 as a result of the discovery in the Base Phase that the IMM solar cells are lighter than assumed at the beginning of the Base Phase. The likelihood of the risk has been increased to a 3 because the Base Phase efficiencies were not as high as hoped.

Risk Context: The context of the risk is the history of increasing solar cell efficiency over the years and the history of the production of gallium arsenide based solar cells.

Likelihood and Consequence to Safety: 1, 5. The likelihood of this risk is based on the safety record of developing and producing Gallium Arsenide based solar cells; and the safety monitoring and interlocks that are in place. SolAero has gone over six years without an injury related to cell manufacture. (The record of safety goes back further than that, but a report for earlier was not available for this document.) The consequence is based on the toxicity of the materials used in the production of the cells. A leak in a reactor could be deadly.

Likelihood and Consequence to Cost: 1, 5. The rationale for this is that APL will trade the cost risk to the technical risk. Essentially, SolAero will accept whatever cell efficiency is obtained for the planned cost. If SolAero do not do this the consequence could be exceeding budget by more than 15%; and, hence is a 5.

Likelihood and Consequence of to Schedule Performance: 1, 5. The rationale for this is that APL will trade the schedule risk to the technical risk. Essentially, SolAero will accept whatever cell efficiency is obtained for the planned schedule. If SolAero do not do this the consequence could be exceeding schedule for several years.

Likelihood and Consequence to Technical Performance: 3, 3. The likelihood of meeting cell efficiency is difficult to determine because the required cells have not been fabricated. However, it is analytically known that the cell efficiency is achievable with available materials and with methods of fabrication that are generally known to be practicable, so calling it a 3. The consequence of not meeting power requirement will be that the Transformational Array will fall short of meeting three of the four efficiency related goals (having already achieved one). SolAero are already at 96% of the BOL efficiency goal, 101% of the end of life blanket efficiency goal, 95% of the specific power goal and 86% of the packaging efficiency goal. SolAero believe this rationale assesses to a level 3 consequence.

Risk Status: Evaluated at the end of the Base Phase; still a risk.

Timeframe: This risk will be present through the start of the contract until the approximately the last 4 months at which time its status will be defined.

Mitigation Plan: SolAero are placing substantial resources into developing IMM solar cells that meet the power requirements. If during the execution of Option I and Option II, it becomes apparent that the efficiency is not increasing as required, SolAero will devote resources to further reducing the mass of the array, which will have a similar effect to increasing the IMM cell efficiency. Depending on the assessment at the time, SolAero will, with the concurrence of Glenn, increase resources to the development of the cell at the expense of other development. This mitigation plan will be in place for the interval from May, 2017 until four months prior to the end of Option II.

ID 2: IMM solar cells do not meet the power requirements after exposure to 4E15 1 MeV electrons

Risk Statement: If the IMM cells do not meet power requirements at end of life, it will be difficult to meet two end of life goals of the contract: over 28% blanket efficiency and over 10 W kg^{-1} specific power. The consequence of this occurring is lowered from a 4 to a 3 as a result of the discovery in the Base Phase that the IMM solar cells are lighter than assumed at the beginning of the Base Phase.

Risk Context: The context of the risk is the history of determining solar cell radiation degradation under charged particle radiation over the past twenty years.

Likelihood and Consequence to Safety: 1, 3. The likelihood of this risk is based on the safety record of exposing solar cells to radiation. The consequence is based on the consequences of exposure to irradiated solar cells that have not been sufficiently “cooled.” The consequence could also be increased to a 5 due to the possibility of increasing the chances of a life ending cancer. SolAero think the 3 is more likely; but it is a judgment call.

Likelihood and Consequence to Cost: 1, 5. The rationale for this is that APL will trade the cost risk to the technical risk. Essentially, SolAero will accept whatever cell performance after exposure to charge particles that SolAero obtain for the planned cost. If SolAero do not do this the consequence could be exceeding budget by more than 15% due to iterations of designing and re-testing cells; and, hence is a 5.

Likelihood and Consequence of to Schedule Performance: 1, 5. The rationale for this is that APL will trade the schedule risk to the technical risk. Essentially, SolAero will accept whatever cell performance is obtained for the planned schedule. If SolAero do not do this the consequence could be exceeding schedule for several years.

Likelihood and Consequence to Technical Performance: 2, 3 - This could happen as these cells are not yet manufactured or tested to 4E15 1 MeV electrons. The likelihood is reduced from 3 to 2 due to comprehensive radiation exposure data now available on IMM+ cells.

Risk Status: Evaluated at the end of the Base Phase; still a risk.

Timeframe: This risk will be present through the start of the contract until the approximately the last 4 months at which time its status will be defined.

Mitigation Plan: As very high efficiency IMM solar cells are required to meet the NRA goals, SolAero are placing substantial resources into developing IMM solar cells that meet the power requirements after exposure to charged particle radiation. If during the execution of Option I and Option II, it becomes apparent that the resistance to charged particle radiation is not as required, SolAero will devote resources to further reducing the mass of the array, which will have a similar effect to increasing the IMM cell efficiency after exposure to charged particle radiation. Depending on the assessment at the time, SolAero with the concurrence of Glenn may also increase resources to the development of cell radiation resistance at the expense of other development. This mitigation plan will be in place from the start of the contract until four months prior to the end of Option II.

ID 3: IMM solar cells will not meet the power requirements after exposure to thermal vacuum cycling, xenon plasma, or electrostatic discharge (or may just plain not meet power requirements).

Risk Statement: If the IMM cells do not meet power requirements at end of life due to failure after exposure to an environment, it will be difficult or impossible to meet four end of life goals of the contract: over 28% blanket efficiency, over 10 W kg^{-1} specific power, operation in a plasma generated by xenon thrusters and capability to operate at over 300 V.

Risk Context: The context of the risk is the history of testing IMM+ solar cells in similar environments.

Likelihood and Consequence to Safety: 1, 3. The likelihood of this risk is based on the author's informal estimation of the safety record of exposing solar cells and arrays to the listed environments. The consequence is based on the possibility of such as receiving a shock in the test of the articles.

Likelihood and Consequence to Cost: 1, 5. The rationale for this is that APL will trade the cost risk to the technical risk. Essentially, SolAero will accept whatever cell performance obtains after exposure to the listed environments that SolAero achieve for the planned cost. If SolAero do not do this the consequence could be exceeding budget by more than 15% due to iterations of designing and re-testing array technology; and, hence is a 5.

Likelihood and Consequence of to Schedule Performance: 1, 5. The rationale for this is that APL will trade the schedule risk to the technical risk. Essentially, SolAero will accept whatever cell performance obtains for the planned schedule. If SolAero do not do this the consequence could be exceeding schedule for several years due to repeated iterations of array tests.

Technical Likelihood and Consequence: 2, 4 **-** This could occur as IMM cells are not yet manufactured or tested to these environments. However, the performance of IMM4, IMM+, and now IMM5 cells in some of these environments and the performance of ZTJ cells in the environments suggest that the IMM cells will not have an issue.

Risk Status: Evaluated at the end of the Base Phase; still a risk.

Timeframe: This risk will be present through the start of the contract until the end of Option I.

Mitigation Plan: The following mitigations will be employed to address this risk.

1. Some mitigation has already been achieved against this risk. SolAero has fabricated IMMX+ solar cells, thermal vacuum cycled them, and exposed them to hard particle radiation. They performed as expected. The slight deficiency to this work is that the IMM+ cells are not identical to the IMM solar cells that the Extreme Environment array requires. Nonetheless, this provides an indication that at least the five junction cells required by the Transformational Array can be fabricated and successfully perform after exposure to thermal vacuum cycling.

2. IMM5 cells were produced during the base phase of the contract and will be tested during the Option 1 phase of the contract. These cells will provide more data reducing the risk to the performance of the IMM cells.
3. APL will devote substantial resources to mitigating this risk.

ID 4: The blanket or associated parts will fail after exposure to thermal vacuum cycling, xenon plasma, or electrostatic discharge.

Risk Statement: If the blanket parts fail after exposure to a test environment, it will be difficult or impossible to meet four end of life goals of the contract: over 28% blanket efficiency, over 10 W kg^{-1} specific power, operation in a plasma generated by xenon thrusters and capability to operate at over 300 V.

Risk Context: The context of the risk is the history of testing the ROSA blankets and other components under similar environments.

Likelihood and Consequence to Safety: 1, 3. The likelihood of this risk is based on the author's informal estimation of the safety record of exposing solar arrays to the listed environments. The consequence is based on the possibility of such as receiving an electric shock in the test of the articles.

Likelihood and Consequence to Cost: 1, 5. The rationale for this is that APL will trade the cost risk to the technical risk. Essentially, SolAero will accept whatever array performance obtains after exposure to the listed environments that SolAero achieve for the planned cost. If SolAero do not do this the consequence could be exceeding budget by more than 15% due to iterations of designing and re-testing array technology; and, hence is a 5.

Likelihood and Consequence of to Schedule Performance: 1, 5. The rationale for this is that APL will trade the schedule risk to the technical risk. Essentially, SolAero will accept whatever array performance obtains for the planned schedule. If SolAero do not do this the consequence could be exceeding schedule for several years due to repeated iterations of array tests.

Technical Likelihood and Consequence: 1, 4 **-** This could occur as some parts are not yet manufactured or tested to these environments. However, the performance of ROSA arrays and the similarity of the vast majority of these parts to the parts in the Transformational array suggest that there will not be an issue.

Risk Status: Evaluated at the end of the Base Phase; still a risk.

Timeframe: This risk will be present through the start of the contract until four months prior to the end of Option II.

Mitigation Plan: Care will be taken to design components close to designs that have already successfully passed exposures to the required environments.

ID 5: Fail to reduce outgassing to an acceptable level for use with concentrators

Risk Statement: If the outgassing is not reduced to an acceptable level, the vast majority of the negative impact will be on cost. This is because the technical performance metrics of the Transformational Array are only slightly reduced if concentrators are not used.

Risk Context: The context of the risk is the history of the poor in-flight performance of reflective concentrator arrays.

Likelihood and Consequence to Safety: 1, 2. The tests to develop low outgassing arrays are generally safe and the consequences of a poorly conducted tests are minimal. Basically, the adhesives are safe to handle and the equipment for the testing is forgiving.

Likelihood and Consequence to Cost: 1, 5. The rationale for this is that APL will trade the cost risk to the technical risk. Essentially, SolAero will accept whatever outgassing is obtained for the planned cost. If SolAero do not do this the consequence could be exceeding budget by more than 15%; and, hence is a 5.

Likelihood and Consequence of to Schedule Performance: 1, 5. The rationale for this is that APL will trade the schedule risk to the technical risk. Essentially, SolAero will accept whatever outgassing is obtained for the planned schedule. If SolAero do not do this the consequence could be exceeding schedule for several years.

Likelihood and Consequence to Technical Performance: 2, 4. There are several possible ways to reduce outgassing and these seem like they have a reasonable chance of success. Therefore, there is a low likelihood of failure. The technical consequences of failure to the technical goals is low because the Transformational Array can perform quite well without the concentrators. However, the cost goal would be adversely affected, hence the consequence of 4.

Risk Status: Evaluated at the end of the Base Phase; still a risk.

Timeframe: This risk will be present through the start of the contract until the end of Option I.

Mitigation Plan: Significant resources are being applied to reduce this risk.

ID 6: Fail to eliminate mirror coating delamination (retired)

Risk Statement: If the risk to obtaining a reliable coating is not reduced to an acceptable level, the vast majority of the negative impact will be on cost. This is because the technical performance metrics of the Transformational Array are only slightly reduced if concentrators are not used. During the interval covered by the status 3 report, DSS developed and tested coating that did not delaminate. As a result, this risk was retired.

Risk Context: The context of the risk is the history of delamination of the mirror coatings on previous FACT work. During the interval covered by the status 3 report, DSS developed and tested coating that did not delaminate.

Likelihood and Consequence to Safety: 1, 2. The tests needed to develop mirror coatings are generally safe and the consequences of a poorly conducted tests are minimal. Basically, the equipment to coat is safe and the equipment for the testing is forgiving.

Likelihood and Consequence to Cost: 1, 5. The rationale for this is that APL will trade the cost risk to the technical risk. Essentially, SolAero will accept whatever delamination is obtained for the planned cost. If SolAero do not do this the consequence could be exceeding budget by more than 15%; and, hence is a 5.

Likelihood and Consequence of to Schedule Performance: 1, 5. The rationale for this is that APL will trade the schedule risk to the technical risk. Essentially, SolAero will accept whatever delamination is obtained for the planned schedule. If SolAero do not do this the consequence could be exceeding schedule for several years.

Likelihood and Consequence to Technical Performance: 1, 4. APL technical experts believe that reliably adhering the coating to the mirrors is tricky but that it is possible. The technical consequence is low because the array can perform well without the concentrators. However, the consequence to the cost goal is relatively high, hence the 4. At the time of the status report the likelihood of this changed from a 3 to a 1 because DSS successfully achieved a coating that passed stringent tape pull tests.

Risk Status: Evaluated at the end of the Option I phase 3 report, this risk is retired.

Timeframe: This risk will be present through the start of the contract until the end of Option I at which time the outgassing work will be stopped.

Mitigation Plan: Significant resources are being applied to reduce this risk. At the end of the phase 3 report, the risk was retired.

ID 7: Fail to eliminate cell shunts

Risk Statement: If SolAero does not eliminate the shunts, the Transformational Array will still meet all of the formally defined specific technical contract goals. If there are no production controls to prevent or at least keep the percentage of shunted cells at an acceptable level, this increases the potential of an undefined cost risk increase.

Risk Context: Shunts were discovered to be an issue at LILT during the execution of the Base Phase.

Likelihood and Consequence to Safety: 1, 5. The likelihood of this risk is based on the safety record of developing and producing Gallium Arsenide based solar cells;
Likelihood and Consequence to Safety: 1, 5. The likelihood of this risk is based on the safety record of developing and producing Gallium Arsenide based solar cells;
and the safety monitoring and interlocks that are in place. SolAero has gone over 5.5 years without an injury related to cell manufacture. (The record of safety goes back further than that, but a report for earlier was not available for this report.) So, the likelihood is evaluated to be 1. The consequence is based on the toxicity of the materials used in the production of the cells. A leak in a reactor could be deadly.

Likelihood and Consequence to Cost: 1, 5. The rationale for this is that APL will trade the cost risk to the technical risk. Essentially, SolAero will accept whatever shunts are obtained for the planned cost. If SolAero do not do this the consequence could be exceeding budget by more than 15%; and, hence is a 5.

Likelihood and Consequence of to Schedule Performance: 1, 5. The rationale for this is that APL will trade the schedule risk to the technical risk. Essentially, SolAero will accept whatever shunts are obtained for the planned schedule. If SolAero do not do this the consequence could be exceeding schedule for several years.

Likelihood and Consequence to Technical Performance: 2, 4. SolAero has identified the cause of the shunts and it believes that there is a good probability of eliminating them. The technical consequence to the array is small because the cells with shunts can be discarded. However, the cost impact is substantial, hence the consequence of 4.

Risk Status: Evaluated at the end of the Base Phase, this risk replaced the risk associated with flat spots. The flat spot risk was retired because none were found in the Base Phase work.

Timeframe: This risk will be present through the start of the contract until four months from the end of Option II, when this work will be completed.

Mitigation: APL and SolAero are applying substantial resources to eliminating the shunts. At the beginning of the base phase this risk was related to flat spots. The likelihood of fixing the problem has increased somewhat as SolAero knows the cause of the shunts and has fixed similar issues on heritage cells.

ID 8: The IMM solar cells cannot be formed into CICS or interconnected. This risk is retired as of the end of the Base Phase.

APL has retired this risk as its likelihood has dropped to the same level of risk that is inherent to the formation of CICS and strings using state of the art cells.

Risk Status: Evaluated at the end of the Base Phase and found not to be a risk worth formally reporting.

ID 9: The ROSA array deployment mechanisms and structure will not attain goal mass

Statement: If this risk manifests, the goals for an array power density of 8 W kg^{-1} and packing density of 66 kW m^{-3} may be slightly exceeded or reserves decreased.

Context: This risk is related to recent work performed on ROSA arrays prior to the Transformational Array.

Likelihood and Consequence to Safety: 1, 2. It is unlikely that anything associated with this work will be unsafe; and if anything did happen the consequence would be slight. Perhaps a finger could be injured during the course of testing the deployment mechanisms.

Likelihood and Consequence to Cost: 1, 5. The rationale for this is that APL will trade the cost risk to the technical risk. Essentially, SolAero will accept whatever ROSA performance are obtained for the planned cost. If SolAero do not do this the consequence could be exceeding budget by more than 15%; and, hence is a 5.

Likelihood and Consequence of to Schedule Performance: 1, 5. The rationale for this is that APL will trade the schedule risk to the technical risk. Essentially, SolAero will accept whatever ROSA performance is obtained for the planned schedule. If SolAero do not do this the consequence could be exceeding schedule for several years.

Likelihood and Consequence to Technical Performance: 1, 4 This is not likely as DSS has sufficient experience with the ROSA mechanisms and structure to make accurate mass estimates. Still SolAero are pushing mass to the lowest possible limits. The likelihood of this occurring has dropped from 2 to 1 at the end of the base phase due to replacement of the heat spreader by a much lighter stiffener. The consequence could be as high as 4.

Risk Status: This risk remains at the end of the Base Phase.

Timeframe: This risk will be present through the start of the contract until four months from the end of Option II, when this work will be completed.

Mitigation: APL and SolAero are applying adequate resources to address this risk.

ID 10: The ROSA array will not deploy

Statement: If this risk manifests, SolAero would not meet contract goals.

Context: This risk is in the context of previous ROSA and previous performance of other types of array. Any failure to deploy would likely be easy to fix.

Likelihood and Consequence to Safety: 1, 2. It is unlikely that anything associated with this work will be unsafe; and if anything did happen the consequence would be slight. Perhaps a finger could be injured during the course of testing the deployment mechanisms.

Likelihood and Consequence to Cost: 1, 4. The rationale for this is that APL will trade the cost risk to the technical risk. Essentially, SolAero will accept whatever ROSA deployment performance is obtained for the planned cost. If SolAero do not do this the consequence could exceed budget.

Likelihood and Consequence of to Schedule Performance: 1, 4. The rationale for this is that APL will trade the schedule risk to the technical risk. Essentially, SolAero will accept whatever ROSA performance is obtained for the planned schedule. If SolAero do not do this the consequence could be exceeding schedule.

Likelihood and Consequence to Technical Performance: 1, 4 This is not likely as DSS has sufficient experience with the ROSA to be certain that it will deploy. This risk is included because array deployment has been a prominent failure mechanism for flight arrays. A failure to deploy in test would be serious to the contract goals as it would mean work would have to be completed to make the technology function properly.

Risk Status: This risk remains at the end of the Base Phase.

Timeframe: This risk will be present through the start of the contract until four months from the end of Option II, when this work will be completed.

Mitigation: APL and SolAero are applying adequate resources to address this risk.

Section III: Work Planned

No additional work is planned for Option I.

Section IV: Analysis

Analysis was performed on outgassing data, for the development of the IMM cells, for the development of the magnetically clean brakes, and for the overall array performance metrics. The analysis was reported in previous sections of this report.

Section V: Financial Reports

Monthly financial reports, 533Ms, were submitted for October, November, and December, 2017; and, January through July of 2018.

Signed

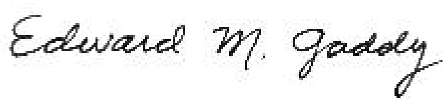

Edward M. Gaddy

Appendix A

Test Summary Report

VTL-R-18-078 I3U02OXX/SEM
August 14, 2018

Program	: JHU/APL – Transformational Array (TA)
Test Description	: Developmental Sinusoidal and Random Vibration
Test Specimen(s)	: TA – Roll Out Solar Array (ROSA) Coupon
Test Date(s)	: August 9-10, 2018
Test Spec. Doc. ID, Date	: ETF Form 7304-8100 for VTL-18-078, rev: June 18, 2008
Test System	: U/D T-4000 Vibration Exciter; m+p VibRunner-1 Control System
VTL Coordinator	: Ken Turner / Luke Boggs
VTL Lead Engineer	: Ken Turner
Responsible Engineer	: Ed Gaddy / Calvin Kee
Test Plan Deviation(s)	: (1) Z-axis run number 010, response accelerometer (R2) came off and was left removed for remaining test sequences
Anomalies	: None

Test Summary **:** The purpose of this test was to expose the Transitional Array Roll Out Solar Array (ROSA), which included a five cell solar string and mass simulators for remaining cells, to developmental sinusoidal and random vibration environments, per the above referenced test specifications to determine the fundamental frequencies and to structurally verify the bonding and integrity of the assembly in its developmental phase. A low level flat-input sine survey sweep was conducted prior to and following the sinusoidal and random vibration test sequences, and resulting response accelerometer inputs were overlaid and compared for any shifting of response natural frequency. Random vibration test input levels were started at -12dB of full-level and increased in upward steps of +3dB to full (0dB) level input, while observing control and response input signals. Response accelerometer limiting of the control input was applied at the discretion of the structural engineer for each test sequence. The ROSA Coupon completed the following vibration test sequences in the mounting configuration order of Y, Z, and X-axes:

Y-axis, Test Sequence

- Pre-Sine Survey; 0.10 g-flat input, 5-2000 Hz frequency spectrum, sweep up rate 4 octaves/minute
- Sine -12dB level; 5.11 g-peak input, 5-100 Hz frequency spectrum, sweep up rate 4 octaves/minute
- Sine -6B level; 10.15 g-peak input, 5-100 Hz frequency spectrum, sweep up rate 4 octaves/minute
- Random -3dB level; 9.25 grms input, 20-2000 Hz frequency spectrum, duration 60 seconds
- Post-Random Survey; 0.10 g-flat input, 5-2000 Hz frequency spectrum, sweep up rate 4 octaves/minute

Next day – repeat Y-axis

- Pre-Sine Survey; 0.10 g-flat input, 5-2000 Hz frequency spectrum, sweep up rate 4 octaves/minute
- Sine -6dB level; 10.21 g-peak input, 5-100 Hz frequency spectrum, sweep up rate 4 octaves/minute
- Sine 0B level; 20.37 g-peak input, 5-100 Hz frequency spectrum, sweep up rate 4 octaves/minute
- Post-Sine Survey; 0.10 g-flat input, 5-2000 Hz frequency spectrum, sweep up rate 4 octaves/minute
- Random 0dB level; 14.13 grms input, 20-2000 Hz frequency spectrum, duration 60 seconds
- Post-Random Survey; 0.10 g-flat input, 5-2000 Hz frequency spectrum, sweep up rate 4 octaves/minute

Z-axis, Test Sequence

- Pre-Sine Survey; 0.10 g-flat input, 5-2000 Hz frequency spectrum, sweep up rate 4 octaves/minute
- Sine -6dB level; 10.2 g-peak input, 5-100 Hz frequency spectrum, sweep up rate 4 octaves/minute
- Sine 0dB level; 20.25 g-peak input, 5-100 Hz frequency spectrum, sweep up rate 4 octaves/minute
- Post-Sine Survey; 0.10 g-flat input, 5-2000 Hz frequency spectrum, sweep up rate 4 octaves/minute
- Random 0dB level; 14.2 grms input, 20-2000 Hz frequency spectrum, duration 60 seconds
- Post-Random Survey; 0.10 g-flat input, 5-2000 Hz frequency spectrum, sweep up rate 4 octaves/minute

X-axis, Test Sequence

- Pre-Sine Survey; 0.10 g-flat input, 5-2000 Hz frequency spectrum, sweep up rate 4 octaves/minute
- Sine -18dB level; 2.5 g-peak input, 5-100 Hz frequency spectrum, sweep up rate 4 octaves/minute
- Sine -6dB level; 10.21 g-peak input, 5-100 Hz frequency spectrum, sweep up rate 4 octaves/minute
- Sine 0dB level; 19.43 g-peak input, 5-100 Hz frequency spectrum, sweep up rate 4 octaves/minute
- Post-Sine Survey; 0.10 g-flat input, 5-2000 Hz frequency spectrum, sweep up rate 4 octaves/minute
- Random 0dB level; 14.2 grms input, 20-2000 Hz frequency spectrum, duration 60 seconds
- Post-Random Survey; 0.10 g-flat input, 5-2000 Hz frequency spectrum, sweep up rate 4 octaves/minute

The vibration test set-up included two "L" mounting end fixtures mounted to the shaker slip-table, and the ROSA assembly was mounted between the two end fixtures per photographs included below. The vibration input was controlled with two PCB model 354M66 tri-axial accelerometers (C1-C2), mounted on the top centers of the two vibration "L" end fixtures. There were six mini tri-axial PCB Model 356A03 response accelerometers (R1-R6) used to capture acceleration responses, and in select test cases some were used for response-limiting of the control input. The six response accelerometers were mounted on the test assembly per the inserted diagram and table located in the test plan paragraph 7.5, Instrumentation Specification.

There was one deviation to the test plan referenced (1); response accelerometer R2 came off during the Y-axis random vibration test run number 010, and was left off of the ROSA assembly for the remaining test sequences. No anomalies occurred during the test sequence. A complete record of test data including; test specifications, test run logs, and set-up photographs is on file in the Environmental Test Facility under the assigned vibration test file number VTL-18-078

Test Set-up Photographs:

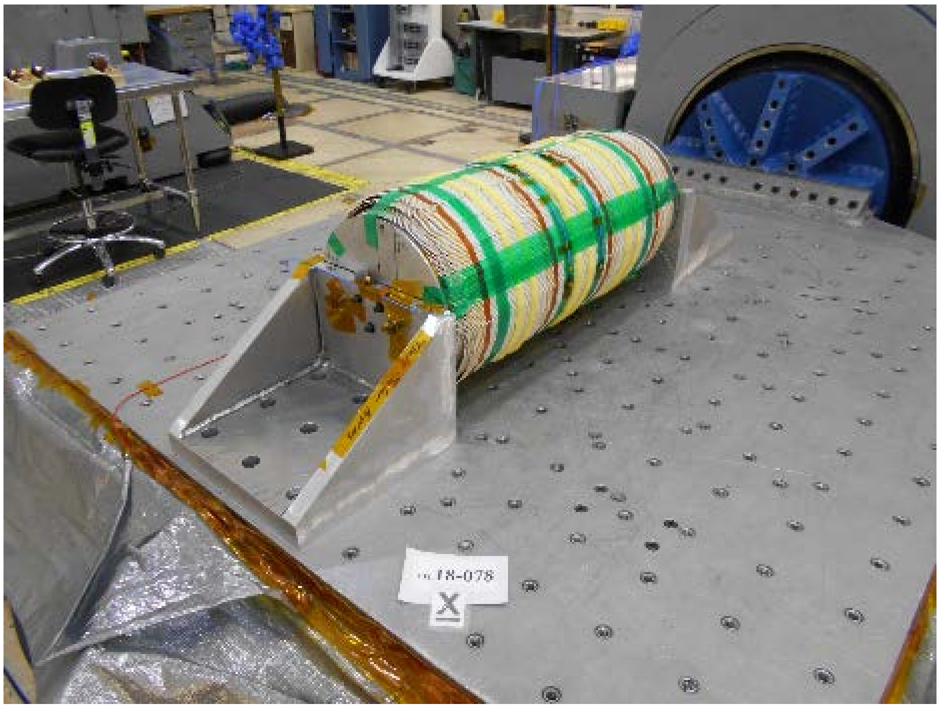

X-axis set-up, Transitional Roll Out Solar Array

Test Set-up Photographs (Continued):

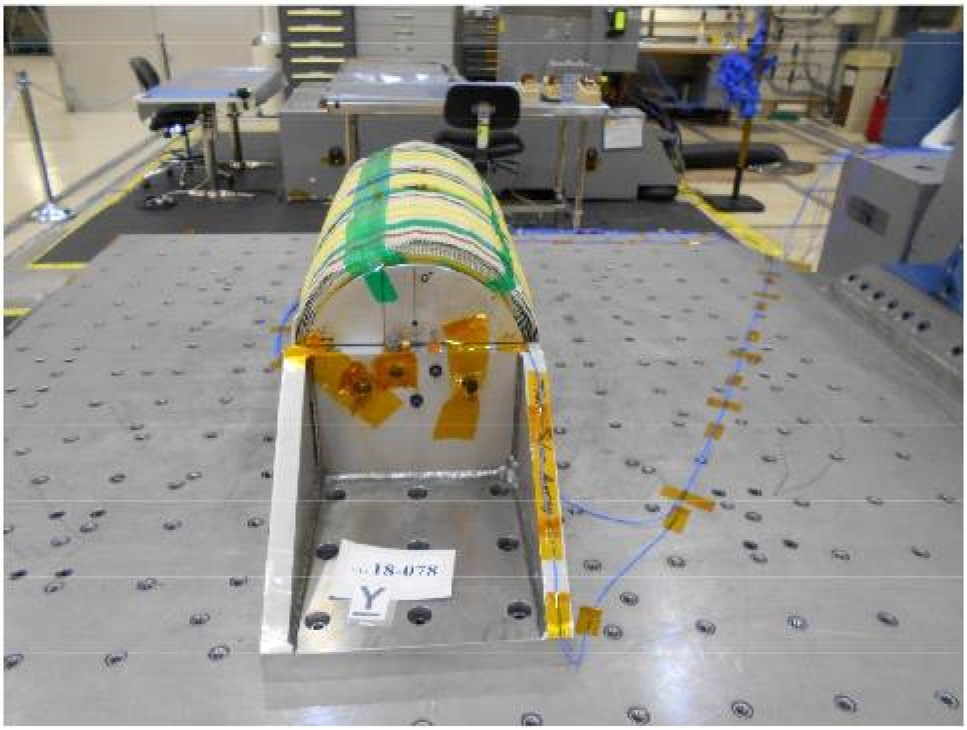

Y-axis set-up, Transitional Roll Out Solar Array

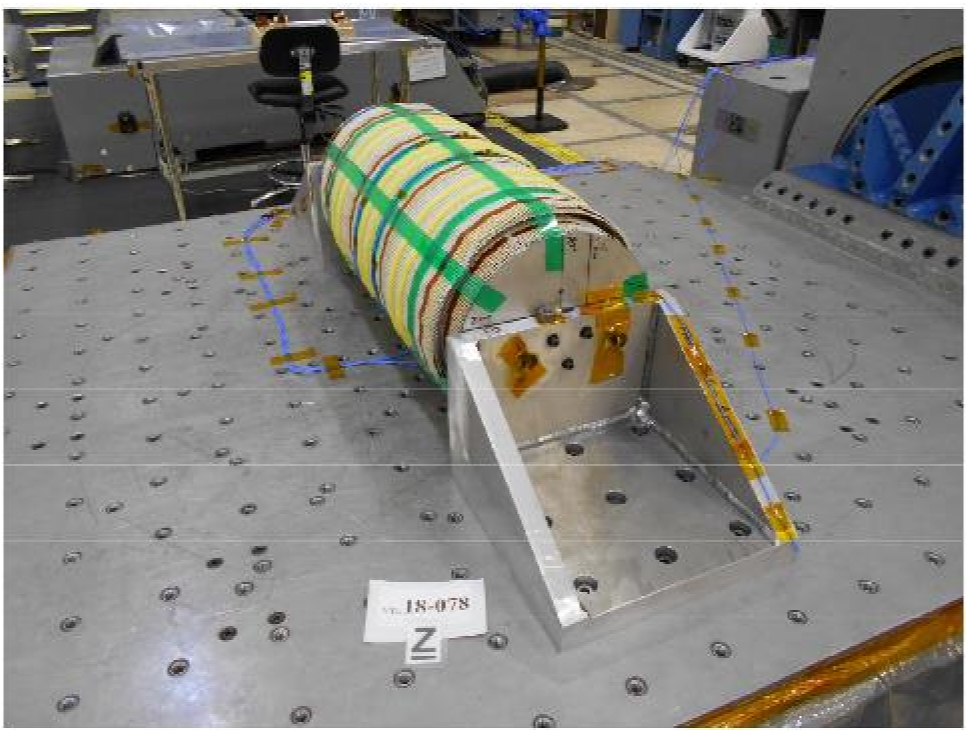

Z-axis set-up, Transitional Roll Out Solar Array